

TeV-scale vector leptoquark from Pati-Salam unification with vectorlike families

Syuhei Iguro¹, Junichiro Kawamura^{2,3}, Shohei Okawa⁴ and Yuji Omura⁵

¹ *Department of Physics, Nagoya University, Nagoya 464-8602, Japan*

² *Center for Theoretical Physics of the Universe, Institute for Basic Science (IBS), Daejeon 34051, Korea*

³ *Department of Physics, Keio University, Yokohama 223-8522, Japan*

⁴ *Department of Physics and Astronomy, University of Victoria, Victoria, BC V8P 5C2, Canada*

⁵ *Department of Physics, Kindai University, Higashi-Osaka, Osaka 577-8502, Japan*

Abstract

In this paper, we show an explicit way to realize a TeV-scale vector leptoquark from the Pati-Salam (PS) unification with extra vectorlike families. The leptoquark mass is constrained to be heavier than PeV-scale by the measurement of a flavor violating kaon decay, $K_L \rightarrow \mu e$, in conventional models. This strong constraint can be avoided by introducing vectorlike families consistently with the quark and lepton masses and CKM and PMNS matrices. The other flavor violating processes are also suppressed. In this model, the vector leptoquark can be sufficiently light to explain the recent $b \rightarrow s\mu\mu$ anomaly, while the $b \rightarrow c\tau\nu$ anomaly is difficult to be explained due to the strong constraints from the Z' boson and vectorlike quark searches at the LHC. When the $b \rightarrow s\mu\mu$ anomaly is explained, we show that $\mathcal{O}(0.2)$ % tuning is required in the fermion matrix, the future experiments in $\mu \rightarrow e\gamma$ and μ - e conversions will cover the most available parameter space, and sizable neutral meson mixings, induced by the extra Higgs doublets, are unavoidable.

Contents

1	Introduction	2
2	Pati-Salam model with vectorlike fermions	3
2.1	Fermion masses	5
2.2	Leptoquark couplings	7
2.3	How to suppress $K_L \rightarrow \mu e$	8
2.4	Parametrization	8
2.5	Fine-tuning	11
3	Phenomenology	12
3.1	Vector leptoquark explanation of the anomalies	12
3.1.1	$b \rightarrow s\mu\mu$ anomaly	12
3.1.2	$b \rightarrow c\tau\nu$ anomaly	13
3.2	Flavor physics	14
3.2.1	μ - e flavor violation versus fine-tuning	15
3.2.2	Flavor violation via Higgs bosons	18
3.3	$n - \bar{n}$ oscillation	21
4	Summary	22
A	Model details	24
A.1	Diagonalization of the fermion mass matrices	24
A.1.1	Dirac mass matrix	24
A.1.2	Neutrino masses	25
A.2	Gauge interactions	26
A.2.1	Symmetry breaking and vector boson masses	26
A.2.2	Gauge interactions with fermions	29
A.3	Scalar Interactions	32
B	Analysis details	35
B.1	Formulas of flavor observables	35
B.1.1	$K_L \rightarrow \mu e$	35
B.1.2	μ - e conversion	36
B.2	Benchmark	37

1 Introduction

Leptoquark is a hypothetical boson that carries both the baryon number and lepton number [1]. Recently, phenomenology of TeV-scale leptoquarks has been discussed particularly to explain the anomalies in the semi-leptonic B decays [2–16]. An attractive extension which predicts leptoquarks is the Pati-Salam (PS) unification [17]. In this paper, we construct an explicit PS model that leads a vector leptoquark at TeV scale.

In the PS model, quarks and leptons are unified into two multiplets under the PS gauge symmetry, $G_{\text{PS}} = SU(4)_C \times SU(2)_L \times SU(2)_R$. The hypercharge is quantized since all gauge symmetries are non-Abelian. A scale of the G_{PS} breaking can be much lower than that of the Grand Unification Theories (GUT) such as $SU(5)$ GUT due to the absence of bosons with di-quark couplings, which induces the proton decay. A vector leptoquarks arises as the massive degree of freedom associated with the G_{PS} breaking, $SU(4)_C \rightarrow SU(3)_C \times U(1)_{B-L}$, and hence its mass will be around the PS breaking scale.

The Yukawa couplings for different types of charged fermions in the Standard Model (SM) are predicted to be unified into one Yukawa coupling at the high-scale where the PS symmetry is restored. In a conventional scenario [18], the Yukawa unification is achieved by taking renormalization group (RG) effects and higher-dimensional operators. This scenario, however, requires that the G_{PS} breaking scale is around the conventional GUT scale, $\mathcal{O}(10^{16} \text{ GeV})$, in order to obtain sizable corrections from the RG effects and higher dimensional operators, which are usually suppressed by the Planck scale. It is proposed in Ref. [19] that the Yukawa unification is achieved by introducing vectorlike fermions even with the TeV-scale G_{PS} breaking¹, and thus the TeV-scale vector leptoquark can be realized in such a model. We also introduce vectorlike fermions in our setup.

One of the recent hot topics in high-energy physics is that experimental results are deviated from the SM predictions in the observables concerned with the semi-leptonic B decays in association with μ or τ lepton [21–35]. The LHCb collaboration reports deviations from the SM predictions in the measurements of the semi-leptonic B decays $B \rightarrow K^{(*)}\ell\ell$ ($\ell = e, \mu$). The LHCb collaboration studies the ratio of the branching ratio of $B \rightarrow K^{(*)}ee$ to that of $B \rightarrow K^{(*)}\mu\mu$ and the result tells that the branching ratio of $B \rightarrow K^{(*)}\mu\mu$ is slightly smaller than the SM prediction. We call this discrepancy the $b \rightarrow s\mu\mu$ anomaly. The collaboration investigates the observables related to the angular distribution of the $B \rightarrow K^*\mu\mu$ decay as well, and the one observable, namely P'_5 , deviates from the SM prediction. The recent observation for the angular observables in charged B meson decay also supports the result [36]. In addition, we can also find the discrepancy in $B \rightarrow D^{(*)}\tau\nu$. The decay mode has been studied in the BaBar, the Belle and the LHCb experiments. The BaBar collaboration has announced that the experimental result on the lepton universality, where the branching ratio of $B \rightarrow D^{(*)}\tau\nu$ is compared with $B \rightarrow D^{(*)}\ell\nu$, is largely deviated from the SM prediction. We call this discrepancy the $b \rightarrow c\tau\nu$ anomaly. The Belle and the LHCb have also studied the decay and have reported their results; the discrepancy becomes milder but the world average is still about 3-4 σ away from the SM value [37–41].

Motivated by those problems, a lot of new physics possibilities have been proposed. The

¹Similar attempts in models with fermions whose representations are different from the SM ones are recently studied in Ref. [20].

leptoquarks provide tree-level explanations of both $b \rightarrow s\mu\mu$ and $b \rightarrow c\tau\nu$ anomalies. Various types of leptoquarks, scalar or vector, representations under the SM gauge group, $G_{\text{SM}} = SU(3)_C \times SU(2)_L \times U(1)_Y$, are discussed in e.g. Refs. [4–6, 9, 42–44]. It is shown that both of the anomalies can be explained by a vector leptoquark with $(\mathbf{3}, \mathbf{1}, 2/3)$ under G_{SM} , which is realized in extensions of the minimal PS model [12, 16, 45–51]. Besides the leptoquarks, the $b \rightarrow s\mu\mu$ anomaly is explained by Z' boson at the tree-level [52–58] or a 1-loop box diagrams mediated by extra fermions [59–68]. However, the explanation of $b \rightarrow c\tau\nu$ anomaly with a charged Higgs boson [69–76] is constrained by the collider search [77] and $B_c \rightarrow \tau\nu$ decay [78, 79].

In this paper, we shall study the phenomenology of the model with TeV-scale G_{PS} breaking and vectorlike fermions. The typical leptoquark is strongly constrained by the measurement of $K_L \rightarrow \mu e$, so that its mass should be heavier than PeV scale. It is, however, pointed out in Ref. [19] that the bound is relaxed to be less than TeV scale if the mixing between the chiral and vectorlike fermions has a certain structure. We explicitly construct a model that realizes such a structure of the fermion mass matrices. We also point out that the parameters of the model should be tuned at $\mathcal{O}(0.1\%)$ level to be consistent with the realistic fermion masses and mixing as well as flavor constraints from $K_L \rightarrow \mu e$ etc., if the $b \rightarrow s\mu\mu$ anomaly is solved by the leptoquark. Interestingly, most of the parameter space will be covered by future experiments searching for the μ - e conversion process and $\mu \rightarrow e\gamma$. We also show that $b \rightarrow c\tau\nu$ anomaly is hardly explained in this model due to the constraints from the Z' boson search at the LHC. Besides, we study flavor violations via the extra Higgs bosons which are inevitably induced to explain the realistic Yukawa couplings.

This paper is organized as follows. We introduce our PS model in Sec. 2, and then the phenomenology is discussed in Sec. 3. Section 4 is devoted to summary. The details of the model and numerical analysis are shown in Appendix A and B, respectively.

2 Pati-Salam model with vectorlike fermions

We shall consider a model with the PS gauge symmetry, $G_{\text{PS}} = SU(4)_C \times SU(2)_L \times SU(2)_R$. In the minimal setup with G_{PS} , there are three generations of chiral fermions L , R and a bi-doublet Higgs field Φ . The Yukawa couplings of the chiral fermions are given by

$$-\mathcal{L}_Y^{\text{Ch}} = \bar{L}y_1\Phi R + \bar{L}y_2\epsilon^T\Phi^*\epsilon R + h.c., \quad (2.1)$$

where $\epsilon := i\sigma_2$ acts onto the $SU(2)_L$ and $SU(2)_R$ indices. Here, y_1 and y_2 are the 3×3 Yukawa matrices in the flavor space. The linear combination of the two terms leads the splittings of the Yukawa couplings between the up-type and down-type quarks, as well as the charged leptons and neutrinos. At the tree-level, however, the Yukawa couplings to the down-type quarks and charged leptons are coincident, and thus there is no mass splitting between them. It is often considered that the mass differences are realized by RG effects after the PS gauge symmetry breaking and/or by incorporating higher-dimensional operators involving symmetry breaking vacuum expectation values (VEVs). The symmetry breaking scale may need to be around the conventional GUT scale $\sim 10^{16}$ GeV, in order to realize sufficiently sizable corrections from the RG effects and/or higher-dimensional operators. Thus, these effects will be too small to explain the realistic fermion masses if the G_{PS} breaking scale is around TeV.

Table 1: The matter content in the Pati-Salam model. Each type of fermion has three flavors.

fields	spin	$SU(4)$	$SU(2)_L$	$SU(2)_R$
L	1/2	4	2	1
R	1/2	4	1	2
F_L	1/2	4	2	1
F_R	1/2	4	2	1
f_L	1/2	4	1	2
f_R	1/2	4	1	2
Δ	0	15	1	1
Σ	0	$\overline{\mathbf{10}}$	1	3
Φ	0	1	2	$\overline{\mathbf{2}}$
S	0	1	1	1

In this paper, we show an explicit model with the TeV-scale vector leptoquark. The matter content and the charge assignment are summarized in Table 1. The PS gauge symmetry is spontaneously broken at the TeV scale in our setup. We introduce extra vectorlike fermions, an $SU(4)_C$ adjoint scalar Δ , and another scalar Σ , $(\overline{\mathbf{10}}, \mathbf{1}, \mathbf{3})$. The mass splittings between the charged leptons and down quarks are generated by the VEV of Δ . The VEV of Σ induces the Majorana masses for the right-handed neutrinos. In this model, the non-zero VEV of Δ breaks $SU(4)_C$ to $SU(3)_C \times U(1)_{B-L}$ and that of Σ breaks $SU(2)_R \times U(1)_{B-L}$ to $U(1)_Y$.

The vectorlike fermions are denoted by F_L , F_R , f_L and f_R . Each type of vectorlike fermion has three flavors as the chiral fermions. As shown in Table 1, the charge assignment of $L(R)$ is the same as that of $F_L(f_R)$. In our work, we simply assume that there is an underlying theory or some symmetry, and they can be distinguished from each other. There are three-generations of vectorlike $SU(2)_L$ and $SU(2)_R$ doublet fermions. This is the minimal setup such that the leptoquark couplings to the SM fermions are vanishing in a certain limit, as shown in later. The vectorlike mass terms and Yukawa couplings are given by

$$\begin{aligned}
-\mathcal{L}_Y^{\text{VL}} = & \overline{F}_L M_L F_R + \overline{f}_L M_R f_R + \overline{f}_L m_R R + \overline{L} m_L F_R \\
& + \overline{F}_L \kappa_L \Delta F_R + \overline{f}_L \kappa_R \Delta f_R + \overline{f}_L \epsilon_R \Delta R + \overline{L} \epsilon_L \Delta F_R \\
& + \overline{F}_L \lambda_1 \Phi R + \overline{F}_L \lambda_2 \epsilon^T \Phi^* \epsilon R + \overline{L} \tilde{\lambda}_1 \Phi f_R + \overline{L} \tilde{\lambda}_2 \epsilon^T \Phi^* \epsilon f_R \\
& + \overline{F}_L \tilde{y}_1 \Phi f_R + \overline{F}_L \tilde{y}_2 \epsilon^T \Phi^* \epsilon f_R + \overline{f}_L \tilde{y}'_1 \Phi^\dagger F_R + \overline{f}_L \tilde{y}'_2 \epsilon^T \Phi^T \epsilon F_R + h.c.,
\end{aligned} \tag{2.2}$$

where all the masses and Yukawa couplings are 3×3 matrices in the flavor space. Here, the first line is the tree-level vectorlike mass terms. The second line is the Yukawa couplings with the $SU(4)_C$ adjoint Δ and the last two lines are the Yukawa couplings with the bi-doublet Φ . The mass splittings between quarks and leptons are induced by the Yukawa couplings involving the adjoint scalar Δ . In the next subsection, we study the fermion mass matrices originated from the

spontaneous PS symmetry breaking.

In addition, there are Yukawa couplings involving Σ , which induce Majorana masses after the symmetry breaking. As discussed in the next subsection, we simply assume that the Yukawa couplings between R and f_R is vanishing and the effective Majorana mass terms consist of only f_R ².

2.1 Fermion masses

After the G_{PS} breaking, the fermion multiplets are decomposed as

$$L = \begin{pmatrix} e_L & n_L \\ d_L & u_L \end{pmatrix}, \quad F_L = \begin{pmatrix} E_L & N_L \\ D_L & U_L \end{pmatrix}, \quad f_L = \begin{pmatrix} \mathcal{E}_L & \mathcal{N}_L \\ \mathcal{D}_L & \mathcal{U}_L \end{pmatrix}, \quad (2.3)$$

$$R = \begin{pmatrix} e_R & n_R \\ d_R & u_R \end{pmatrix}, \quad F_R = \begin{pmatrix} E_R & N_R \\ D_R & U_R \end{pmatrix}, \quad f_R = \begin{pmatrix} \mathcal{E}_R & \mathcal{N}_R \\ \mathcal{D}_R & \mathcal{U}_R \end{pmatrix}, \quad (2.4)$$

where the rows are the $SU(4)_C$ space and the columns are the $SU(2)_{L(R)}$ space for the $SU(2)_{L(R)}$ doublets. We parametrize the Dirac mass matrices as

$$\begin{aligned} & -\mathcal{L}_Y^{\text{Ch}} - \mathcal{L}_Y^{\text{VL}} \quad (2.5) \\ & = \begin{pmatrix} \bar{u}_L \\ \bar{U}_L \\ \bar{\mathcal{U}}_L \end{pmatrix}^T \begin{pmatrix} y_u v_H & \tilde{\lambda}_u v_H & m_{Q_L} \\ \lambda_u v_H & \tilde{y}_u v_H & M_{Q_L} \\ m_{Q_R} & M_{Q_R} & \tilde{y}'_u v_H \end{pmatrix} \begin{pmatrix} u_R \\ \mathcal{U}_R \\ U_R \end{pmatrix} + \begin{pmatrix} \bar{d}_L \\ \bar{D}_L \\ \bar{\mathcal{D}}_L \end{pmatrix}^T \begin{pmatrix} y_d v_H & \tilde{\lambda}_d v_H & m_{Q_L} \\ \lambda_d v_H & \tilde{y}_d v_H & M_{Q_L} \\ m_{Q_R} & M_{Q_R} & \tilde{y}'_d v_H \end{pmatrix} \begin{pmatrix} d_R \\ \mathcal{D}_R \\ D_R \end{pmatrix} \\ & + \begin{pmatrix} \bar{e}_L \\ \bar{E}_L \\ \bar{\mathcal{E}}_L \end{pmatrix}^T \begin{pmatrix} y_u v_H & \tilde{\lambda}_u v_H & m_{\ell_L} \\ \lambda_u v_H & \tilde{y}_u v_H & M_{\ell_L} \\ m_{\ell_R} & M_{\ell_R} & \tilde{y}'_u v_H \end{pmatrix} \begin{pmatrix} e_R \\ \mathcal{E}_R \\ E_R \end{pmatrix} + \begin{pmatrix} \bar{n}_L \\ \bar{N}_L \\ \bar{\mathcal{N}}_L \end{pmatrix}^T \begin{pmatrix} y_u v_H & \tilde{\lambda}_u v_H & m_{\ell_L} \\ \lambda_u v_H & \tilde{y}_u v_H & M_{\ell_L} \\ m_{\ell_R} & M_{\ell_R} & \tilde{y}'_u v_H \end{pmatrix} \begin{pmatrix} n_R \\ \mathcal{N}_R \\ N_R \end{pmatrix} + h.c. \\ & = \bar{\mathbf{u}}_L \mathcal{M}_u \mathbf{u}_R + \bar{\mathbf{d}}_L \mathcal{M}_d \mathbf{d}_R + \bar{\mathbf{e}}_L \mathcal{M}_e \mathbf{e}_R + \bar{\mathbf{n}}_L \mathcal{M}_n \mathbf{n}_R + h.c., \quad (2.6) \end{aligned}$$

where $\lambda_{u,d}$, $\tilde{\lambda}_{u,d}$, $y_{u,d}$, $\tilde{y}_{u,d}$ are the linear combinations of $\lambda_{1,2}$, $\tilde{\lambda}_{1,2}$, $y_{1,2}$ and $\tilde{y}_{1,2}$, respectively³. The VEVs of the bi-doublet and adjoint are defined as

$$\langle \Phi \rangle = v_H \times \text{diag}(s_\beta, c_\beta), \quad \langle \Delta \rangle = \frac{v_\Delta}{2\sqrt{3}} \times \text{diag}(3, -1, -1, -1), \quad (2.7)$$

where $s_\beta^2 + c_\beta^2 = 1$ and $v_H \simeq 174$ GeV. The mass matrices $M_{\mathcal{F}}$ and $m_{\mathcal{F}}$ ($\mathcal{F} = Q_{L,R}, \ell_{L,R}$) are defined as

$$\begin{aligned} M_{\ell_{L,R}} &= M_{L,R} + \frac{3}{2\sqrt{3}} \kappa_{L,R} v_\Delta, & M_{Q_{L,R}} &= M_{L,R} - \frac{1}{2\sqrt{3}} \kappa_{L,R} v_\Delta, \\ m_{\ell_{L,R}} &= m_{L,R} + \frac{3}{2\sqrt{3}} \epsilon_{L,R} v_\Delta, & m_{Q_{L,R}} &= m_{L,R} - \frac{1}{2\sqrt{3}} \epsilon_{L,R} v_\Delta. \end{aligned} \quad (2.8)$$

²We note that this situation can be realized by assigning extra symmetry to distinguish f_R from R .

³Their explicit relations are shown in Appendix A.3.

Here, \mathcal{M}_u , \mathcal{M}_d , \mathcal{M}_e and \mathcal{M}_n respectively represent 9×9 mass matrices for the 9 generations of fermions $\mathbf{u}_{L,R}$, $\mathbf{d}_{L,R}$, $\mathbf{e}_{L,R}$ and $\mathbf{n}_{L,R}$. The Yukawa couplings with the SM Higgs bosons are the same for the down quarks and charged leptons, as well as the up quarks and neutrinos, while the vectorlike masses and Yukawa couplings with Δ are common in each of the quarks and leptons. Note that the orderings of the $SU(2)_L$ singlet and doublet states are flipped for which the electroweak (EW) gauge couplings are simplified. We define the mass basis for the charged fermions as

$$\hat{\mathbf{u}}_{L,R} = (U_{L,R}^u)^\dagger \mathbf{u}_{L,R}, \quad \hat{\mathbf{d}}_{L,R} = (U_{L,R}^d)^\dagger \mathbf{d}_{L,R}, \quad \hat{\mathbf{e}}_{L,R} = (U_{L,R}^e)^\dagger \mathbf{e}_{L,R}. \quad (2.9)$$

The unitary matrices diagonalize the mass matrices as

$$(U_L^f)^\dagger \mathcal{M}_f U_R^f = \text{diag} \left(m_1^f, m_2^f, \dots, m_9^f \right), \quad (2.10)$$

where $f = e, d, u$. The singular values are in ascending ordered, i.e. $m_a^f \leq m_{a+1}^f$ ($a = 1, \dots, 8$). The SM fermion masses are given by m_1^f , m_2^f and m_3^f :

$$(m_1^e, m_2^e, m_3^e) = (m_e, m_\mu, m_\tau), \quad (m_1^d, m_2^d, m_3^d) = (m_d, m_s, m_b), \quad (m_1^u, m_2^u, m_3^u) = (m_u, m_c, m_t).$$

The neutrino masses are explained by the type-I seesaw mechanism with Majorana masses for the right-handed neutrinos. In this model, the Yukawa couplings with Σ are given by

$$-\mathcal{L}_\Sigma^y = \frac{1}{2} \bar{f}_R^c h \epsilon^T \Sigma f_R + h.c., \quad (2.11)$$

where h is the 3×3 symmetric Yukawa matrix. The scalar Σ is represented as

$$\Sigma_{\alpha\beta} = \Sigma_{\alpha\beta}^{k_R} T^{k_R} = \frac{1}{2} \begin{pmatrix} \Sigma_{\alpha\beta}^3 & \sqrt{2}\Sigma_{\alpha\beta}^+ \\ \sqrt{2}\Sigma_{\alpha\beta}^- & -\Sigma_{\alpha\beta}^3 \end{pmatrix}, \quad \Sigma_{\alpha\beta}^\pm = \frac{\Sigma_{\alpha\beta}^1 \pm i\Sigma_{\alpha\beta}^2}{\sqrt{2}}, \quad (2.12)$$

where $k_R = 1, 2, 3$ is $SU(2)_R$ index and $\alpha, \beta = 1, 2, 3, 4$ are the $SU(4)_C$ indices. We shall assume that Σ obtains the VEV as

$$\langle \Sigma_{11}^+ \rangle = \frac{v_\Sigma}{\sqrt{2}} \neq 0, \quad \text{others} = 0, \quad (2.13)$$

where $\alpha, \beta = 1$ is the leptonic direction in the $SU(4)_C$ space. After the symmetry breaking, the Majorana mass term is given by

$$-\mathcal{L}_{h,\Sigma} \supset \frac{1}{2} \bar{\mathcal{N}}_R^c M_R \mathcal{N}_R + h.c., \quad M_R = \frac{h}{\sqrt{2}} v_\Sigma. \quad (2.14)$$

The full neutrino mass term is given by

$$-\mathcal{L}_N = \frac{1}{2} \bar{\mathbf{N}}_L \mathcal{M}_N \mathbf{N}_R := \begin{pmatrix} \bar{\mathbf{n}}_L & \bar{\mathbf{n}}_R^c \end{pmatrix} \begin{pmatrix} 0_9 & \mathcal{M}_n \\ \mathcal{M}_n^T & \mathcal{M}_R \end{pmatrix} \begin{pmatrix} \mathbf{n}_L^c \\ \mathbf{n}_R \end{pmatrix}, \quad \mathcal{M}_R = \begin{pmatrix} 0_3 & 0_3 & 0_3 \\ 0_3 & M_R & 0_3 \\ 0_3 & 0_3 & 0_3 \end{pmatrix}, \quad (2.15)$$

where the Dirac mass matrix is defined in Eq. (2.5)⁴. Note that $\mathbf{N}_R^c = \mathbf{N}_L$. The mass eigenstate is defined as

$$\hat{\mathbf{N}}_R = U_N^\dagger \mathbf{N}_R, \quad \hat{\mathbf{N}}_L = U_N^T \mathbf{N}_L, \quad [U_N^T \mathcal{M}_N U_N]_{xy} = m_{\nu_x} \delta_{xy}, \quad (2.16)$$

with $x, y = 1, 2, 3, \dots, 18$. Here, U_N is an 18×18 unitary matrix. We define the 9×18 matrices,

$$U_L^n := \mathcal{P}_L U_N^*, \quad U_R^n := \mathcal{P}_R U_N, \quad (2.17)$$

where the projection matrices for the neutrino flavors are defined as

$$\mathcal{P}_L := \begin{pmatrix} \mathbf{1}_9 & 0_9 \end{pmatrix}, \quad \mathcal{P}_R := \begin{pmatrix} 0_9 & \mathbf{1}_9 \end{pmatrix}. \quad (2.18)$$

2.2 Leptoquark couplings

The spontaneous PS gauge symmetry breaking generates the mass of the vector leptoquark, that is part of the $SU(4)_C$ gauge field. The gauge couplings with the vector leptoquark, X^μ , are given by

$$\begin{aligned} \mathcal{L}_X &= \frac{g_4}{\sqrt{2}} X^\mu \left(\bar{\mathbf{d}}_L \gamma_\mu \mathbf{e}_L + \bar{\mathbf{u}}_L \gamma_\mu \mathbf{n}_L + \bar{\mathbf{d}}_R \gamma_\mu \mathbf{e}_R + \bar{\mathbf{u}}_R \gamma_\mu X^\mu \mathbf{n}_R \right) + h.c. \\ &= X^\mu \left(\hat{\mathbf{d}}_L \hat{g}_{d_L}^X \gamma_\mu \hat{\mathbf{e}}_L + \hat{\mathbf{u}}_L \hat{g}_{u_L}^X \gamma_\mu \hat{\mathbf{N}}_L + \hat{\mathbf{d}}_R \hat{g}_{d_R}^X \gamma_\mu \hat{\mathbf{e}}_R + \hat{\mathbf{u}}_R \hat{g}_{u_R}^X \gamma_\mu \hat{\mathbf{N}}_R \right) + h.c.. \end{aligned} \quad (2.19)$$

Here, the coupling matrices in the mass basis are given by

$$\begin{aligned} \hat{g}_{d_L}^X &= \frac{g_4}{\sqrt{2}} (U_L^d)^\dagger U_L^e, & \hat{g}_{d_R}^X &= \frac{g_4}{\sqrt{2}} (U_R^d)^\dagger U_R^e, \\ \hat{g}_{u_L}^X &= \frac{g_4}{\sqrt{2}} (U_L^u)^\dagger U_L^n, & \hat{g}_{u_R}^X &= \frac{g_4}{\sqrt{2}} (U_R^u)^\dagger U_R^n. \end{aligned} \quad (2.20)$$

The couplings of the fermions to the other gauge bosons and scalars are shown in Appendix A.

All the SM fermion masses and mixings can be explained consistently with the PS relations by the mass splittings via the Yukawa couplings with the bi-doublets Φ and adjoint Δ even if the G_{PS} breaking scale is at the TeV scale. The leptoquark, however, couples to the SM charged leptons and down-type quarks if the SM fermions dominantly come from the chiral fermions, L and R . When the leptoquark has sizable couplings to the light flavor fermions, particularly electron and down-type quarks simultaneously, it is known that the limit from $K_L \rightarrow \mu e$ gives the most stringent bound on the leptoquark mass, that is the G_{PS} breaking scale [80, 81]⁵. If $\hat{g}_{d_L}^X = \hat{g}_{d_R}^X = (g_4/\sqrt{2}) \cdot \mathbf{1}_9$, the branching fraction of $K_L \rightarrow \mu e$ is estimated as⁶.

$$\text{BR}(K_L \rightarrow \mu e) \sim 1.4 \times 10^{-11} \times \left(\frac{1 \text{ PeV}}{m_X} \right)^4 \left(\frac{g_4}{1.0} \right)^4, \quad (2.21)$$

⁴In this paper, 0_n is a $n \times n$ zero matrix. Similarly, $\mathbf{1}_n$ is an $n \times n$ identity matrix.

⁵We note that the flavor constraints from $K \rightarrow \pi \mu e$ are milder than the one obtained from $K_L \rightarrow \mu e$ [82].

⁶See Eq. (B.1) for the full formula.

while the current upper bound is 4.7×10^{-12} . Thus the leptoquark should be heavier than 1 PeV in this case, that is too heavy to explain the current flavor anomalies. The couplings to light flavor fermions could be suppressed by introducing vectorlike fermions [19] as in our model. In the following, we will show explicit mass matrices which are consistent with the TeV-scale vector leptoquark, SM fermion mass and mixing. We also see that most of flavor violating processes as well as $K_L \rightarrow \mu e$ are sufficiently suppressed.

2.3 How to suppress $K_L \rightarrow \mu e$

We propose an explicit way to avoid the strong constraint from the $K_L \rightarrow \mu e$ at the tree level, by tuning the vectorlike masses such that

$$m_{Q_R} \ll M_{Q_R}, \quad M_{Q_L} \ll m_{Q_L}, \quad M_{\ell_R} \ll m_{\ell_R}, \quad m_{\ell_L} \ll M_{\ell_L}. \quad (2.22)$$

The mass matrices of the down quarks and charged leptons are schematically given by

$$\mathcal{M}_d \sim \begin{pmatrix} 0_3 & \hat{m}_e & m_{Q_L} \\ \hat{m}_d & 0_3 & 0_3 \\ 0_3 & M_{Q_R} & 0_3 \end{pmatrix}, \quad \mathcal{M}_e \sim \begin{pmatrix} 0_3 & \hat{m}_e & 0_3 \\ \hat{m}_d & 0_3 & M_{\ell_L} \\ m_{\ell_R} & 0_3 & 0_3 \end{pmatrix}, \quad (2.23)$$

where \hat{m}_d and \hat{m}_e are the 3×3 mass matrices proportional to v_H . The same structure will arise in the up quark and neutrino sector due to the hierarchy in Eq. (2.22). With this texture, \hat{m}_d and \hat{m}_e are approximately the mass matrices for the down-type quarks and charged leptons in the SM generations since the mixing with the other blocks are suppressed. The down quarks are originated from (F_L, R) , while the charged leptons are originated from (L, f_R) . Thus, the masses and mixing of the SM fermions can be explained separately, and the leptoquark couplings to the SM down-type fermions are more suppressed as the hierarchical structure in Eq. (2.22) is more strict.

2.4 Parametrization

In our notation, it is convenient to express the mass matrices by a 6×6 block on the upper-left and a 3×3 block on the bottom-right. Without loss of generality ⁷, we can parametrize the Dirac mass matrices in the gauge basis as

$$\mathcal{M}_d = \begin{pmatrix} \tilde{D}_d & V_{Q_L} \tilde{D}_{Q_L} W_{Q_R}^\dagger \\ W_{Q_L} \tilde{D}_{Q_R} V_{Q_R}^\dagger & \Delta_d \end{pmatrix}, \quad \mathcal{M}_e = \begin{pmatrix} \tilde{D}_d & V_{\ell_L} \tilde{D}_{\ell_L} W_{\ell_R}^\dagger \\ W_{\ell_L} \tilde{D}_{\ell_R} V_{\ell_R}^\dagger & \Delta_d \end{pmatrix}, \quad (2.24)$$

$$\mathcal{M}_u = \begin{pmatrix} v_{u_L} \tilde{D}_u v_{u_R}^\dagger & V_{Q_L} \tilde{D}_{Q_L} W_{Q_R}^\dagger \\ W_{Q_L} \tilde{D}_{Q_R} V_{Q_R}^\dagger & w_{u_L} \Delta_u w_{u_R}^\dagger \end{pmatrix}, \quad \mathcal{M}_n = \begin{pmatrix} v_{u_L} \tilde{D}_u v_{u_R}^\dagger & V_{\ell_L} \tilde{D}_{\ell_L} W_{\ell_R}^\dagger \\ W_{\ell_L} \tilde{D}_{\ell_R} V_{\ell_R}^\dagger & w_{u_L} \Delta_u w_{u_R}^\dagger \end{pmatrix},$$

⁷Here, the mass matrices are expressed by the singular value decomposition, as usually applied to the Dirac mass matrix.

where

$$\tilde{D}_d = \begin{pmatrix} 0_3 & D_e \\ D_d & 0_3 \end{pmatrix}, \quad \tilde{D}_u = \begin{pmatrix} 0_3 & D_n \\ D_u & 0_3 \end{pmatrix}, \quad (2.25)$$

and

$$\tilde{D}_{Q_R} = \begin{pmatrix} 0_3 & D_{Q_R} \end{pmatrix}, \quad \tilde{D}_{Q_L} = \begin{pmatrix} D_{Q_L} \\ 0_3 \end{pmatrix}, \quad \tilde{D}_{\ell_R} = \begin{pmatrix} D_{\ell_R} & 0_3 \end{pmatrix}, \quad \tilde{D}_{\ell_L} = \begin{pmatrix} 0_3 \\ D_{\ell_L} \end{pmatrix}. \quad (2.26)$$

Here, D_f ($f = u, d, e, n$) and $D_{F_{L,R}}$ ($F = Q, \ell$) are 3×3 diagonal matrices. There are four 6×6 unitary matrices $V_{Q_{L,R}}, V_{\ell_{L,R}}$ and eight 3×3 unitary matrices $W_{Q_{L,R}}, W_{\ell_{L,R}}$ and $v_{u_{L,R}}, w_{u_{L,R}}$. By definition, the mass matrices are unchanged under

$$V_{\ell_{L,R}} \rightarrow \begin{pmatrix} u_{\ell_{L,R}} & 0_3 \\ 0_3 & \mathbf{1}_3 \end{pmatrix} V_{\ell_{L,R}}, \quad V_{Q_{L,R}} \rightarrow \begin{pmatrix} u_{Q_{L,R}} & 0_3 \\ 0_3 & \mathbf{1}_3 \end{pmatrix} V_{Q_{L,R}}, \quad (2.27)$$

where $u_{F_{L,R}}$ are arbitrary 3×3 unitary matrices. We start from a basis in which D_d, D_e and Δ_d are diagonalized, which can be done without changing any couplings with the gauge bosons or scalars. See Appendix A.1 for more details. We further assume that the Majorana matrix M_R is proportional to an identity matrix in this basis for simplicity.

This parametrization is defined such that the SM-like fermion masses and couplings are realized when all the unitary matrices are identity matrices except v_{u_L} which should be

$$v_{u_L} = \begin{pmatrix} U_{\text{PMNS}} & 0_3 \\ 0_3 & V_{\text{CKM}}^\dagger \end{pmatrix}, \quad (2.28)$$

so that the CKM and PMNS matrices are realized. In this canonical case, the (Dirac) mass matrices are diagonalized by the following unitary matrices,

$$\begin{aligned} U_L^{0,d} = U_R^{0,e} = U_R^{0,n} &= \begin{pmatrix} 0_3 & \mathbf{1}_3 & 0_3 \\ \mathbf{1}_3 & 0_3 & 0_3 \\ 0_3 & 0_3 & \mathbf{1}_3 \end{pmatrix}, & U_L^{0,u} &= \begin{pmatrix} 0_3 & \mathbf{1}_3 & 0_3 \\ V_{\text{CKM}}^\dagger & 0_3 & 0_3 \\ 0_3 & 0_3 & \mathbf{1}_3 \end{pmatrix}, \\ U_R^{0,u} = U_R^{0,d} = U_L^{0,e} &= \begin{pmatrix} \mathbf{1}_3 & 0_3 & 0_3 \\ 0_3 & 0_3 & \mathbf{1}_3 \\ 0_3 & \mathbf{1}_3 & 0_3 \end{pmatrix}, & U_L^{0,n} &= \begin{pmatrix} U_{\text{PMNS}} & 0_3 & 0_3 \\ 0_3 & 0_3 & \mathbf{1}_3 \\ 0_3 & \mathbf{1}_3 & 0_3 \end{pmatrix}, \end{aligned} \quad (2.29)$$

up to $\mathcal{O}(v_H^2/v_\Delta)$ corrections. For the full neutrino matrix, the diagonalization matrix is given by

$$U_N^0 \sim \begin{pmatrix} (U_L^{0,n})^* & 0_9 \\ 0_9 & U_R^{0,n} \end{pmatrix}. \quad (2.30)$$

Then, the leptoquark couplings are approximately given by

$$\hat{g}_{d_L}^X \sim (\hat{g}_{d_R}^X)^T \sim \mathcal{P}_R (\hat{g}_{u_R}^X)^T \sim \frac{g_4}{\sqrt{2}} \begin{pmatrix} 0_3 & 0_3 & \mathbf{1}_3 \\ \mathbf{1}_3 & 0_3 & 0_3 \\ 0_3 & \mathbf{1}_3 & 0_3 \end{pmatrix}, \quad \hat{g}_{u_L}^X \mathcal{P}_L^T \sim \frac{g_4}{\sqrt{2}} \begin{pmatrix} 0_3 & 0_3 & V_{\text{CKM}} \\ U_{\text{PMNS}} & 0_3 & 0_3 \\ 0_3 & \mathbf{1}_3 & 0_3 \end{pmatrix}. \quad (2.31)$$

Hence, the leptoquark couplings to the SM fermions, which corresponds to the most upper-left block in the coupling matrix, e.g. $[\hat{g}_{d_L}^X]_{ij}$ ($i, j \leq 3$), are vanishing. Thus, in this canonical case, there is no flavor violation at the tree-level, although there might be flavor violation, such as $\mu \rightarrow e\gamma$, from the loop-effects involving the vectorlike states. In order to explain the flavor anomalies, the leptoquark should couple to the SM fermions with a certain pattern. In the following, we will turn on the mixing angles in the unitary matrices which are chosen to be identity in the canonical limit. The diagonalization for a general case with the parametrization in Eq. (2.24) is discussed in Appendix A.1.

For simplicity, we assume that the singular values for vectorlike fermions and $\Delta_{u,d}$ are universal⁸, i.e.

$$D_{Q_L} = d_{Q_L} \mathbf{1}_3, \quad D_{Q_R} = d_{Q_R} \mathbf{1}_3, \quad D_{\ell_L} = d_{\ell_L} \mathbf{1}_3, \quad D_{\ell_R} = d_{\ell_R} \mathbf{1}_3, \quad (2.32)$$

and

$$\Delta_d = \delta_d \mathbf{1}_3, \quad \Delta_u = \delta_u \mathbf{1}_3. \quad (2.33)$$

We also assume that the Majorana mass matrix is given by

$$\mathcal{M}_R = m_N \begin{pmatrix} 0_3 & 0_3 & 0_3 \\ 0_3 & \mathbf{1}_3 & 0_3 \\ 0_3 & 0_3 & 0_3 \end{pmatrix}. \quad (2.34)$$

Further, we take $W_{Q_{L,R}}$, $W_{\ell_{L,R}}$ and $w_{u_{L,R}}$ identity matrices, since these are not significant for the SM fermion couplings.

When the $V_{Q_{L,R}}$ and $V_{\ell_{L,R}}$ are not identity matrices, the diagonalization matrices for the down-type fermions in Eq. (2.24) are approximately given by

$$U_{e_L} \sim \begin{pmatrix} 0_{6 \times 3} & V_{\ell_L} \\ W_{\ell_L} & 0_{3 \times 6} \end{pmatrix} P_1, \quad U_{e_R} \sim \begin{pmatrix} V_{\ell_R} & 0_{6 \times 3} \\ 0_{3 \times 6} & W_{\ell_R} \end{pmatrix} P_1, \quad (2.35)$$

$$U_{d_L} \sim \begin{pmatrix} V_{Q_L} & 0_{6 \times 3} \\ 0_{3 \times 6} & W_{Q_L} \end{pmatrix} P_1, \quad U_{d_R} \sim \begin{pmatrix} 0_{6 \times 3} & V_{Q_R} \\ W_{Q_R} & 0_{3 \times 6} \end{pmatrix} P_1, \quad (2.36)$$

⁸Precisely, we introduce $\mathcal{O}(0.1 \text{ GeV})$ corrections to the vectorlike fermion masses to avoid numerical instabilities due to the degeneracy as can be seen in Appendix B.

where

$$P_1 := \begin{pmatrix} 0_3 & \mathbf{1}_3 & 0_3 \\ \mathbf{1}_3 & 0_3 & 0_3 \\ 0_3 & 0_3 & \mathbf{1}_3 \end{pmatrix}, \quad (2.37)$$

is introduced so that the singular values are increasingly ordered. The derivation and those for the up-type fermions are shown in Appendix A.1. With this parametrization, the leptoquark couplings to the SM fermions are approximately given by

$$[\hat{g}_{dL}^X]_{ij} \sim [\hat{g}_{uL}^X]_{ij} \sim \frac{g_4}{\sqrt{2}} [V_{QL}^\dagger V_{\ell L}]_{3+i,j}, \quad [\hat{g}_{dR}^X]_{ij} \sim [\hat{g}_{uR}^X]_{ij} \sim \frac{g_4}{\sqrt{2}} [V_{QR}^\dagger V_{\ell R}]_{i,j+3}, \quad (2.38)$$

with $i, j = 1, 2, 3$. Hence, the leptoquark couplings to the SM families are induced from the mixing between the first three and the second three states. We parametrize the unitary matrices, V_{FX} , $F = \ell, Q$, $X = L, R$, as ⁹

$$V_{FX} := R_{FX}^{11} R_{FX}^{12} R_{FX}^{13} R_{FX}^{21} R_{FX}^{22} R_{FX}^{23} R_{FX}^{31} R_{FX}^{32} R_{FX}^{33}, \quad (2.39)$$

where the rotation matrix R_{FX}^{ij} mixes the i -th and $(j+3)$ -th elements, i.e.

$$R_{FX}^{ij} = \begin{pmatrix} 1 & \cdots & 0 & \cdots & 0 & \cdots & 0 \\ \vdots & & \vdots & & \vdots & & \vdots \\ 0 & \cdots & c_{FX}^{ij} & \cdots & s_{FX}^{ij} & \cdots & 0 \\ \vdots & & \vdots & & \vdots & & \vdots \\ 0 & \cdots & -s_{FX}^{ij} & \cdots & c_{FX}^{ij} & \cdots & 0 \\ \vdots & & \vdots & & \vdots & & \vdots \\ 0 & \cdots & 0 & \cdots & 0 & \cdots & 1 \end{pmatrix}, \quad (2.40)$$

where $(c_{FX}^{ij})^2 + (s_{FX}^{ij})^2 = 1$. In our analysis, we assume that V_{FX} 's are real and we will not consider the mixing inside the first three and second three states.

In our numerical analysis of Section 3, the vectorlike fermion masses $d_{Q_{L,R}}, d_{\ell_{L,R}}, \delta_{u,d}$ and the unitary matrices V_{FX} are input parameters. The rest of parameters, \tilde{D}_d, \tilde{D}_u and v_{uL}, v_{uR} are fitted to explain the observed fermion masses and mixing for a given set of input parameters.

2.5 Fine-tuning

The texture in Eq. (2.23), or the hierarchy in Eq. (2.22) requires fine-tunings between the PS symmetric mass parameters in the first line of Eq. (2.2) and the mass terms originated from the $SU(4)_C$ adjoint $\langle \Delta \rangle$. To quantify the degree of tunings, we define the tuning measure Δ_{FT} as

$$\Delta_{\text{FT}} := \min_{A,B} ([\Delta_{dL}]_A, [\Delta_{dR}]_B), \quad (2.41)$$

⁹Here, we assumed the matrices are real for simplicity.

where

$$[\Delta_{d_L}]_A := \frac{\min \left(\left| [\mathcal{M}_d]_{A,6+\tilde{A}} \right|, \left| [\mathcal{M}_e]_{A,6+\tilde{A}} \right| \right)}{\max \left(\left| [\mathcal{M}_d]_{A,6+\tilde{A}} \right|, \left| [\mathcal{M}_e]_{A,6+\tilde{A}} \right| \right)}, \quad [\Delta_{d_R}]_B := \frac{\min \left(\left| [\mathcal{M}_d]_{6+B,\tilde{B}} \right|, \left| [\mathcal{M}_e]_{6+B,\tilde{B}} \right| \right)}{\max \left(\left| [\mathcal{M}_d]_{6+B,\tilde{B}} \right|, \left| [\mathcal{M}_e]_{6+B,\tilde{B}} \right| \right)}. \quad (2.42)$$

Here, $A, B = 1, 2, 3, \dots, 6$ and \tilde{A}, \tilde{B} are respectively residues of A, B divided by 3, so that it measures the degree of cancellations in the diagonal elements of the vectorlike masses. For instance, 10 % tuning is required if Δ_{FT} is 0.1.

3 Phenomenology

We study phenomenology in this setup. We have seen the way to suppress $K_L \rightarrow \mu e$. The suppression, however, may require severe fine-tuning. If the fine-tuning is relaxed, other flavor violating processes would become sizable. First of all, we discuss the possibility that the TeV-scale leptoquark explains the anomalies in the semi-leptonic B meson decays. Then, we investigate the other flavor violating processes paying attention to the degree of tuning.

3.1 Vector leptoquark explanation of the anomalies

Interestingly, the TeV-scale leptoquark may be able to explain all anomalies in the semi-leptonic B meson decays, $B \rightarrow K^{(*)} \mu \mu$ and $B \rightarrow D^{(*)} \tau \nu$. It has been pointed out in the literature that the vector leptoquark from the PS model can explain both anomalies simultaneously, but we show that the $b \rightarrow c \tau \nu$ anomaly is hardly solved in our model due to the correlation between the leptoquark and Z' boson masses¹⁰.

3.1.1 $b \rightarrow s \mu \mu$ anomaly

The $b \rightarrow s \mu \mu$ anomaly may be a signal of new physics. The effective Hamiltonian is given by

$$\mathcal{H}_{\text{eff}}^{b \rightarrow s \mu \mu} = -\frac{4G_F}{\sqrt{2}} \frac{\alpha}{4\pi} \sum_{a=9,10} (C_a \mathcal{O}_a + C'_a \mathcal{O}'_a), \quad (3.1)$$

where

$$\mathcal{O}_9 = (\bar{s} \gamma^\rho P_L b) (\bar{\mu} \gamma_\rho \mu), \quad \mathcal{O}_{10} = (\bar{s} \gamma^\rho P_L b) (\bar{\mu} \gamma_\rho \gamma_5 \mu), \quad (3.2)$$

$$\mathcal{O}'_9 = (\bar{s} \gamma^\rho P_R b) (\bar{\mu} \gamma_\rho \mu), \quad \mathcal{O}'_{10} = (\bar{s} \gamma^\rho P_R b) (\bar{\mu} \gamma_\rho \gamma_5 \mu). \quad (3.3)$$

¹⁰The correlation between leptoquark and Z' has been also studied in a more generic way [83].

The leptoquark contributions to the Wilson coefficients, C_9 and C_{10} , are given by

$$\begin{aligned}\Delta C_9 = -\Delta C_{10} &= -\frac{\sqrt{2}}{4G_F} \frac{4\pi}{\alpha} \frac{1}{V_{tb}^* V_{ts}} \frac{1}{2m_X^2} [\hat{g}_{d_L}^X]_{32}^* [\hat{g}_{d_L}^X]_{22} \\ &\sim -0.51 \times \left(\frac{5 \text{ TeV}}{m_X}\right)^2 \left(\frac{[\hat{g}_{d_L}^X]_{32}^* [\hat{g}_{d_L}^X]_{22}}{0.02}\right).\end{aligned}\quad (3.4)$$

The experimental results favor $-0.59 \lesssim \Delta C_9 \lesssim -0.41$ at 1σ level [84], and thus $m_X \sim \mathcal{O}(10 \text{ TeV})$ is a suitable size to explain the $b \rightarrow s\mu\mu$ anomaly. The Z' boson would contribute to the $b \rightarrow s\mu\mu$ anomaly, but the flavor violating effects from the Z' boson is expected to be very suppressed in our model as discussed in Appendix A.2.

With the parametrization of Eq. (2.39), the relevant couplings are given by

$$\begin{aligned}[\hat{g}_{d_L}^X]_{22} &= \frac{g_4}{\sqrt{2}} c_{\ell_L}^{23} (s_{Q_L}^{22} c_{\ell_L}^{22} - c_{Q_L}^{22} s_{\ell_L}^{22}), \\ [\hat{g}_{d_L}^X]_{32} &= \frac{g_4}{\sqrt{2}} \{s_{Q_L}^{23} c_{\ell_L}^{23} (c_{Q_L}^{22} c_{\ell_L}^{22} + s_{Q_L}^{22} s_{\ell_L}^{22}) - s_{\ell_L}^{23} c_{Q_L}^{23}\},\end{aligned}\quad (3.5)$$

if the angles only in $R_{Q_L}^{22}$, $R_{Q_L}^{23}$, $R_{\ell_L}^{22}$ and $R_{\ell_L}^{23}$ are turned on. We fix the angles at

$$s_{Q_L}^{23} = -s_{\ell_L}^{23} = \frac{1}{\sqrt{2}}, \quad s_{Q_L}^{22} = -s_{\ell_L}^{22} = 0.04 \times \frac{1}{\sqrt{2}},\quad (3.6)$$

so that the $b \rightarrow s\mu\mu$ anomaly is explained with $m_X \sim 5 \text{ TeV}$ and $|[\hat{g}_{d_L}^X]_{22}/[\hat{g}_{d_L}^X]_{23}| \sim 0.04$. As discussed in later, $[\hat{g}_{d_L}^X]_{22}$ should be small to suppress $K_L \rightarrow \mu e$. Note that this model, in general, predicts the leptoquark contributions to the other lepton flavors, as well as $C'_{9,10}$. In our analysis, we will consider the parameter space where these are negligibly small.

3.1.2 $b \rightarrow c\tau\nu$ anomaly

The effective Hamiltonian relevant to $b \rightarrow c\tau\nu$ within the our model is given by

$$\mathcal{H}_{\text{eff}}^{b \rightarrow c\tau\nu} = \frac{4G_F}{\sqrt{2}} V_{cb} C_{V_1} (\bar{c}\gamma^\mu P_L b) (\bar{\tau} P_L \nu_\tau).\quad (3.7)$$

The leptoquark contribution to the Wilson coefficients C_{V_1} is given by

$$\begin{aligned}\Delta C_{V_1} &= \frac{\sqrt{2}}{4G_F} \frac{1}{V_{cb}} \frac{1}{m_X^2} [\hat{g}_{d_L}^X]_{33}^* [\hat{g}_{u_L}^X]_{2\nu} \\ &\sim 0.092 \times \left(\frac{1.4 \text{ TeV}}{m_X}\right)^2 \left(\frac{[\hat{g}_{d_L}^X]_{33}^* [\hat{g}_{u_L}^X]_{2\nu}}{0.25}\right),\end{aligned}\quad (3.8)$$

where $[\hat{g}_{u_L}^X]_{2\nu} := \sum_{i=1,2,3} [\hat{g}_{u_L}^X]_{2i}$. The experimental results favor $0.052 \lesssim \Delta C_{V_1} \lesssim 0.124$ at 2σ level [85]. Note that $[\hat{g}_{d_L}^X]_{33}^* [\hat{g}_{d_L}^X]_{2\nu} \sim g_4^2/4 \sim 0.25$ is the maximal value as far as the $SU(4)_C$

gauge coupling constant is $g_4 \sim 1.0$ that is consistent with the strong coupling constant at the TeV scale [86]. Thus, $\Delta C_{V_1} \sim 0.09$ (0.057) could be explained if $m_X \sim 1.4$ (1.8) TeV.

The LHC result [87] searching for di-lepton resonance severely constraints a Z' boson mass if the Z' boson decays to a pair of electrons or muons. In our model, the Z' boson couples to the fermions in the similar way as the Z boson. Therefore the resonant production cross section via the Drell-Yan process can be large as long as Z' boson is light, and there are sizable branching fractions to di-leptons, as we see in Eq. (A.60) of Appendix A.2. If all the vectorlike fermions are heavier than the half of the Z' mass, the limit is about 5 TeV. The limit is relaxed to about 4.5 TeV if Z' boson can decay to vectorlike fermions, since the branching fractions to di-leptons are suppressed by $1/3$ ¹¹. From Eqs. (A.22) and (A.37) in Appendix A.2, the Z' boson mass is bounded by the leptoquark mass,

$$m_{Z'} < \sqrt{\frac{2g_R^2 + 3g_4^2}{g_4^2}} m_X \sim 3.5 \text{ TeV} \times \left(\frac{m_X}{1.8 \text{ TeV}} \right), \quad (3.9)$$

where the upper bound is saturated when $v_\Delta = 0$. Hence, the Z' boson is too light to be consistent with the current limit. Furthermore, the vectorlike fermions will have masses of $\mathcal{O}(v_\Delta)$ unless the Yukawa couplings are non-perturbatively large. The LHC limit on a single vectorlike quark is about 1.2 TeV when a vectorlike quark decays to a SM boson and a quark in the third generation [88]. Thus, the vector leptoquark explanation of the $b \rightarrow c\tau\nu$ anomaly is excluded by the Z' and vectorlike quark searches. We note that it would be possible that the $b \rightarrow c\tau\nu$ anomaly is explained in the scalar leptoquarks in PS models as studied in e.g. Ref. [89].

3.2 Flavor physics

We shall discuss the flavor physics induced by the leptoquark and the extra Higgs bosons when $m_X = 5$ TeV and the sizable leptoquark couplings are given by Eqs. (3.5) and (3.6), so that the $b \rightarrow s\mu\mu$ anomaly is explained. The formulas and values of constants used in our numerical analysis are shown in Appendix B.

In this paper, we study our predictions at the tree level in flavor physics, except for $\mu \rightarrow e\gamma$. We do not include tree-level contributions of the $SU(4)_C$ adjoint Δ and $SU(2)_R$ triplet Σ . As shown in Appendix A.3, the adjoint Δ does not couple to two SM fermions up to $\mathcal{O}(v_H/v_\Delta)$. Hence tree-level processes induced by those scalars are very suppressed. The loop effects would be as large as those from the leptoquark if the Yukawa couplings are $\mathcal{O}(1)$. The loop corrections involving both scalars and leptoquark possibly enhance flavor violating processes, such as $K_L \rightarrow \mu e$, even if all $s_{F_X}^{ij}$ are vanishing. This study is work in progress and will be shown near future. For Σ , it is shown that the scalar leptoquarks from it can explain both $b \rightarrow s\mu\mu$ and $b \rightarrow c\tau\nu$ anomalies [89] as well as inducing various flavor violations if the corresponding Yukawa couplings have a certain structure. The phenomenology of those scalar fields are interesting subject, but this is beyond the scope of this paper. We simply assume that v_Δ is so large that the corresponding Yukawa couplings are negligible and the Yukawa coupling $h \propto \mathbf{1}_3$, and thus we expect that flavor violating effects from those scalar fields are negligibly small.

¹¹The larger decay width will also relax the limit.

3.2.1 μ - e flavor violation versus fine-tuning

As discussed in Sec. 2.2, the flavor violating decay of K meson, $K_L \rightarrow \mu e$, gives the most stringent bound to the leptoquark mass if it is coupled to the first generation fermions. The branching fraction is approximately given by

$$\begin{aligned} \text{BR}(K_L \rightarrow \mu e) &\sim \frac{\tau_{K_L}}{128\pi m_X^4} \frac{m_K^5 f_K^2}{m_s^2} \left(1 - \frac{m_\mu^2}{m_K^2}\right)^2 \left| [\hat{g}_{d_L}^X]_{22} [\hat{g}_{d_R}^X]_{11} \right|^2 \\ &\sim 2.3 \times 10^{-12} \times \left(\frac{5 \text{ TeV}}{m_X}\right)^4 \left(\frac{\left| [\hat{g}_{d_L}^X]_{22} [\hat{g}_{d_R}^X]_{11} \right|}{10^{-5}}\right)^2. \end{aligned} \quad (3.10)$$

Here we assume that $[\hat{g}_{d_L}^X]_{22}$ is much larger than the other couplings except for those involving the third generation. The experimental upper bound on the branching ratio is 4.7×10^{-12} [90].

The leptoquark coupling will be also strongly constrained by the measurements of the μ - e conversion for an aluminum (gold) target in the future (current) experiments. The conversion per capture rate for an aluminum target is approximately given by

$$\begin{aligned} \text{BR}(\mu \rightarrow e)^{\text{Al}} &\sim \frac{16m_\mu^5 S_p^2 m_p^2}{m_X^4 \Gamma_{\text{capt}}} \left| \frac{f_{S_p}^s}{m_s} [\hat{g}_{d_R}]_{21}^* [\hat{g}_{d_L}]_{22} + \frac{2}{27} \frac{f_G^p}{m_b} [\hat{g}_{d_R}]_{31}^* [\hat{g}_{d_L}]_{32} \right|^2 \\ &\sim 1.5 \times 10^{-14} \times \left(\frac{5 \text{ TeV}}{m_X}\right)^2 \left| 0.45 \left(\frac{[\hat{g}_{d_R}]_{21}^* [\hat{g}_{d_L}]_{22}}{10^{-5}}\right) + 0.016 \left(\frac{[\hat{g}_{d_R}]_{31}^* [\hat{g}_{d_L}]_{32}}{10^{-5}}\right) \right|^2, \end{aligned} \quad (3.11)$$

where the mass and form factors for the neutron are set to be those for the proton for simplicity in the second line. This rate is the same order of magnitude for the gold target. The future (current) limit on the conversion rate per capture rate is [91–94]

$$\text{BR}(\mu \rightarrow e)^{\text{Al(Au)}} = \frac{\Gamma_{\text{conv}}}{\Gamma_{\text{capt}}} < 6 \times 10^{-17} \quad (7 \times 10^{-13}). \quad (3.12)$$

We note that even if the $K_L \rightarrow \mu e$ is sufficiently suppressed, the μ - e conversion rate can be larger than the future sensitivity because of the contribution from the other coupling parameters.

There may be constraints from $\mu \rightarrow e\gamma$ induced by the loop effects mediated by the leptoquarks and vectorlike down quarks. The branching fraction is given by [95],

$$\text{BR}(\mu \rightarrow e\gamma) = \tau_\mu \frac{\alpha_e m_\mu^3}{1024\pi^4 m_X^4} \left(|C_L^{\mu e}|^2 + |C_R^{\mu e}|^2 \right), \quad (3.13)$$

where τ_μ denotes the muon lifetime and

$$C_L^{\mu e} = \sum_{A=1}^9 \left[m_\mu [\hat{g}_{d_L}^X]_{A1}^* [\hat{g}_{d_L}^X]_{A2} F\left(\frac{m_{d_A}^2}{m_X^2}\right) + m_{d_A} [\hat{g}_{d_L}^X]_{A1}^* [\hat{g}_{d_R}^X]_{A2} G\left(\frac{m_{d_A}^2}{m_X^2}\right) \right]. \quad (3.14)$$

$C_R^{\mu e}$ is obtained by formally replacing $L \leftrightarrow R$. The loop functions are defined as

$$F(t) = -\frac{4 - 16t + 39t^2 - 28t^3 + t^4 + 6t^2(1 + 2t) \log t}{4(t - 1)^4}, \quad (3.15)$$

$$G(t) = \frac{-4 + 27t - 24t^2 + t^3 + 6t(1 + 2t) \log t}{2(t - 1)^3}. \quad (3.16)$$

The second term will be the dominant due to the chiral enhancement by the Yukawa coupling with Higgs bosons if $\delta_d \leq \mathcal{O}(v_H)$ in Eq. (2.24) is larger than the muon mass. Since the muon couples to one vectorlike down quark with $\mathcal{O}(1)$ mixing, the branching fraction is estimated as

$$\text{BR}(\mu \rightarrow e\gamma) \sim 1.2 \times 10^{-13} \times \left(\frac{5.0 \text{ TeV}}{m_X}\right)^4 \left(\frac{g_L^X g_R^X}{0.005}\right)^2 \left(\frac{\delta_d}{100 \text{ MeV}}\right)^2, \quad (3.17)$$

where $g_{L(R)}^X$ is a typical size of leptoquark couplings to mu/electron in the left (right)-current. Thus the Higgs boson couplings with the vectorlike down-type fermions should be so suppressed that the current limit $\text{BR}(\mu \rightarrow e\gamma) < 4.2 \times 10^{-13}$ [96] is satisfied. This process can probe different parameter space from the $K_L \rightarrow \mu e$ decay and μ - e conversion which are induced at the tree-level, since it directly constrains the leptoquark couplings to the SM charged leptons and vectorlike quarks. We will see that there are parameter spaces that can be probed only by $\mu \rightarrow e\gamma$ even if $\delta_d = 10^{-4}v_H$ and the chiral enhancement effect is suppressed.

With the severe constraint from $\mu \rightarrow e\gamma$, the muon anomalous magnetic moment $\Delta a_\mu \sim \mathcal{O}(10^{-9})$ is difficult to be explained by the 1-loop effects of the leptoquark and vectorlike quark. It is roughly estimated as

$$\Delta a_\mu \lesssim \frac{m_\mu \delta_d}{16\pi^2 m_X^2} N_c N_{\text{VL}} \sim 5 \times 10^{-11} \times \left(\frac{5 \text{ TeV}}{m_X}\right)^2 \left(\frac{\delta_d}{100 \text{ MeV}}\right), \quad (3.18)$$

where $N_c = 3$ and $N_{\text{VL}} = 6$. Thus it is, at least, two orders of magnitude smaller than the currently preferred value as far as $\delta_d \lesssim m_\mu$ to suppress $\mu \rightarrow e\gamma$.

In our model, the stringent constraints on the μ - e flavor violation can be avoided due to the texture of Eq. (2.23) which is achieved by tuning the vectorlike mass terms such that there are cancellations between the mass parameters and the adjoint VEV $\langle \Delta \rangle$, see Eq. (2.8). To quantify how accurately this cancellation should be hold, we turn on the angles universally except for those relevant to the $b \rightarrow s\mu\mu$ anomaly,

$$s_{Q_L} := s_{q_L}^{\hat{i}\hat{j}}, \quad s_{Q_R} := s_{q_R}^{ij}, \quad s_{\ell_R} := s_{\ell_L}^{\hat{i}\hat{j}}, \quad s_{\ell_R} := s_{\ell_R}^{ij}. \quad (3.19)$$

where $i, j = 1, 2, 3$ run over all the combinations and $\hat{i}, \hat{j} = 1, 2, 3$ also run over all the combinations except $(\hat{i}, \hat{j}) = (2, 2), (2, 3)$, to keep ΔC_9 unchanged approximately. In our numerical analysis, we set $\delta_u = \delta_d = 10^{-4}$, so that the chiral enhancement effect to $\mu \rightarrow e\gamma$ is negligible and obtain conservative limits.

Figure 1 shows the degree of tuning Δ_{FT} and constraints from the μ - e violations on the $(s_Q + s_\ell)$ vs $(s_Q - s_\ell)$ plane, where

$$s_Q := s_{Q_L} = s_{Q_R} \quad s_\ell := s_{\ell_L} = s_{\ell_R}. \quad (3.20)$$

The density plot shows Δ_{FT}^{-1} . The gray (blue) region is excluded by the current limit on $\text{BR}(K_L \rightarrow \mu e)$ ($\text{BR}(\mu \rightarrow e\gamma)$). The blue lines are the future sensitivity of $\text{BR}(\mu \rightarrow e\gamma) = 6 \times 10^{-14}$ at the MEG experiment [97]. The green lines show $\text{BR}(\mu \rightarrow e)^{\text{Al}}$ and it is below the future sensitivity of $\text{BR}(\mu \rightarrow e)^{\text{Al}} = 6 \times 10^{-17}$ [93] between the solid green lines. There is no region excluded by

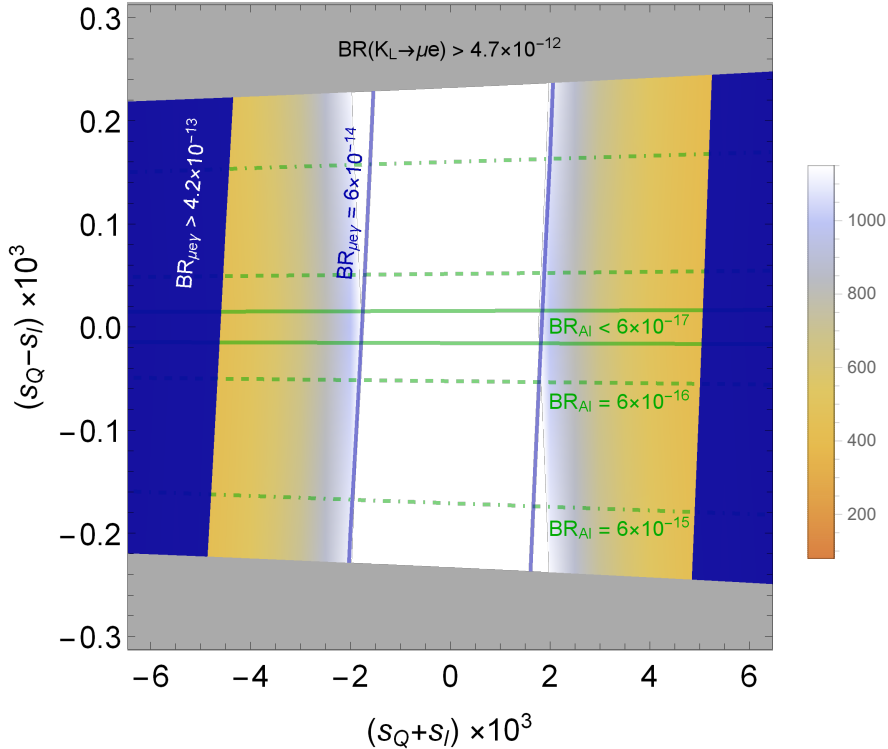


Figure 1: The degree of tuning Δ_{FT}^{-1} , constraints and values of the μ - e violation observables. See the text for details.

the current limit on $\text{BR}(\mu \rightarrow e)^{\text{Au}}$ [91]. Since the leptoquark couplings to the SM fermions are induced by $|s_Q - s_\ell|$, the tree-level μ - e violations are enhanced in the upper and lower regions. On the other hand, $\text{BR}(\mu \rightarrow e\gamma)$ is enhanced as $|s_Q + s_\ell|$ increases since it comes from the coupling with the vectorlike quarks. The limit from $\text{BR}(\mu \rightarrow e\gamma)$ will be tightened if δ_d is larger. Note that the $b \rightarrow s\mu\mu$ anomaly is explained in the whole region in this plot.

The degree of tuning $\Delta_{\text{FT}}^{-1} \gtrsim 500$ (1000) at $|s_Q + s_\ell| \gtrsim 0.005$ (0.002). One may concern about the tuning between s_Q and s_ℓ , but the cancellation is mild since $(s_Q - s_\ell)/(s_Q + s_\ell) \gtrsim \mathcal{O}(0.01)$ even if $\text{BR}(\mu \rightarrow e)^{\text{Al}} < 6 \times 10^{-17}$. Therefore, we conclude that the degree of tuning to explain the $b \rightarrow s\mu\mu$ anomaly consistently with the current limit is $\Delta_{\text{FT}}^{-1} \sim 500$ which corresponds to $\mathcal{O}(0.2\%)$ tuning. Most of the parameter space, outside of the two green solid lines, will be tested by the future experiments of the μ - e conversion.

Figure 2 shows the same plot as Fig. 1, but on (s_L, s_R) plane, where

$$s_L := s_{Q_L} = -s_{\ell_L}/1.1, \quad s_R := s_{Q_R} = -s_{\ell_R}/1.1. \quad (3.21)$$

We keep $s_{Q_L} \sim s_{\ell_L}$ and $s_{Q_R} \sim s_{\ell_R}$ to avoid the large μ - e violation. The tree-level μ - e flavor violations are sensitive to s_R , since $[\hat{g}_{d_L}^X]_{s\mu}$ is sizable to explain the $b \rightarrow s\mu\mu$ anomaly. The future measurement of the $\mu \rightarrow e$ conversion will cover $\Delta_{\text{FT}}^{-1} \lesssim 3000$ in the case of Eq. (3.21). The radiative decay, $\mu \rightarrow e\gamma$ is equally sensitive to s_L and s_R , and the region surrounded by the blue line will be covered by the MEG experiment.

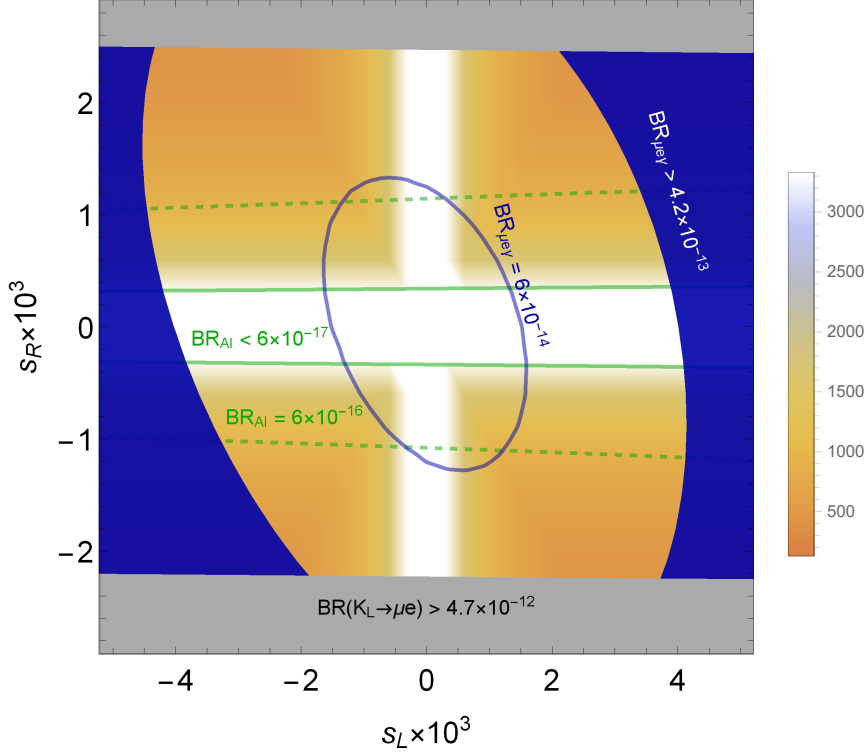


Figure 2: The same plot as Fig. 1 on (s_L, s_R) plane.

3.2.2 Flavor violation via Higgs bosons

This model predicts sizable tree-level flavor violating couplings involving Higgs bosons as well. Even in the canonical limit, the heavy Higgs boson couplings to the down-type SM quarks are given by

$$\begin{aligned} [\hat{Y}_d^H]_{ij} &\sim -i [\hat{Y}_d^A]_{ij} \sim \frac{1}{\sqrt{2}} [\hat{Y}_d^{H^+}]_{ij} \\ &\sim -\frac{1}{\sqrt{2}v_H} \left(\frac{2 \tan \beta}{1 - \tan^2 \beta} [D_d]_{ij} + \frac{1 + \tan^2 \beta}{1 - \tan^2 \beta} [V_{\text{CKM}}^\dagger D_u]_{ij} \right), \end{aligned} \quad (3.22)$$

where $i, j = 1, 2, 3$. Here we take the decoupling limit of the Higgs bosons¹². In this limit, all the scalar masses of the heavy Higgs doublet are degenerate. The second term in the parenthesis inevitably induces flavor violations whose typical values are estimated as

$$v_H^{-1} |V_{\text{CKM}}^\dagger D_u| \sim \begin{pmatrix} 5 \times 10^{-5} & 0.0006 & 0.007 \\ 1 \times 10^{-6} & 0.003 & 0.03 \\ 2 \times 10^{-8} & 0.0001 & 0.78 \end{pmatrix}. \quad (3.23)$$

¹²See Appendix A.3 for more details of the Higgs couplings.

As we see, flavor violating couplings, that are off-diagonal elements, are sizable and hence flavor violating processes will be large if the Higgs bosons are light, although the chirality structure may suppress them because only the upper-right elements are sizable.

In the charged lepton sector, similarly, there are flavor violations, that are estimated as $U_{\text{PMNS}} D_n / v_H$. The effects are, however, expected to be negligible because the Yukawa coupling to the neutrinos is estimated as $D_n / v_H \sim \mathcal{O}(10^{-5})$ to explain the neutrino masses with the $\mathcal{O}(10 \text{ TeV})$ Majorana masses. Therefore the neutral meson mixing is the most sensitive process to the flavor violation via the Higgs bosons. The effective interactions relevant to our model are given by ¹³

$$\mathcal{H}_{\text{eff}}^{\Delta F=2} = \sum_{I,A} C_I^A Q_I^A, \quad (3.24)$$

where $(I, A) = (1, \text{VLL}), (2, \text{LR}), (1, \text{SLL}), (1, \text{SRR})$. The four-Fermi operators are defined as

$$Q_1^{\text{VLL}} = (\bar{F}^a \gamma_\mu P_L f^a) (\bar{F}^b \gamma^\mu P_L f^b), \quad Q_2^{\text{LR}} = (\bar{F}^a P_L f^a) (\bar{F}^b P_R f^b), \quad (3.25)$$

$$Q_1^{\text{SLL}} = (\bar{F}^a P_L f^a) (\bar{F}^b P_L f^b), \quad Q_1^{\text{SRR}} = (\bar{F}^a P_R f^a) (\bar{F}^b P_R f^b), \quad (3.26)$$

where $a, b = 1, 2, 3$ are the color indices. Here, $(F, f) = (s, d), (b, d), (b, s)$ for $K-\bar{K}$, $B_d-\bar{B}_d$ and $B_s-\bar{B}_s$ mixing, respectively. We define the ratios of off-diagonal matrix element of our model to that of the SM as

$$C_M := \frac{\langle M | \mathcal{H}_{\text{eff}}^{\Delta F=2} | \bar{M} \rangle}{\langle M | \mathcal{H}_{\text{eff}}^{\text{SM}} | \bar{M} \rangle} = \frac{C_{\text{SM}}^M \mathcal{O}_1^{\text{VLL}} + C_2^{\text{LR}} \mathcal{O}_2^{\text{LR}} + (C_1^{\text{SLL}} + C_1^{\text{SRR}}) \mathcal{O}_1^{\text{SLL}}}{C_{\text{SM}}^M \mathcal{O}_1^{\text{VLL}}}. \quad (3.27)$$

Here, $\mathcal{O}_I^A := \langle M | Q_I^A | \bar{M} \rangle / (2m_M)$ with m_M is the meson mass. We use the values of \mathcal{O}_I^A shown in Ref. [58]. The SM contribution C_{SM}^M is shown in e.g. Ref. [99]. In our model, the Wilson coefficients are given by

$$C_2^{\text{LR}} = - \sum_{S=h,H,A} \frac{y_L^S y_R^S}{2m_S^2}, \quad C_1^{\text{SLL}} = - \sum_{S=h,H,A} \frac{y_L^S y_L^S}{2m_S^2}, \quad C_1^{\text{SRR}} = - \sum_{S=h,H,A} \frac{y_R^S y_R^S}{2m_S^2}, \quad (3.28)$$

where

$$y_L^S = [\hat{Y}_d^S]_{ji}^*, \quad y_R^S = [\hat{Y}_d^S]_{ij}, \quad (3.29)$$

with $(i, j) = (2, 1), (3, 1), (3, 2)$ for $M = K, B_d, B_s$, respectively. The flavor violation from the adjoint field is negligible as discussed in Appendix A.3. We neglect loop corrections from the leptoquarks in our analysis. The current constraints at 95% C.L. given by the UT-Fit [100, 101] are

$$0.87 \leq \text{Im } C_K \leq 1.39, \quad 0.83 \leq |C_{B_d}| \leq 1.29, \quad 0.942 \leq |C_{B_s}| \leq 1.288. \quad (3.30)$$

¹³We use the basis of the operators used in e.g. Ref. [98].

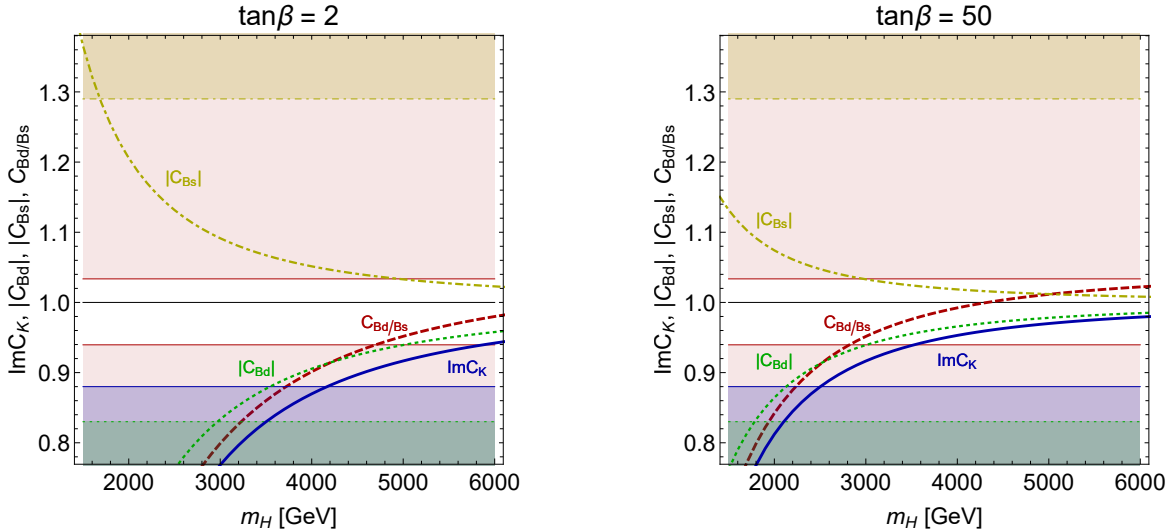


Figure 3: The limits on the heavy Higgs boson mass m_H from the observables concerned with the neutral meson mixings: $|C_{B_d}|$ (green), $|C_{B_s}|$ (yellow), C_{B_d/B_s} (red) and $\text{Im} C_K$ (blue). The excluded region for each observable is colored in the same color as the corresponding line. $\tan \beta$ is fixed at $\tan \beta = 2.0$ (50) in the left (right) panel.

As pointed out in Ref. [102], the uncertainties are reduced in the ratio of mass differences of the B_d and B_s meson mixing,

$$\frac{\Delta M_d}{\Delta M_s} = 0.0298^{+0.0005}_{-0.0009}. \quad (3.31)$$

We define the parameter,

$$C_{B_d/B_s} := \frac{1}{0.0298} \times \left| \frac{\langle B_d | \mathcal{H}_{\text{eff}}^{\Delta F=2} | \bar{B}_d \rangle}{\langle B_s | \mathcal{H}_{\text{eff}}^{\Delta F=2} | \bar{B}_s \rangle} \right|. \quad (3.32)$$

Figure 3 shows experimental limits from the neutral meson mixing on the heavy Higgs boson mass for $\tan \beta = 2.0$ (50) on the left (right) panel. Our predictions for $|C_{B_d}|$, $|C_{B_s}|$, C_{B_d/B_s} and $\text{Im} C_K$ are depicted by the green, yellow, red, and blue lines, respectively. The excluded region for each observable is colored in the same color as the corresponding line. In the red regions, the deviation of C_{B_d/B_s} from the central value is more than twice as large as the uncertainties. In this figure, our parameters satisfy $s_Q + s_\ell = 0.0015$ and $s_Q - s_\ell = 0.6 \times 10^{-5}$ that can not be probed by looking for the μ - e flavor violations. The limits for the cases with larger angles s_Q , s_ℓ are quite similar to this result because the dominant effect comes from Eq. (3.22) which is independent of the angles, although there are mild dependence on them. We see that C_{B_d/B_s} gives the most stringent limits for both $\tan \beta = 2$ and 50. Interestingly, the bound from C_{B_d/B_s} is stronger than the others, since the uncertainty is small and our predictions of $|C_{B_s}|$ and $|C_{B_d}|$ move in the opposite directions. The limits from the phases of $C_{B_{d,s}}$ are weaker than those from the absolute values. The lower bound on the heavy Higgs boson mass is about 4.8 (2.8) TeV for $\tan \beta = 2.0$ (50). The limit is stronger for smaller $\tan \beta$ since the up-type Yukawa coupling constants are enhanced, see Eq. (3.22).

3.3 $n - \bar{n}$ oscillation

Before closing this section, let us discuss neutron anti-neutron ($n-\bar{n}$) oscillation. In general, gauge unified models predict baryon number violating processes, such as proton decays and $n-\bar{n}$ oscillation, that provide a useful tool to test the unification models. In the PS unification, the gauge bosons from the PS symmetry breaking do not mediate the baryon number violating processes, since their interactions respect the $B - L$ and $B + L$ symmetries. However, the scalars responsible for the PS symmetry breaking can generate the baryon number violation, depending on the representations. Since the PS breaking scale is relatively low in our model, the baryon number violation induced by such scalars may provide a stringent constraint.

In our model, three (non-singlet) scalar fields, namely $\Phi : (\mathbf{1}, \mathbf{2}, \mathbf{2})$, $\Delta : (\mathbf{15}, \mathbf{1}, \mathbf{1})$ and $\Sigma : (\overline{\mathbf{10}}, \mathbf{1}, \mathbf{3})$, are introduced. With these representations, the stability of proton is ensured even after the PS symmetry breaking because of the discrete symmetry under the following transformation [103],

$$\Sigma_{ab} \rightarrow e^{-2i\pi/3} \Sigma_{ab}, \quad \Sigma_{a1} \rightarrow e^{-i\pi/3} \Sigma_{a1}, \quad \Sigma_{11} \rightarrow \Sigma_{11}, \quad (3.33)$$

$$\mathbf{u}_{L,R} \rightarrow e^{i\pi/3} \mathbf{u}_{L,R}, \quad \mathbf{d}_{L,R} \rightarrow e^{i\pi/3} \mathbf{d}_{L,R}, \quad (3.34)$$

where $a, b = 2, 3, 4$ are the color indices. Since this symmetry does not protect processes that change the baryon number by an even integer, the $n-\bar{n}$ oscillation can occur in our model. In what follows, we shall estimate the transition amplitude and discuss the compatibility with the TeV-scale leptoquark scenario.

Of three scalars in our model, only the symmetric representation scalar Σ breaks the baryon number symmetry when it develops the VEV, and hence contributes to the $n - \bar{n}$ transition. The transition requires three $\Sigma \bar{f}_R^c h f_R$ vertices, the VEV of Σ and the following quartic coupling of Σ ,

$$V_{n-\bar{n}} = \lambda_\Sigma \left[\text{Tr} (\Sigma_{\alpha\zeta} \Sigma_{\beta\eta}) \text{Tr} (\Sigma_{\gamma\kappa} \Sigma_{\delta\lambda}) \epsilon^{\alpha\beta\gamma\delta} \epsilon^{\zeta\eta\kappa\lambda} + h.c. \right], \quad (3.35)$$

where $\alpha, \beta, \dots, \lambda = 1, 2, 3, 4$ are the $SU(4)_C$ indices and the trace is for the $SU(2)_R$ indices. After the PS symmetry breaking, the interactions relevant to the $n - \bar{n}$ oscillation are given by

$$V_{n-\bar{n}} \supset 2\lambda_\Sigma v_\Sigma \epsilon^{abc} \epsilon^{def} \Sigma_{ad}^{2/3} \left(\Sigma_{be}^{-1/3} \Sigma_{cf}^{-1/3} + 2\Sigma_{be}^{2/3} \Sigma_{cf}^{-4/3} \right) + h.c., \quad (3.36)$$

where $a, b, \dots, f = 1, 2, 3$ are the $SU(3)_c$ indices and we denote the scalars of symmetric representation under $SU(3)_c$ as $\Sigma^Y : (\overline{\mathbf{6}}, \mathbf{1}, Y)$, with $Y = -4/3, -1/3, 2/3$, under G_{SM} . Their masses are denoted by m_{Σ^Y} . Integrating out these heavy scalars induces six-quark operators,

$$\mathcal{L}_{\text{eff}}^{n-\bar{n}} = -\lambda_\Sigma v_\Sigma \epsilon^{abc} \epsilon^{def} \left[\frac{h_{dd}^2 h_{uu}}{m_{\Sigma^{-4/3}}^4 m_{\Sigma^{2/3}}^2} (\bar{d}_{R,a}^c d_{R,d}) (\bar{d}_{R,b}^c d_{R,e}) (\bar{u}_{R,c}^c u_{R,f}) \right. \\ \left. - 2 \frac{h_{dd} h_{ud}^2}{m_{\Sigma^{-4/3}}^2 m_{\Sigma^{-1/3}}^4} (\bar{d}_{R,a}^c d_{R,d}) (\bar{d}_{R,b}^c u_{R,e}) (\bar{u}_{R,c}^c d_{R,f}) \right], \quad (3.37)$$

where $h_{qq'}$ ($q, q' = u, d$) is the Yukawa coupling of Σ to q and q' quarks in the mass basis, given by

$$h_{qq'} = \sum_{i,j=1,2,3} \frac{1}{\sqrt{2}} [h]_{ij} [U_R^q]_{3+i,1} [U_R^{q'}]_{3+j,1}. \quad (3.38)$$

Assuming, for simplicity,

$$m_\Sigma := m_{\Sigma^{-4/3}} = m_{\Sigma^{2/3}} = m_{\Sigma^{-1/3}}, \quad h_Q := h_{uu} = h_{dd} = h_{ud}. \quad (3.39)$$

The Yukawa coupling of the SM quarks to Σ is estimated to be $h_Q \sim s_Q^2$ when the Yukawa coupling in the gauge basis $h \sim \mathcal{O}(1)$, and hence it is suppressed by the mixing between the chiral and vectorlike quarks which is at most 0.005 as read from Fig. 1. With the naive dimensional analysis [104], we find the transition amplitude to be

$$\begin{aligned} \tau_{n-\bar{n}} &\sim \frac{m_\Sigma^6}{\lambda_\Sigma v_\Sigma h_Q^3 \Lambda_{\text{QCD}}^6} \quad (3.40) \\ &\sim 1.2 \times 10^{14} \text{ sec} \times \left(\frac{m_\Sigma}{10 \text{ TeV}}\right)^6 \left(\frac{10 \text{ TeV}}{v_\Sigma}\right) \left(\frac{180 \text{ MeV}}{\Lambda_{\text{QCD}}}\right)^6 \left(\frac{0.005}{s_Q}\right)^6 \left(\frac{1.0}{h}\right)^3 \left(\frac{0.1}{\lambda_\Sigma}\right). \end{aligned}$$

Here, Λ_{QCD} denotes the QCD scale. It follows that the $n - \bar{n}$ transition is very sensitive to the Σ mass. The current limit is

$$\tau_{n-\bar{n}} \geq \begin{cases} 2.7 \times 10^8 \text{ sec} & \text{bound neutron [105]} \\ 8.6 \times 10^7 \text{ sec} & \text{reactor free neutron [104]} \end{cases} \quad (3.41)$$

Therefore, the constraint from the $n - \bar{n}$ oscillation can be avoided even if the relevant couplings, h and λ_Σ , are of order unity.

4 Summary

In this paper, we have proposed an explicit model with the PS gauge symmetry and extra vectorlike fermions that realizes

- a vector leptoquark which accounts for the $b \rightarrow s\mu\mu$ anomaly
- the realistic mass spectrum of the SM fermions
- sufficiently suppressed μ - e flavor violations due to tuning of the parameters.

The texture in Eq. (2.23) of the vectorlike fermion masses is a key idea to suppress the μ - e flavor violation, especially $K_L \rightarrow \mu e$ decay. We have showed in Fig. 1 that $\text{BR}(K_L \rightarrow e\mu)$ is less than the current limit if we adopt the $\mathcal{O}(0.2\%)$ tuning of the parameters. With this texture, the TeV-scale vector leptoquark is allowed and thus the $b \rightarrow s\mu\mu$ anomaly can be explained. We have, on the other hand, pointed out that the combination of the Z' boson and vectorlike quark searches exclude the light leptoquark to explain the $b \rightarrow c\tau\nu$ anomaly.

The idea to relax the bound from $K_L \rightarrow \mu e$ by introducing vectorlike families was proposed in Ref. [19]. In this paper, we have shown an explicit texture of the mass matrices to suppress the $K_L \rightarrow \mu e$ together with the SM fermion mass and mixing matrices. By this explicit construction, we found that the $b \rightarrow c\tau\nu$ anomaly is difficult to be explained, the $\mathcal{O}(0.1)\%$ tuning is required

to satisfy the phenomenological conditions for the $\mathcal{O}(1)$ TeV leptoquark, and the flavor violating couplings of the heavy Higgs boson are unavoidable.

On top of these, we conclude that the available parameter space to explain the $b \rightarrow s\mu\mu$ anomaly is probed by future searches for $\mu \rightarrow e\gamma$ and $\mu\text{Al} \rightarrow e\text{Al}$ processes. The former process is sensitive to the couplings with the SM leptons and vectorlike quarks, while the later is sensitive to the SM leptons and SM down quarks. The future experiments cover the parameter space that satisfies $|s_Q + s_\ell| \gtrsim 0.002$ and $|s_Q - s_\ell| \gtrsim 3.0 \times 10^{-5}$. We have also found the fact that the flavor violating couplings of the extra Higgs bosons are inevitable. It is shown in Fig. 3 that the heavy Higgs bosons lighter than 4.8 (2.8) TeV are excluded by the measurement of B meson mixing when $\tan\beta = 2$ (50). In our model, the neutron oscillation is also predicted by the couplings involving Σ . We estimate the transition amplitude and conclude that our prediction is much below the current experimental bound.

Before closing our discussion, let us comment on loop corrections to the flavor violating processes, e.g. $K_L \rightarrow \mu e$. In our setup, the tree-level contributions via Δ and leptoquark exchanging are very suppressed because of the unique structure in the fermion mass matrices. This setup leads almost flavor-diagonal couplings, and we concentrate on the tree-level predictions induced by leptoquark exchanging. However, the leptoquark and scalar couplings between quarks/leptons and heavy fermions could be sizable. The one-loop corrections involving heavy fermions and scalars may be large in the TeV-scale scenario. The study on the loop effect is not so simple because of many parameters. We need more careful study, taking into account the mass spectrum of all fermions as well. This study is work in progress and will be shown near future.

Acknowledgment

S. I. would like to thank the warm hospitality at KEK where he stayed during the work. The work of S. I. is supported by the Japan Society for the Promotion of Science (JSPS) Research Fellowships for Young Scientists, No. 19J10980 and the JSPS Core-to-Core Program, No. JPJSCCA20200002. The work of J.K. is supported in part by the Institute for Basic Science (IBS-R018-D1), the Department of Energy (DOE) under Award No. DE-SC0011726, and the Grant-in-Aid for Scientific Research from the Ministry of Education, Science, Sports and Culture (MEXT), Japan No. 18K13534. S. O. is supported in part by NSERC, Canada. The work of Y. O. is supported by Grant-in-Aid for Scientific research from the MEXT, Japan, No. 19H04614, No. 19H05101, and No. 19K03867.

A Model details

A.1 Diagonalization of the fermion mass matrices

A.1.1 Dirac mass matrix

Let us discuss the fermion mass matrices parametrized as in Eq. (2.24). The unitary matrices

$$U_{\ell_L}^0 = \begin{pmatrix} 0_{6 \times 3} & V_{\ell_L} \\ W_{\ell_L} & 0_{3 \times 6} \end{pmatrix}, \quad U_{\ell_R}^0 = \begin{pmatrix} V_{\ell_R} & 0_{6 \times 3} \\ 0_{3 \times 6} & W_{\ell_R} \end{pmatrix}, \quad U_{Q_L}^0 = \begin{pmatrix} V_{Q_L} & 0_{6 \times 3} \\ 0_{3 \times 6} & W_{Q_L} \end{pmatrix}, \quad U_{Q_R}^0 = \begin{pmatrix} 0_{6 \times 3} & V_{Q_R} \\ W_{Q_R} & 0_{3 \times 6} \end{pmatrix}, \quad (\text{A.1})$$

approximately diagonalize the mass matrices as

$$(U_{\ell_L}^0)^\dagger \mathcal{M}_e U_{\ell_R}^0 = \begin{pmatrix} D_{\ell_R} & 0_3 & \cdot \\ \cdot & d_e & 0_3 \\ \cdot & \cdot & D_{\ell_L} \end{pmatrix}, \quad (U_{Q_L}^0)^\dagger \mathcal{M}_d U_{Q_R}^0 = \begin{pmatrix} D_{Q_L} & \cdot & \cdot \\ 0_3 & d_d & \cdot \\ \cdot & 0_3 & D_{Q_R} \end{pmatrix}, \quad (\text{A.2})$$

$$(U_{\ell_L}^0)^\dagger \mathcal{M}_n U_{\ell_R}^0 = \begin{pmatrix} D_{\ell_R} & 0_3 & \cdot \\ \cdot & m_n & 0_3 \\ \cdot & \cdot & D_{\ell_L} \end{pmatrix}, \quad (U_{Q_L}^0)^\dagger \mathcal{M}_u U_{Q_R}^0 = \begin{pmatrix} D_{Q_L} & \cdot & \cdot \\ 0_3 & m_u & \cdot \\ \cdot & 0_3 & D_{Q_R} \end{pmatrix}, \quad (\text{A.3})$$

where \cdot represents $\mathcal{O}(v_H)$ entries. Here, d_e and d_d are chosen to be diagonal by using the redundancies of Eq.(2.27) in $V_{\ell_{L,R}}$ and $V_{Q_{L,R}}$. To make the singular values in increasing order and the SM up-type quark and neutrino masses, M_u and M_n , diagonalized, we introduce

$$\tilde{U}_{e_{L,R}} := U_{\ell_{L,R}}^0 \begin{pmatrix} 0_3 & \mathbf{1}_3 & 0_3 \\ \mathbf{1}_3 & 0_3 & 0_3 \\ 0_3 & 0_3 & \mathbf{1}_3 \end{pmatrix}, \quad \tilde{U}_{n_{L,R}} := U_{\ell_{L,R}}^0 \begin{pmatrix} 0_3 & \mathbf{1}_3 & 0_3 \\ u_{n_{L,R}} & 0_3 & 0_3 \\ 0_3 & 0_3 & \mathbf{1}_3 \end{pmatrix}, \quad (\text{A.4})$$

$$\tilde{U}_{d_{L,R}} := U_{Q_{L,R}}^0 \begin{pmatrix} 0_3 & \mathbf{1}_3 & 0_3 \\ \mathbf{1}_3 & 0_3 & 0_3 \\ 0_3 & 0_3 & \mathbf{1}_3 \end{pmatrix}, \quad \tilde{U}_{u_{L,R}} := U_{Q_{L,R}}^0 \begin{pmatrix} 0_3 & \mathbf{1}_3 & 0_3 \\ u_{u_{L,R}} & 0_3 & 0_3 \\ 0_3 & 0_3 & \mathbf{1}_3 \end{pmatrix}, \quad (\text{A.5})$$

where the unitary matrices $u_{u_{L,R}}$ and $u_{n_{L,R}}$ diagonalize m_u and m_n respectively,

$$u_{n_L}^\dagger m_n u_{n_R} = d_n, \quad u_{u_L}^\dagger m_u u_{u_R} = d_u. \quad (\text{A.6})$$

The Dirac mass matrices are diagonalized as

$$\begin{aligned} (\tilde{U}_{e_L})^\dagger \mathcal{M}_e \tilde{U}_{e_R} &\sim \text{diag}(d_e, D_{\ell_R}, D_{\ell_L}), & (\tilde{U}_{n_L})^\dagger \mathcal{M}_n \tilde{U}_{n_R} &\sim \text{diag}(d_n, D_{\ell_R}, D_{\ell_L}), \\ (\tilde{U}_{d_L})^\dagger \mathcal{M}_d \tilde{U}_{d_R} &\sim \text{diag}(d_d, D_{Q_R}, D_{Q_L}), & (\tilde{U}_{u_L})^\dagger \mathcal{M}_u \tilde{U}_{u_R} &\sim \text{diag}(d_u, D_{Q_R}, D_{Q_L}). \end{aligned} \quad (\text{A.7})$$

The corrections from the off-diagonal blocks to the SM fermion mass matrix are $\mathcal{O}(d_f^2/v_\Delta)$, $f = e, n, d, u$, so it may be sub-dominant compared with the leading matrix $\sim d_f$.

A.1.2 Neutrino masses

The 18×18 mass matrix is given by

$$-\mathcal{L}_N = \frac{1}{2} \bar{\mathbf{N}}_L \mathcal{M}_N \mathbf{N}_R = \begin{pmatrix} \bar{\mathbf{n}}_L & \bar{\mathbf{n}}_R^c \end{pmatrix} \begin{pmatrix} 0 & \mathcal{M}_n \\ \mathcal{M}_n^T & \mathcal{M}_R \end{pmatrix} \begin{pmatrix} \mathbf{n}_L^c \\ \mathbf{n}_R \end{pmatrix},$$

where the Dirac mass matrix \mathcal{M}_n and Majorana mass matrix \mathcal{M}_R are given in Eqs. (2.24) and (2.14), respectively. The mass basis is defined as

$$\hat{\mathbf{N}}_R = U_N^\dagger \mathbf{N}_R, \quad \hat{\mathbf{N}}_L = U_N^T \mathbf{N}_L,$$

where $U_N^T \mathcal{M}_N U_N$ is diagonalized.

We introduce the unitary matrices,

$$\tilde{U}_N = \begin{pmatrix} \tilde{U}_{n_L}^* & 0_9 \\ 0_9 & \tilde{U}_{n_R} \end{pmatrix}, \quad (\text{A.8})$$

where $\tilde{U}_{n_{L,R}}$ are defined in Eq. (A.4). After multiplying these matrices, we obtain

$$\tilde{\mathcal{M}}_N := \tilde{U}_N^T \mathcal{M}_N \tilde{U}_N = \begin{pmatrix} 0_3 & 0_3 & 0_3 & d_n & \cdot & 0_3 \\ 0_3 & 0_3 & 0_3 & 0_3 & D_{n_R} & \cdot \\ 0_3 & 0_3 & 0_3 & \cdot & \cdot & D_{n_L} \\ d_n & 0_3 & \cdot & \tilde{M}_R & \tilde{\mu}_N & 0_3 \\ \cdot & D_{n_R} & \cdot & \tilde{\mu}_N^T & \tilde{M}_N & 0_3 \\ 0_3 & \cdot & D_{n_L} & 0_3 & 0_3 & 0_3 \end{pmatrix}, \quad (\text{A.9})$$

where

$$\begin{pmatrix} \tilde{M}_R & \tilde{\mu}_N \\ \tilde{\mu}_N^T & \tilde{M}_N \end{pmatrix} = \begin{pmatrix} 0_3 & u_{n_R}^T \\ \mathbf{1}_3 & 0_3 \end{pmatrix} V_{\ell_R}^T \begin{pmatrix} M_R & 0_3 \\ 0_3 & 0_3 \end{pmatrix} V_{\ell_R} \begin{pmatrix} 0_3 & \mathbf{1}_3 \\ u_{n_R} & 0_3 \end{pmatrix}. \quad (\text{A.10})$$

In numerical analysis, we studied the case which $V_{\ell_R} \sim \mathbf{1}_6$, $u_{n_R} \sim \mathbf{1}_3$ and $M_R \propto \mathbf{1}_3$. We assume this structure in the analytical analysis in this Appendix, but the non-zero effects are included in our numerical analysis. The SM Majorana neutrino masses arise after the block-diagonalization by

$$\tilde{U}_N^1 \sim \begin{pmatrix} \mathbf{1}_3 & 0_3 & 0_3 & d_n \tilde{M}_R^{-1} & 0_3 & 0_3 \\ 0_3 & \mathbf{1}_3 & 0_3 & 0_3 & 0_3 & 0_3 \\ 0_3 & 0_3 & \mathbf{1}_3 & 0_3 & 0_3 & 0_3 \\ -\tilde{M}_R^{-1} d_n & 0_3 & 0_3 & \mathbf{1}_3 & 0_3 & 0_3 \\ 0_3 & 0_3 & 0_3 & 0_3 & \mathbf{1}_3 & 0_3 \\ 0_3 & 0_3 & 0_3 & 0_3 & 0_3 & \mathbf{1}_3 \end{pmatrix}. \quad (\text{A.11})$$

The other states have diagonal Dirac mass matrices. In this case, the active neutrino mass is approximately given by

$$\tilde{M}_\nu \sim -d_n \tilde{M}_R^{-1} d_n, \quad (\text{A.12})$$

and this is already diagonalized. The total unitary matrix is thus given by $U_N \sim \tilde{U}_N \tilde{U}_N^1$.

A.2 Gauge interactions

We shall discuss gauge interactions. The PS symmetry is broken by non-zero VEVs of Δ and Σ . We name the massive gauge bosons in $SU(4)_C/SU(3)_C \times U(1)_{B-L}$ as leptoquark X_μ , and those in $SU(2)_R \times U(1)_{B-L}/U(1)_Y$ as Z'_μ and $W_{R\mu}^\pm$. In this subsection for the gauge interactions, $A, B, \dots = 1, 2, \dots, 15$ and $\alpha, \beta, \dots = 1, 2, 3, 4$ are for the $SU(4)_C$ indices of adjoint and fundamental representations, respectively. The $SU(2)_X$, $X = L, R$, indices of adjoint and fundamental representations are respectively denoted as $k_X, \dots = 1, 2, 3$ and $\alpha_X, \dots = 1, 2, 3$.

A.2.1 Symmetry breaking and vector boson masses

The covariant derivative terms of the symmetry breaking scalar fields are given by

$$\mathcal{L}_{\text{kin}}^{\text{SC}} = \text{Tr}_4 (D^\mu \Delta \cdot D_\mu \Delta) + \sum_{\alpha, \beta} \text{Tr}_2 \left[(D^\mu \Sigma_{\alpha\beta})^\dagger D_\mu \Sigma_{\alpha\beta} \right] + \text{Tr}_2 \left[(D^\mu \Phi)^\dagger D_\mu \Phi \right], \quad (\text{A.13})$$

where Tr_4 is the trace for the $SU(4)_C$ indices and Tr_2 is that for the $SU(2)_L$ and $SU(2)_R$ indices. The covariant derivatives are given by

$$D_\mu \Delta = \partial_\mu \Delta - ig_4 [\mathcal{V}_\mu, \Delta], \quad (\text{A.14})$$

$$D_\mu \Sigma_{\alpha\beta} = \partial_\mu \Sigma_{\alpha\beta} - ig_R [W_{R\mu}, \Sigma_{\alpha\beta}] + ig_4 \Sigma_{\gamma\delta} (\mathcal{V}_{\alpha\mu}^\gamma \delta_\beta^\delta + \mathcal{V}_{\beta\mu}^\delta \delta_\alpha^\gamma), \quad (\text{A.15})$$

$$D_\mu \Phi = \partial_\mu \Phi - ig_L W_{L\mu} \Phi + ig_R \Phi W_{R\mu}, \quad (\text{A.16})$$

where the indices of the fields are

$$\Delta = \Delta_\beta^\alpha = \Delta^A T^A, \quad \Sigma_{\alpha\beta} = \sqrt{1 + \delta_{\alpha\beta}} \Sigma_{\alpha\beta}^{k_R} \tau_R^{k_R}, \quad \Phi = \begin{pmatrix} H_1 & \tilde{H}_2 \end{pmatrix}, \quad (\text{A.17})$$

$$\mathcal{V}_\mu = \mathcal{V}_\mu^A T^A, \quad W_{L\mu} = W_{L\mu}^{k_L} \tau_L^{k_L}, \quad W_{R\mu} = W_{R\mu}^{k_R} \tau_R^{k_R}, \quad (\text{A.18})$$

where $\Sigma^{\alpha\beta} = \Sigma^{\beta\alpha}$. Here, the scalar fields Δ^A and $\Sigma_{\alpha\beta}^{k_R}$ are canonically normalized. The hermitian matrices T^A and $\tau_{L(R)}^{k_{L(R)}}$ are the generators of fundamental representation of $SU(4)_C$ and $SU(2)_{L(R)}$, respectively. H_1 and $\tilde{H}_2 := \epsilon H_2^*$ are the $SU(2)_L$ doublets.

In this paper, we assume a certain potential gives the following VEVs,

$$\langle \Delta \rangle = \frac{v_\Delta}{2\sqrt{3}} \begin{pmatrix} 3 & 0 \\ 0 & -\mathbf{1}_3 \end{pmatrix}, \quad \langle \Sigma_{\alpha\beta} \rangle = \frac{v_\Sigma}{\sqrt{2}} \begin{pmatrix} 0 & 1 \\ 0 & 0 \end{pmatrix} \otimes \delta_{\alpha 1} \delta_{\beta 1}, \quad \langle \Phi \rangle = v_H \begin{pmatrix} c_\beta & 0 \\ 0 & s_\beta \end{pmatrix}. \quad (\text{A.19})$$

where $s_\beta^2 + c_\beta^2 = 1$. The $SU(4)_C$ gauge boson \mathcal{V}_μ and $SU(2)_{L,R}$ gauge boson $\mathcal{W}_{L,R\mu}$ are decomposed as

$$\begin{aligned} \mathcal{V} &= \sqrt{\frac{3}{8}} \begin{pmatrix} 1 & 0 \\ 0 & -\frac{1}{3} \cdot \mathbf{1}_3 \end{pmatrix} V_\mu^{B-L} + \begin{pmatrix} 0 & X^\dagger/\sqrt{2} \\ X/\sqrt{2} & G \end{pmatrix}, \\ W_{L,R} &= \frac{1}{2} \begin{pmatrix} W_{L,R}^3 & \sqrt{2}W_{L,R}^+ \\ \sqrt{2}W_{L,R}^- & -W_{L,R}^3 \end{pmatrix}, \quad W_{L,R}^\pm = \frac{W_{L,R}^1 \pm iW_{L,R}^2}{\sqrt{2}} \end{aligned} \quad (\text{A.20})$$

where the Lorentz index is omitted. Here, V^{B-L} , X , G are $B-L$ gauge boson, leptoquarks and gluon, respectively. The mass terms of the gauge bosons are given by

$$\mathcal{L}_{\text{mass}}^V = m_X^2 X_\mu^\dagger X^\mu + \mathcal{W}_\mu^+ \mathcal{M}_W^2 \mathcal{W}^{-\mu} + \frac{1}{2} \mathcal{Z}_\mu \mathcal{M}_Z^2 \mathcal{Z}^\mu, \quad (\text{A.21})$$

where the mass and matrices are given by

$$m_X = g_4 \sqrt{\frac{4}{3}v_\Delta^2 + \frac{1}{2}v_\Sigma^2}, \quad \mathcal{M}_W^2 = \frac{1}{2} \begin{pmatrix} g_L^2 v_H^2 & -s_{2\beta} g_L g_R v_H^2 \\ -s_{2\beta} g_L g_R v_H^2 & g_R^2 (v_H^2 + v_\Sigma^2) \end{pmatrix}, \quad (\text{A.22})$$

$$\mathcal{M}_Z^2 = \frac{1}{2} \begin{pmatrix} g_L^2 v_H^2 & -g_L g_R v_H^2 & 0 \\ -g_L g_R v_H^2 & g_R^2 v_H^2 + 2g_\Sigma^2 v_\Sigma^2 & -\sqrt{6}g_R g_4 v_\Sigma^2 \\ 0 & -\sqrt{6}g_R g_4 v_\Sigma^2 & 3g_4^2 v_\Sigma^2 \end{pmatrix}, \quad (\text{A.23})$$

with the gauge bosons

$$\mathcal{W}_\mu^\pm := \begin{pmatrix} W_{L\mu}^\pm \\ W_{R\mu}^\pm \end{pmatrix}, \quad \mathcal{Z}_\mu := \begin{pmatrix} W_{L\mu}^3 \\ W_{R\mu}^3 \\ V_\mu^{B-L} \end{pmatrix}. \quad (\text{A.24})$$

Here, $s_{2\beta} = 2c_\beta s_\beta$ and $c_{2\beta} = c_\beta^2 - s_\beta^2$. The mass basis of the gauge bosons are defined as

$$\mathcal{W}_\mu^\pm = R_W \begin{pmatrix} W_\mu^\pm \\ W_\mu^{\prime\pm} \end{pmatrix}, \quad \mathcal{Z}_\mu = R_Z \begin{pmatrix} A_\mu \\ Z_\mu \\ Z'_\mu \end{pmatrix}, \quad (\text{A.25})$$

where R_W and R_Z are orthogonal matrices diagonalizing \mathcal{M}_W^2 and \mathcal{M}_Z^2 , respectively.

The rotation matrix R_W and eigenvalues of the mass matrix, m_W and $m_{W'}$ are exactly given by

$$R_W = \begin{pmatrix} c_\omega & s_\omega \\ -s_\omega & c_\omega \end{pmatrix}, \quad (\text{A.26})$$

$$m_W^2 = \frac{v_\Sigma^2}{4} [g_R^2 + (g_R^2 + g_L^2)\eta - D_W], \quad m_{W'}^2 = \frac{v_\Sigma^2}{4} [g_R^2 + (g_R^2 + g_L^2)\eta + D_W], \quad (\text{A.27})$$

where

$$D_W = \sqrt{g_R^4 + 2g_R^2(g_R^2 - g_L^2)\eta + \left\{ (g_R^2 - g_L^2)^2 + 4s_{2\beta}^2 g_L^2 g_R^2 \right\} \eta^2}, \quad (\text{A.28})$$

$$c_\omega = \frac{1}{\sqrt{2}} \sqrt{1 + \frac{g_R^2 + (g_R^2 - g_L^2)\eta}{D_W}}, \quad s_\omega = -\frac{1}{\sqrt{2}} \sqrt{1 - \frac{g_R^2 + (g_R^2 - g_L^2)\eta}{D_W}}, \quad (\text{A.29})$$

and $\eta := v_H^2/v_\Sigma^2$. The rotation matrix for the neutral bosons are given by

$$R_Z = \begin{pmatrix} c_{12} & s_{12} & 0 \\ -s_{12} & c_{12} & 0 \\ 0 & 0 & 1 \end{pmatrix} \begin{pmatrix} c_{13} & 0 & s_{13} \\ 0 & 1 & 0 \\ -s_{13} & 0 & c_{13} \end{pmatrix} \begin{pmatrix} 1 & 0 & 0 \\ 0 & c_{23} & s_{23} \\ 0 & -s_{23} & c_{23} \end{pmatrix}. \quad (\text{A.30})$$

Here, the angles are given by

$$c_{12} = \frac{g_R}{\sqrt{g_L^2 + g_R^2}}, \quad s_{12} = -\frac{g_L}{\sqrt{g_L^2 + g_R^2}}, \quad c_{13} = -\sqrt{3(g_L^2 + g_R^2)} \frac{g_4}{\tilde{g}^2}, \quad s_{13} = \sqrt{2} \frac{g_L g_R}{\tilde{g}^2}, \quad (\text{A.31})$$

$$c_{23} = \frac{1}{\sqrt{2}} \sqrt{1 - \frac{s - 2\tilde{g}^4/(g_L^2 + g_R^2)}{D_Z}}, \quad s_{23} = \frac{1}{\sqrt{2}} \sqrt{1 + \frac{s - 2\tilde{g}^4/(g_L^2 + g_R^2)}{D_Z}}, \quad (\text{A.32})$$

where

$$\tilde{g}^2 = \sqrt{2g_R^2 g_L^2 + 3g_4^2 (g_L^2 + g_R^2)}, \quad s = 3g_4^2 + 2g_R^2 + (g_L^2 + g_R^2)\eta, \quad D_Z = \sqrt{s^2 - 4\tilde{g}^4 \eta}. \quad (\text{A.33})$$

The Z and Z' boson masses are given by

$$m_Z^2 = \frac{v_\Sigma^2}{4} (s - D_Z), \quad m_{Z'}^2 = \frac{v_\Sigma^2}{4} (s + D_Z). \quad (\text{A.34})$$

The rotation matrices R_W , R_Z diagonalize the mass matrices as

$$R_W^T \mathcal{M}_W^2 R_W = \text{diag}(m_W^2, m_{W'}^2), \quad R_Z^T \mathcal{M}_Z^2 R_Z = \text{diag}(0, m_Z^2, m_{Z'}^2). \quad (\text{A.35})$$

If the sub-leading terms in η are neglected, the vector boson masses are given by

$$m_W^2 = \frac{g_L^2}{2} v_H^2, \quad m_{W'}^2 = \frac{g_R^2}{2} v_\Sigma^2, \quad (\text{A.36})$$

and

$$m_Z^2 = \frac{\tilde{g}^4}{3g_4^2 + 2g_R^2} \frac{v_H^2}{2}, \quad m_{Z'}^2 = (3g_4^2 + 2g_R^2) \frac{v_\Sigma^2}{2}. \quad (\text{A.37})$$

A.2.2 Gauge interactions with fermions

With the PS symmetry, the covariant derivatives terms for the fermions, $\mathcal{F}_L \in (L, F_L, f_L)$ and $\mathcal{F}_R \in (R, f_R, F_R)$, are given by

$$D^\mu \mathcal{F}_L = \partial^\mu \mathcal{F}_L - ig_L W_L^\mu \mathcal{F}_L - ig_A \mathcal{V}^\mu \mathcal{F}_L, \quad D^\mu \mathcal{F}_R = \partial^\mu \mathcal{F}_R - ig_R W_R^\mu \mathcal{F}_L - ig_A \mathcal{V}^\mu \mathcal{F}_R, \quad (\text{A.38})$$

The gauge couplings to the vector leptoquarks are shown in Eqs. (2.19) and (2.20).

The gauge couplings with the charged $SU(2)$ bosons, (W_L^-, W_R^-) are given by

$$\begin{aligned} \mathcal{L}_W &= \frac{g_L}{\sqrt{2}} W_{L\mu}^- (\bar{\mathbf{u}}_L \gamma^\mu P_6 \mathbf{d}_L + \bar{\mathbf{n}}_L \gamma^\mu P_6 \mathbf{e}_L + \bar{\mathbf{u}}_R \gamma^\mu P_{\bar{6}} \mathbf{d}_R + \bar{\mathbf{n}}_R \gamma^\mu P_6 \mathbf{e}_R) \\ &\quad + \frac{g_R}{\sqrt{2}} W_{R\mu}^- (\bar{\mathbf{u}}_L \gamma^\mu P_{\bar{6}} \mathbf{d}_L + \bar{\mathbf{n}}_L \gamma^\mu P_6 \mathbf{e}_L + \bar{\mathbf{u}}_R \gamma^\mu P_6 \mathbf{d}_R + \bar{\mathbf{n}}_R \gamma^\mu P_6 \mathbf{e}_R) + h.c. \\ &= W_{L\mu}^- \left(\hat{\mathbf{u}}_L \hat{g}_{qL}^{W_L} \gamma^\mu \hat{\mathbf{d}}_L + \hat{\mathbf{n}}_L \hat{g}_{\ell_L}^{W_L} \gamma^\mu \hat{\mathbf{e}}_L + \hat{\mathbf{u}}_R \hat{g}_{qR}^{W_L} \gamma^\mu \hat{\mathbf{d}}_R + \hat{\mathbf{n}}_R \hat{g}_{\ell_R}^{W_L} \gamma^\mu \hat{\mathbf{e}}_R \right) \\ &\quad + W_{R\mu}^- \left(\hat{\mathbf{u}}_L \hat{g}_{qL}^{W_R} \gamma^\mu \hat{\mathbf{d}}_L + \hat{\mathbf{n}}_L \hat{g}_{\ell_L}^{W_R} \gamma^\mu \hat{\mathbf{e}}_L + \hat{\mathbf{u}}_R \hat{g}_{qR}^{W_R} \gamma^\mu \hat{\mathbf{d}}_R + \hat{\mathbf{n}}_R \hat{g}_{\ell_R}^{W_R} \gamma^\mu \hat{\mathbf{e}}_R \right) + h.c., \end{aligned} \quad (\text{A.39})$$

where the couplings in the mass basis of the fermions are given by

$$\begin{aligned} \hat{g}_{qL}^{W_L} &= \frac{g_L}{\sqrt{2}} (U_L^u)^\dagger P_6 U_L^d, & \hat{g}_{\ell_L}^{W_L} &= \frac{g_L}{\sqrt{2}} (U_L^n)^\dagger P_6 U_L^e, \\ \hat{g}_{qR}^{W_L} &= \frac{g_L}{\sqrt{2}} (U_R^u)^\dagger P_{\bar{6}} U_R^d, & \hat{g}_{\ell_R}^{W_L} &= \frac{g_L}{\sqrt{2}} (U_R^n)^\dagger P_{\bar{6}} U_R^e, \\ \hat{g}_{qL}^{W_R} &= \frac{g_R}{\sqrt{2}} (U_L^u)^\dagger P_{\bar{6}} U_L^d, & \hat{g}_{\ell_L}^{W_R} &= \frac{g_R}{\sqrt{2}} (U_L^n)^\dagger P_{\bar{6}} U_L^e, \\ \hat{g}_{qR}^{W_R} &= \frac{g_R}{\sqrt{2}} (U_R^u)^\dagger P_6 U_R^d, & \hat{g}_{\ell_R}^{W_R} &= \frac{g_R}{\sqrt{2}} (U_R^n)^\dagger P_6 U_R^e. \end{aligned} \quad (\text{A.40})$$

Here, the projection matrices are defined as

$$P_6 := \begin{pmatrix} \mathbf{1}_6 & 0_{6 \times 3} \\ 0_{3 \times 6} & 0_3 \end{pmatrix}, \quad P_{\bar{6}} := \mathbf{1}_9 - P_6. \quad (\text{A.41})$$

Note that (W_L, W_R) is not a mass base of the gauge bosons. For instance, the couplings to the left-handed quarks are given by

$$\begin{pmatrix} \hat{g}_{qL}^W \\ \hat{g}_{qL}^{W'} \end{pmatrix} = R_W^T \begin{pmatrix} \hat{g}_{qL}^{W_L} \\ \hat{g}_{qL}^{W_R} \end{pmatrix}, \quad (\text{A.42})$$

and those for the fermions can be obtained in the same way.

The gauge couplings with the neutral gauge bosons (W_L^3, W_R^3, V^{B-L}) are given by

$$\mathcal{L}_Z = \frac{g_L}{2} W_{L\mu}^3 \sum_{\mathbf{f}=\mathbf{u},\mathbf{d},\mathbf{e},\mathbf{n}} I_{\mathbf{f}} (\bar{\mathbf{f}}_L \gamma^\mu P_6 \mathbf{f}_L + \bar{\mathbf{f}}_R \gamma^\mu P_6 \mathbf{f}_R) \quad (\text{A.43})$$

$$\begin{aligned} &+ \frac{g_R}{2} W_{R\mu}^3 \sum_{\mathbf{f}=\mathbf{u},\mathbf{d},\mathbf{e},\mathbf{n}} I_{\mathbf{f}} (\bar{\mathbf{f}}_L \gamma^\mu P_{\bar{6}} \mathbf{f}_L + \bar{\mathbf{f}}_R \gamma^\mu P_6 \mathbf{f}_R) \\ &- \sqrt{\frac{3}{8}} g_4 V_\mu^{B-L} \sum_{\mathbf{f}=\mathbf{u},\mathbf{d},\mathbf{e},\mathbf{n}} Q_{B-L}^{\mathbf{f}} (\bar{\mathbf{f}}_L \gamma^\mu \mathbf{f}_L + \bar{\mathbf{f}}_R \gamma^\mu \mathbf{f}_R) \\ &= \sum_{V=W_L^3, W_R^3, V^{B-L}} V_\mu \sum_{\mathbf{f}=\mathbf{u},\mathbf{d},\mathbf{e},\mathbf{n}} \left(\bar{\mathbf{f}}_L \hat{g}_{f_L}^V \gamma^\mu \hat{\mathbf{f}}_L + \bar{\mathbf{f}}_R \hat{g}_{f_R}^V \gamma^\mu \hat{\mathbf{f}}_R \right), \end{aligned} \quad (\text{A.44})$$

where $I_{\mathbf{f}} = +1$ (-1) for $\mathbf{f} = \mathbf{e}, \mathbf{d}$ (\mathbf{u}, \mathbf{n}). $Q_{B-L}^{\mathbf{f}}$ is the $B-L$ number of a fermion \mathbf{f} . The gauge coupling matrices in the fermion mass basis are given by

$$\hat{g}_{f_L}^{W_L^3} = \frac{g_L}{2} I_L^f (U_L^f)^\dagger P_6 U_L^f, \quad \hat{g}_{f_R}^{W_L^3} = \frac{g_L}{2} I_L^f (U_R^f)^\dagger P_6 U_R^f, \quad (\text{A.45})$$

$$\hat{g}_{f_L}^{W_R^3} = \frac{g_R}{2} I_R^f (U_L^f)^\dagger P_{\bar{6}} U_L^f, \quad \hat{g}_{f_R}^{W_R^3} = \frac{g_R}{2} I_R^f (U_R^f)^\dagger P_6 U_R^f, \quad (\text{A.46})$$

$$\hat{g}_{f_L}^{V^{B-L}} = -\sqrt{\frac{3}{8}} g_4 Q_{B-L}^f (U_L^f)^\dagger U_L^f, \quad \hat{g}_{f_R}^{V^{B-L}} = -\sqrt{\frac{3}{8}} g_4 Q_{B-L}^f (U_R^f)^\dagger U_R^f. \quad (\text{A.47})$$

The coupling matrices in the mass basis are

$$\begin{pmatrix} \hat{g}_{f_L}^A \\ \hat{g}_{f_L}^Z \\ \hat{g}_{f_L}^{Z'} \end{pmatrix} = R_Z^T \begin{pmatrix} \hat{g}_{f_L}^{W_L^3} \\ \hat{g}_{f_L}^{W_R^3} \\ \hat{g}_{f_L}^{V^{B-L}} \end{pmatrix}, \quad \begin{pmatrix} \hat{g}_{f_R}^A \\ \hat{g}_{f_R}^Z \\ \hat{g}_{f_R}^{Z'} \end{pmatrix} = R_Z^T \begin{pmatrix} \hat{g}_{f_R}^{W_L^3} \\ \hat{g}_{f_R}^{W_R^3} \\ \hat{g}_{f_R}^{V^{B-L}} \end{pmatrix}. \quad (\text{A.48})$$

Approximately, R_W and R_Z are given by

$$R_W = \begin{pmatrix} 1 & 0 \\ 0 & 1 \end{pmatrix} + \mathcal{O}(\eta), \quad R_Z = \begin{pmatrix} -\sqrt{3}g_4g_R/\tilde{g}^2 & -\sqrt{s}g_L/\tilde{g}^2 & 0 \\ -\sqrt{3}g_4g_L/\tilde{g}^2 & 3g_4^2g_R/(\sqrt{s}\tilde{g}^2) & \sqrt{2}g_R/\sqrt{s} \\ -\sqrt{2}g_Lg_R/\tilde{g}^2 & \sqrt{6}g_4g_R^2/(\sqrt{s}\tilde{g}^2) & -\sqrt{3}g_4/\sqrt{s} \end{pmatrix} + \mathcal{O}(\eta). \quad (\text{A.49})$$

At the leading order in η , $W \sim W_L$ and $W' \sim W_R$. The coupling matrices to the fermions are approximately given by

$$\hat{g}_{qL}^W \sim \frac{g_L}{\sqrt{2}} \begin{pmatrix} u_{uL}^\dagger & 0_3 & 0_3 \\ 0_3 & \mathbf{1}_3 & 0_3 \\ 0_3 & 0_3 & 0_3 \end{pmatrix}, \quad \hat{g}_{qR}^W \sim \frac{g_L}{\sqrt{2}} \begin{pmatrix} 0_3 & 0_3 & 0_3 \\ 0_3 & \mathbf{1}_3 & 0_3 \\ 0_3 & 0_3 & 0_3 \end{pmatrix}, \quad (\text{A.50})$$

$$\mathcal{P}_L \hat{g}_{\ell L}^W \sim \frac{g_L}{\sqrt{2}} \begin{pmatrix} u_{nL}^\dagger & 0_3 & 0_3 \\ 0_3 & 0_3 & 0_3 \\ 0_3 & 0_3 & \mathbf{1}_3 \end{pmatrix}, \quad \mathcal{P}_R \hat{g}_{\ell R}^W \sim \frac{g_L}{\sqrt{2}} \begin{pmatrix} 0_3 & 0_3 & 0_3 \\ 0_3 & 0_3 & 0_3 \\ 0_3 & 0_3 & \mathbf{1}_3 \end{pmatrix}, \quad (\text{A.51})$$

$$\hat{g}_{qL}^{W'} \sim \frac{g_R}{\sqrt{2}} \begin{pmatrix} 0_3 & 0_3 & 0_3 \\ 0_3 & 0_3 & 0_3 \\ 0_3 & 0_3 & \mathbf{1}_3 \end{pmatrix}, \quad \hat{g}_{qR}^{W'} \sim \frac{g_R}{\sqrt{2}} \begin{pmatrix} u_{uR}^\dagger & 0_3 & 0_3 \\ 0_3 & 0_3 & 0_3 \\ 0_3 & 0_3 & \mathbf{1}_3 \end{pmatrix}, \quad (\text{A.52})$$

$$\mathcal{P}_L \hat{g}_{\ell L}^{W'} \sim \frac{g_R}{\sqrt{2}} \begin{pmatrix} 0_3 & 0_3 & 0_3 \\ 0_3 & \mathbf{1}_3 & 0_3 \\ 0_3 & 0_3 & 0_3 \end{pmatrix}, \quad \mathcal{P}_R \hat{g}_{\ell R}^{W'} \sim \frac{g_R}{\sqrt{2}} \begin{pmatrix} u_{nR}^\dagger & 0_3 & 0_3 \\ 0_3 & \mathbf{1}_3 & 0_3 \\ 0_3 & 0_3 & 0_3 \end{pmatrix}. \quad (\text{A.53})$$

The other blocks in the neutrino couplings are vanishing. For the SM families, the W boson couples via the left-current, while the W' boson couples via the right-current. Their flavor structure depends on independent unitary matrices, $u_{uL,R}$ and $u_{nL,R}$. In particular, u_{uL}^\dagger and u_{nL}^\dagger correspond to the CKM and PMNS matrices, respectively.

The coupling matrices to the neutral bosons (W_L^3, W_R^3, V^{B-L}) are given by

$$\hat{g}_{qL}^{W_L^3} \sim \frac{g_L}{2} I_q P_{qL}^Z, \quad \hat{g}_{qL}^{W_R^3} \sim \frac{g_R}{2} I_q P_{qL}^{Z'}, \quad \hat{g}_{qL}^{V^{B-L}} \sim -g_4 \sqrt{\frac{1}{24}} \mathbf{1}_9, \quad (\text{A.54})$$

$$\hat{g}_{qR}^{W_L^3} \sim \frac{g_L}{2} I_q P_{qR}^Z, \quad \hat{g}_{qR}^{W_R^3} \sim \frac{g_R}{2} I_q P_{qR}^{Z'}, \quad \hat{g}_{qR}^{V^{B-L}} \sim -g_4 \sqrt{\frac{1}{24}} \mathbf{1}_9, \quad (\text{A.55})$$

$$\hat{g}_{\ell L}^{W_L^3} \sim \frac{g_L}{2} I_\ell P_{\ell L}^Z, \quad \hat{g}_{\ell L}^{W_R^3} \sim \frac{g_R}{2} I_\ell P_{\ell L}^{Z'}, \quad \hat{g}_{\ell L}^{V^{B-L}} \sim g_4 \sqrt{\frac{3}{8}} \mathbf{1}_9, \quad (\text{A.56})$$

$$\hat{g}_{\ell R}^{W_L^3} \sim \frac{g_L}{2} I_\ell P_{\ell R}^Z, \quad \hat{g}_{\ell R}^{W_R^3} \sim \frac{g_R}{2} I_\ell P_{\ell R}^{Z'}, \quad \hat{g}_{\ell R}^{V^{B-L}} \sim g_4 \sqrt{\frac{3}{8}} \mathbf{1}_9, \quad (\text{A.57})$$

where $q = u, d$ and $\ell = e, n$. The coupling matrices are given by

$$P_{qL}^Z = P_{\ell R}^{Z'} = \begin{pmatrix} \mathbf{1}_3 & 0_3 & 0_3 \\ 0_3 & \mathbf{1}_3 & 0_3 \\ 0_3 & 0_3 & 0_3 \end{pmatrix}, \quad P_{qR}^Z = P_{\ell L}^{Z'} = \begin{pmatrix} 0_3 & 0_3 & 0_3 \\ 0_3 & \mathbf{1}_3 & 0_3 \\ 0_3 & 0_3 & 0_3 \end{pmatrix}, \quad (\text{A.58})$$

$$P_{\ell L}^Z = P_{qR}^{Z'} = \begin{pmatrix} \mathbf{1}_3 & 0_3 & 0_3 \\ 0_3 & 0_3 & 0_3 \\ 0_3 & 0_3 & \mathbf{1}_3 \end{pmatrix}, \quad P_{\ell R}^Z = P_{qL}^{Z'} = \begin{pmatrix} 0_3 & 0_3 & 0_3 \\ 0_3 & 0_3 & 0_3 \\ 0_3 & 0_3 & \mathbf{1}_3 \end{pmatrix}. \quad (\text{A.59})$$

For the neutrinos, these are the 9×9 upper-left (bottom-right) block in the 18×18 coupling matrices for the left-handed (right-handed) neutrinos. Using Eq. (A.49), the gauge couplings to the neutral gauge bosons in the mass basis, (A, Z, Z') are approximately given by

$$\hat{g}_{fX}^A \sim e Q_e^f \mathbf{1}_9, \quad \hat{g}_{fX}^Z \sim \frac{g_L}{c_W} \left(-\frac{I_f}{2} P_{fX}^Z - s_W^2 Q_e^f \mathbf{1}_9 \right), \quad \hat{g}_{fX}^{Z'} \sim \frac{g_{Z'}}{2} \left(s_{Z'}^2 P_{fX}^{Z'} I_f + c_{Z'}^2 Q_{B-L}^f \mathbf{1}_9 \right), \quad (\text{A.60})$$

where the electric charge, coupling constant and Z' gauge coupling constant are given by

$$Q_e^f = \frac{Q_{B-L}^f - I_f}{2}, \quad e = \sqrt{3} \frac{g_A g_L g_R}{\tilde{g}^2}, \quad g_{Z'} = \sqrt{\frac{2g_R^2 + 3g_4^2}{2}}. \quad (\text{A.61})$$

For the Z and Z' boson couplings, the angles are defined as

$$c_W = \frac{g_L \sqrt{3g_4^2 + 2g_R^2}}{\tilde{g}^2}, \quad s_W = \frac{\sqrt{3}g_A g_R}{\tilde{g}^2}, \quad c_{Z'} = \sqrt{\frac{2g_R^2}{2g_R^2 + 3g_4^2}}, \quad s_{Z'} = \sqrt{\frac{3g_4^2}{2g_R^2 + 3g_4^2}}. \quad (\text{A.62})$$

Therefore, the EW gauge couplings coincides with the SM values when $\mathcal{O}(\eta)$ effects are negligible.

In the above approximate formulas, we neglected $\mathcal{O}(v_H^2/v_\Delta^2, \eta)$ effects in the diagonalization unitary matrices for the fermion and gauge boson mass matrices. In the fermion mass matrix, the $\mathcal{O}(v_H)$ elements, denoted by \cdot in Eq. (A.2), in the off-diagonal blocks are neglected. These off-diagonal entries will induce flavor violating couplings with the EW gauge bosons. The flavor violating coupling to $f_i f_j$ will be $\mathcal{O}(g_L [d_f]_i [d_f]_j / v_\Delta^2)$, where $[d_f]_i$ is the mass of the SM fermion of i -th generation¹⁴. Here we assume that all the vectorlike fermion masses are $\mathcal{O}(v_\Delta)$. If $v_\Delta \sim \mathcal{O}(10 \text{ TeV})$ as considered in this paper, the induced flavor violating coupling is at most $\mathcal{O}(10^{-6})$ for top and charm quarks, and the smaller for the light flavor fermions. Thus the flavor violation from the EW gauge bosons are too small to be measured by experiments. The mixing of Z - Z' and W - W' will affect to EW precision observables, since these induce exotic right-current interactions. Again, when $v_\Sigma \sim \mathcal{O}(10 \text{ TeV})$, the effect is $\mathcal{O}(10^{-4})$, and thus may be too small to be measured. Note that Z' and W' can be lighter while keeping the leptoquark $\mathcal{O}(10 \text{ TeV})$ if $v_\Sigma \ll v_\Delta$. This would be an interesting possibility but is beyond the scope of this paper. In our numerical analysis, flavor violating effects from the extra gauge bosons are neglected.

A.3 Scalar Interactions

In our model, there are three scalar fields Δ , Σ and Φ introduced to break the PS to SM symmetry. In this paper, we will not consider the scalar potential explicitly, and we assume that the scalar potential has the global minimum at the VEVs which we assumed.

The EW symmetry is broken by the VEV of bi-doublet Φ ,

$$\Phi = \begin{pmatrix} H_1^0 & H_2^{+*} \\ H_1^+ & -H_2^{0*} \end{pmatrix} = (H_1 \ \tilde{H}_2),$$

where, $H_{1,2}$ are the $SU(2)_L$ doublets which can be expanded as

$$H_k = \begin{pmatrix} H_k^0 \\ H_k^+ \end{pmatrix} = \frac{1}{\sqrt{2}} \begin{pmatrix} v_k + h_k + ia_k \\ \sqrt{2}H_k^+ \end{pmatrix}, \quad k = 1, 2. \quad (\text{A.63})$$

¹⁴See Refs. [57, 58] for the similar analysis in a model with one vectorlike generation.

The mass basis of the doublet Higgs bosons are defined as

$$\begin{pmatrix} h_1 \\ h_2 \end{pmatrix} = R_\alpha \begin{pmatrix} h \\ H \end{pmatrix}, \quad \begin{pmatrix} a_1 \\ a_2 \end{pmatrix} = R_{\beta_0} \begin{pmatrix} G^0 \\ A \end{pmatrix}, \quad \begin{pmatrix} H_1^+ \\ H_2^+ \end{pmatrix} = R_{\beta_+} \begin{pmatrix} G^+ \\ H^+ \end{pmatrix}, \quad (\text{A.64})$$

where G^0, G^+ are the NG bosons. The rotations matrices are defined with the angles as

$$R_\phi = \begin{pmatrix} \cos \phi & -\sin \phi \\ \sin \phi & \cos \phi \end{pmatrix}, \quad \phi = \alpha, \beta_0, \beta_\pm. \quad (\text{A.65})$$

In the decoupling limit ($m_A, m_{H^\pm} \gg m_h$), these angles are aligned as $\alpha = \beta_0 = \beta_\pm = \beta$ where $\tan \beta \equiv v_2/v_1$. The Higgs couplings to the fermions are given by

$$\begin{aligned} -\mathcal{L}_H = & \sum_{S=h,H,A} S \left(\bar{u}_L Y_u^S \mathbf{u}_R + \bar{d}_L Y_d^S \mathbf{d}_R + \bar{e}_L Y_e^S \mathbf{e}_R + \bar{n}_L Y_n^S \mathbf{n}_R \right) \\ & + H^+ \left(\bar{u}_L Y_d^{H^+} \mathbf{d}_R + \bar{\nu}_L Y_e^{H^+} \mathbf{e}_R \right) + H^- \left(\bar{d}_L Y_u^{H^-} \mathbf{u}_R + \bar{e}_L Y_n^{H^-} \mathbf{n}_R \right) + h.c.. \end{aligned} \quad (\text{A.66})$$

The Yukawa matrices Y_f^S are given by linear combinations of

$$Y_a = \begin{pmatrix} y_a & \tilde{\lambda}_a & 0_3 \\ \lambda_a & \tilde{y}_a & 0_3 \\ 0_3 & 0_3 & \tilde{y}'_a \end{pmatrix}, \quad a = 1, 2, \quad (\text{A.67})$$

where the 3×3 Yukawa matrices are defined in Eqs. (2.1) and (2.2). The relation of these Yukawa matrices to the quark Yukawa matrix is given by

$$\begin{pmatrix} Y_d \\ Y_u \end{pmatrix} := \frac{d}{dv_H} \begin{pmatrix} \mathcal{M}_d \\ \mathcal{M}_u \end{pmatrix} = \begin{pmatrix} c_\beta & -s_\beta \\ -s_\beta & c_\beta \end{pmatrix} \begin{pmatrix} Y_1 \\ Y_2 \end{pmatrix}, \quad (\text{A.68})$$

where Y_d and Y_u are the Yukawa matrices aligned to the relevant block of the mass matrix. The Yukawa matrices for $S = h, H, A, H^\pm$ are given by

$$\begin{pmatrix} Y_d^h \\ Y_u^h \end{pmatrix} = \frac{1}{\sqrt{2} \cos 2\beta} \begin{pmatrix} \cos(\alpha + \beta) & -\sin(\alpha - \beta) \\ -\sin(\alpha - \beta) & \cos(\alpha + \beta) \end{pmatrix} \begin{pmatrix} Y_d \\ Y_u \end{pmatrix}, \quad (\text{A.69})$$

$$\begin{pmatrix} Y_d^H \\ Y_u^H \end{pmatrix} = \frac{-1}{\sqrt{2} \cos 2\beta} \begin{pmatrix} \sin(\alpha + \beta) & \cos(\alpha - \beta) \\ \cos(\alpha - \beta) & \sin(\alpha + \beta) \end{pmatrix} \begin{pmatrix} Y_d \\ Y_u \end{pmatrix}, \quad (\text{A.70})$$

$$\begin{pmatrix} Y_d^A \\ Y_u^A \end{pmatrix} = \frac{-i}{\sqrt{2} \cos 2\beta} \begin{pmatrix} \sin(\beta_0 + \beta) & \cos(\beta_0 - \beta) \\ -\cos(\beta_0 - \beta) & -\sin(\beta_0 + \beta) \end{pmatrix} \begin{pmatrix} Y_d \\ Y_u \end{pmatrix}, \quad (\text{A.71})$$

$$\begin{pmatrix} Y_d^{H^\pm} \\ Y_u^{H^\pm} \end{pmatrix} = \frac{-1}{\cos 2\beta} \begin{pmatrix} \sin(\beta_\pm + \beta) & \cos(\beta_\pm - \beta) \\ -\cos(\beta_\pm - \beta) & -\sin(\beta_\pm + \beta) \end{pmatrix} \begin{pmatrix} Y_d \\ Y_u \end{pmatrix}. \quad (\text{A.72})$$

In the gauge basis, the lepton Yukawa couplings are the same as those of the quarks, e.g. $Y_d^h = Y_e^h$. The Yukawa matrices in the mass basis are given by

$$\hat{Y}_f^{S^0} = \left(U_L^f\right)^\dagger Y_f^{S^0} U_R^f, \quad (\text{A.73})$$

where $S^0 = h, H, A$ and $f = u, d, e, n$. The charge Higgs couplings are given by

$$\hat{Y}_d^{H^+} = (U_L^u)^\dagger Y_d^{H^+} U_R^d, \quad \hat{Y}_u^{H^-} = (U_L^d)^\dagger Y_u^{H^-} U_R^u, \quad (\text{A.74})$$

$$\hat{Y}_e^{H^+} = (U_L^n)^\dagger Y_e^{H^+} U_R^e, \quad \hat{Y}_n^{H^-} = (U_L^e)^\dagger Y_n^{H^-} U_R^n. \quad (\text{A.75})$$

In the decoupling limit, the SM Higgs couplings are aligned with the mass matrix, i.e. $Y_{d(u)}^h \propto Y_{d(u)}$, while the Yukawa couplings to the heavier Higgs bosons are not. Therefore the heavy Higgs bosons generically induce flavor violation.

The $SU(4)_C$ adjoint scalar Δ is expanded as

$$\Delta = \frac{1}{2\sqrt{3}} \left(v_\Delta + \frac{h_\Delta}{\sqrt{2}} \right) \begin{pmatrix} 3 & 0 \\ 0 & -\mathbf{1}_3 \end{pmatrix} + \begin{pmatrix} 0 & 0 \\ 0 & \Delta_8 \end{pmatrix}. \quad (\text{A.76})$$

Here, h_Δ is a CP-even neutral scalar and Δ_8 is a $SU(3)_C$ adjoint scalar field. The Yukawa couplings involving Δ and Δ_8 are given by

$$-\mathcal{L}_\Delta = \sum_{\mathbf{f}=\mathbf{u},\mathbf{d},\mathbf{e},\mathbf{n}} \sqrt{\frac{3}{8}} h_\Delta Q_{B-L}^{\mathbf{f}} \bar{\mathbf{f}}_L Y_\Delta \mathbf{f}_R + \sum_{\mathbf{f}=\mathbf{u},\mathbf{d}} \bar{\mathbf{f}}_L Y_\Delta \Delta_8 \mathbf{f}_R + h.c., \quad (\text{A.77})$$

where the Yukawa coupling matrices in the gauge basis are common for the fermions,

$$Y_\Delta = \begin{pmatrix} 0_3 & 0_3 & \epsilon_L \\ 0_3 & 0_3 & \kappa_L \\ \epsilon_R & \kappa_R & 0_3 \end{pmatrix} = \frac{\sqrt{3}}{2v_\Delta} (\mathcal{M}_e - \mathcal{M}_d). \quad (\text{A.78})$$

In the mass basis, the couplings are given by

$$\hat{Y}_\Delta^f = \left(U_L^f\right)^\dagger Y_\Delta U_R^f, \quad f = u, d, e, n. \quad (\text{A.79})$$

The flavor violation is also induced by the Δ couplings, although the sizable contributions appear only with vectorlike generations. For instance, the Yukawa coupling to the charged leptons is approximately given by,

$$\hat{Y}_\Delta^e \sim \left(\tilde{U}_{eL}\right)^\dagger Y_\Delta \tilde{U}_{eR} = \begin{pmatrix} 0_3 & 0_3 & \Lambda_{L_1}^e \\ \Lambda_{R_2}^e & \Lambda_{R_1}^e & 0_3 \\ 0_3 & 0_3 & \Lambda_{L_2}^e \end{pmatrix} + \mathcal{O}\left(\frac{v_H}{v_\Delta}\right), \quad (\text{A.80})$$

Table 2: Values of parameters of the mesons taken from PDG and HFLAG2019 [106]. The units of masses and decay constants are GeV, that of lifetime is GeV^{-1} .

m_{B_d}	5.280	$\tau_{B_d} \times 10^{-12}$	2.3230	f_{B_d}	0.1920	B_{B_d}	1.30
m_{B_s}	5.367	$\tau_{B_s} \times 10^{-12}$	2.2930	f_{B_s}	0.2284	B_{B_s}	1.35
m_{B_c}	6.275	$\tau_{B_c} \times 10^{-12}$	0.7703	f_{B_c}	0.4340	-	-
m_K	0.4976	$\tau_{K_L} \times 10^{-17}$	7.7730	f_K	0.1552	B_K	0.717

where the 3×3 coupling matrices $\Lambda_{L,R_{1,2}}^e$ are given by

$$\begin{pmatrix} \Lambda_{R_1}^e & \Lambda_{R_2}^e \end{pmatrix} = \tilde{D}_{\ell_R} - W_{\ell_L}^\dagger W_{Q_L} \tilde{D}_{Q_R} V_{Q_R}^\dagger V_{\ell_R}, \quad (\text{A.81})$$

$$\begin{pmatrix} \Lambda_{L_1}^e \\ \Lambda_{L_2}^e \end{pmatrix} = \tilde{D}_{\ell_L} - V_{\ell_L}^\dagger V_{Q_L} \tilde{D}_{Q_L} W_{Q_R}^\dagger W_{\ell_R}. \quad (\text{A.82})$$

Thus, there is no couplings of Δ with two SM fermions at the leading order. It might be possible that loop effects mediated by the vectorlike fermions induce flavor violations, such as $\mu \rightarrow e\gamma$. For $\mu \rightarrow e\gamma$, the chirality enhanced effect enhanced by v_H will be proportional to $[\hat{Y}_\Delta^e]_{1a} [\hat{Y}_\Delta^e]_{a2}$, $a = 1, 2, \dots, 9$, which are all zero in Eq. (A.80). Hence, we expect that Δ will not give significant flavor violating effects no matter how the leptoquark couplings are.

B Analysis details

B.1 Formulas of flavor observables

B.1.1 $K_L \rightarrow \mu e$

The branching fraction of $K_L \rightarrow e_i e_j$ is given by

$$\begin{aligned} \text{BR}(K_L \rightarrow e_i e_j) & \quad (\text{B.1}) \\ &= \frac{\tau_{K_L}}{512\pi m_X^4} (m_{e_i} + m_{e_j})^2 m_K f_K^2 \sqrt{\left(1 - \frac{(m_{e_i} + m_{e_j})^2}{m_K^2}\right) \left(1 - \frac{(m_{e_i} - m_{e_j})^2}{m_K^2}\right)} \\ &\times \left[\left| [\hat{g}_{d_L}^X]_{2i} [\hat{g}_{d_L}^X]_{1j}^* + [\hat{g}_{d_R}^X]_{2i} [\hat{g}_{d_R}^X]_{1j}^* \right. \right. \\ &\quad \left. \left. - \frac{2m_K^2}{(m_{e_i} + m_{e_j})(m_d + m_s)} \left([\hat{g}_{d_R}^X]_{2i} [\hat{g}_{d_L}^X]_{1j}^* + [\hat{g}_{d_L}^X]_{2i} [\hat{g}_{d_R}^X]_{1j}^* \right) \right|^2 \left(1 - \frac{(m_{e_i} - m_{e_j})^2}{m_K^2}\right) \right. \\ &\quad \left. + \left| \frac{2m_K^2}{(m_{e_i} + m_{e_j})(m_d + m_s)} \left([\hat{g}_{d_R}^X]_{2i} [\hat{g}_{d_L}^X]_{1j}^* - [\hat{g}_{d_L}^X]_{2i} [\hat{g}_{d_R}^X]_{1j}^* \right) \right|^2 \left(1 - \frac{(m_{e_i} + m_{e_j})^2}{m_K^2}\right) \right] \\ &\quad + (i \leftrightarrow j), \end{aligned}$$

where $m_{e_{i(j)}}$ is the masses of $i(j)$ -th generation charged lepton. In our numerical analysis, we included contributions from the Higgs bosons and adjoint scalar h_Δ, Δ_8 , but we have seen that

Table 3: Values of vector [107] and scalar [108] form factors. The coefficients S_N, V_N are calculated in Ref. [109]. The capture rates are given in Ref. [109, 110].

$f_{V_p}^u$	$f_{V_p}^d$	$f_{V_n}^u$	$f_{V_n}^d$	$f_{V_p}^s = f_{V_n}^s$
2	1	1	2	0
$f_{S_p}^u$	$f_{S_p}^d$	$f_{S_n}^u$	$f_{S_n}^d$	$f_{S_p}^s = f_{S_n}^s$
0.0191	0.0363	0.0171	0.0404	0.043

Target	S_p	S_n	V_p	V_n	$\Gamma_{\text{capt}} [10^6 \cdot s^{-1}]$
Au	0.0614	0.0918	0.0974	0.146	13.07
Al	0.0155	0.0167	0.0161	0.0173	0.705

these are always negligible compared with those from the leptoquark due to the small flavor violating coupling to the charged leptons as discussed in Appendix A. We use the same formula for the other leptonic decays of B, B_s and B_c mesons by formally replacing coupling matrices and flavor indices appropriately. The values of constants used in our numerical analysis is shown in Table 2, and the values of observables at the benchmark point are shown in the next section.

B.1.2 μ - e conversion

For the flavor violation involving the electron, μ - e conversion is also severely constrained particularly in the future experiments. The conversion rate is given by [107]

$$\Gamma_{\text{conv}} = 4m_\mu^5 \left(\left| \sum_{N=p,n} \left(\tilde{C}_{VL}^N V_N + m_N \tilde{C}_{SL}^N S_N \right) \right|^2 + \left| \sum_{N=p,n} \left(\tilde{C}_{VR}^N V_N + m_N \tilde{C}_{SR}^N S_N \right) \right|^2 \right), \quad (\text{B.2})$$

where

$$\tilde{C}_{VL}^N = \sum_{q=u,d,s} C_{VL}^q f_{V_N}^q, \quad \tilde{C}_{SL}^N = \sum_{q=u,d,s} C_{SL}^q f_{S_N}^q + \frac{2}{27} f_G^N \sum_{Q=c,b,t} C_{SL}^Q, \quad (\text{B.3})$$

$$\tilde{C}_{VR}^N = \sum_{q=u,d,s} C_{VR}^q f_{V_N}^q, \quad \tilde{C}_{SR}^N = \sum_{q=u,d,s} C_{SR}^q f_{S_N}^q + \frac{2}{27} f_G^N \sum_{Q=c,b,t} C_{SR}^Q. \quad (\text{B.4})$$

The values for form factors are shown in Table 3 and $f_G^N = 1 - \sum_{q=u,d,s} f_{S_N}^q$. In our model, the coefficients are given by

$$C_{VL}^{d_i} = \frac{[\hat{g}_{d_L}^X]^* [\hat{g}_{d_L}^X]_{i2}}{2m_X^2}, \quad C_{VR}^{d_i} = \frac{[\hat{g}_{d_R}^X]^* [\hat{g}_{d_R}^X]_{i2}}{2m_X^2}, \quad (\text{B.5})$$

and

$$C_{SL}^{d_i} = -\frac{1}{m_{d_i}} \left[\frac{[\hat{g}_{d_L}^X]^* [\hat{g}_{d_R}^X]_{i2}}{m_X^2} + \sum_S \frac{1}{2m_S^2} [\hat{Y}_e^S]_{12} \operatorname{Re} \left([\hat{Y}_d^S]_{ii} \right) \right], \quad (\text{B.6})$$

$$C_{SR}^{d_i} = -\frac{1}{m_{d_i}} \left[\frac{[\hat{g}_{d_R}^X]^* [\hat{g}_{d_L}^X]_{i2}}{m_X^2} + \sum_S \frac{1}{2m_S^2} [\hat{Y}_e^S]_{21}^* \operatorname{Re} \left([\hat{Y}_d^S]_{ii} \right) \right], \quad (\text{B.7})$$

$$C_{SL}^{u_i} = -\frac{1}{m_{u_i}} \sum_S \frac{1}{2m_S^2} [\hat{Y}_e^S]_{12} \operatorname{Re} \left([\hat{Y}_u^S]_{ii} \right), \quad (\text{B.8})$$

$$C_{SR}^{u_i} = -\frac{1}{m_{u_i}} \sum_S \frac{1}{2m_S^2} [\hat{Y}_e^S]_{21}^* \operatorname{Re} \left([\hat{Y}_u^S]_{ii} \right), \quad (\text{B.9})$$

where S runs over all the neutral scalar fields.

B.2 Benchmark

We show the values of parameters at a benchmark point whose the input parameters are given by

$$D_{Q_{L,R}} \sim D_{\ell_{L,R}} \sim 5 \text{ TeV}, \quad m_N = 10 \text{ TeV}, \quad \delta_u = \delta_d = 10^{-4}, \quad (\text{B.10})$$

and the angles for $V_{Q_{L,R}}, V_{\ell_{L,R}}$ are $s_Q = 0.00078$ and $s_\ell = 0.00072$. The other unitary matrices in $W_{Q_{L,R}}, W_{\ell_{L,R}}$ and $w_{Q_{L,R}}, w_{\ell_{L,R}}$ are taken to be identity. The other parameters are fitted such that the SM fermion masses, CKM and PMNS matrices are explained. The mass matrices in Eq. (2.24) are given by

$$\bar{D}_d = \begin{pmatrix} 0 & 0 & 0 & 0.000502716 & 0. & 0. \\ 0 & 0 & 0 & 0. & 0.146787 & 0. \\ 0 & 0 & 0 & 0. & 0. & 1.80177 \\ 0.00211529 & 0. & 0. & 0. & 0 & 0 \\ 0. & 0.0417809 & 0. & 0 & 0 & 0 \\ 0. & 0. & 2.97755 & 0 & 0 & 0 \end{pmatrix}, \quad (\text{B.11})$$

$$\bar{D}_u = \begin{pmatrix} 0.00000060 \cdot e^{-2.2460i} & 0.00001279 \cdot e^{-1.0960i} & 0.00488531 \cdot e^{-2.7440i} & 0.00001386 \cdot e^{0.0987i} & 0.00015155 \cdot e^{0.0092i} & 0.00013351 \cdot e^{2.1100i} \\ 0.00000181 \cdot e^{-3.1020i} & 0.00002292 \cdot e^{-3.1350i} & 0.00697150 \cdot e^{-3.0540i} & 0.00007441 \cdot e^{3.1210i} & 0.00003288 \cdot e^{0.5167i} & 0.00036822 \cdot e^{0.0012i} \\ 0.00000197 \cdot e^{-3.0910i} & 0.00006067 \cdot e^{-3.1380i} & 0.00863796 \cdot e^{-3.0440i} & 0.00006500 \cdot e^{0.0333i} & 0.00002488 \cdot e^{1.1330i} & 0.00051000 \cdot e^{0.0012i} \\ 0.00111051 \cdot e^{0.0579i} & 0.10784074 \cdot e^{3.1410i} & 1.22353000 \cdot e^{0.3833i} & 0.00080864 \cdot e^{-2.7230i} & 0.00080780 \cdot e^{-2.7230i} & 0.00081043 \cdot e^{-2.7230i} \\ 0.00057303 \cdot e^{3.1160i} & 0.46812929 & 5.64585730 \cdot e^{3.1230i} & 0.00371601 \cdot e^{-0.0204i} & 0.00371740 \cdot e^{-0.0204i} & 0.00373373 \cdot e^{-0.0203i} \\ 0.02694553 \cdot e^{0.0001i} & 0.01657569 & 191.73898000 & 0.13766851 \cdot e^{-3.1420i} & 0.13769853 \cdot e^{-3.1420i} & -0.13788805 \end{pmatrix}, \quad (\text{B.12})$$

$$V_{Q_R}^* \bar{D}_{Q_R}^T = \begin{pmatrix} 3.90023160 & 3.90030370 & 3.90037580 \\ 3.90023280 & 3.90030730 & 3.90038170 \\ 3.90023400 & 3.90031080 & 3.90038760 \\ 5000.29540000 & -0.00912672 & -0.00912690 \\ 0.00000000 & 5000.39540000 & -0.00912691 \\ 0.00000000 & 0.00000000 & 5000.49540000 \end{pmatrix}, \quad V_{Q_L} \bar{D}_{Q_L} = \begin{pmatrix} 4999.99540000 & -2.82413960 & -0.00818287 \\ 0.00000000 & 3551.78620000 & -2.85575350 \\ 0.00000000 & 0.00000000 & 5000.19540000 \\ -3.89999760 & -2.76819210 & -3.89792210 \\ -3.89999880 & -99.99485400 & -3.82138210 \\ -3.90000000 & -3517.92550000 & -2.77154640 \end{pmatrix}, \quad (\text{B.13})$$

$$V_{\ell_R}^* \bar{D}_{\ell_R}^T = \begin{pmatrix} 5000.89610000 & -0.00777755 & -0.00777770 \\ 0.00000000 & 5000.99610000 & -0.00777771 \\ 0.00000000 & 0.00000000 & 5001.09610000 \\ -3.60064610 & -3.60071350 & -3.60078080 \\ -3.60064710 & -3.60071630 & -3.60078550 \\ -3.60064800 & -3.60071910 & -3.60079010 \end{pmatrix}, \quad V_{\ell_L} \bar{D}_{\ell_L} = \begin{pmatrix} 3.60043010 & 3.59914710 & 2.48918270 \\ 3.60043110 & -140.73388000 & -3517.02360000 \\ 3.60043200 & 3.60050310 & 3.60057410 \\ 5000.59610000 & 0.09614469 & 2.52787370 \\ 0.00000000 & 4998.71670000 & -99.02272300 \\ 0.00000000 & 0.00000000 & 3553.69030000 \end{pmatrix}, \quad (\text{B.14})$$

The charged fermion Dirac masses are given by

$$\begin{aligned}
m_i^e &= (0.00050112, 0.105789, 1.80177, 4999.87, 5000.6, 5000.7, 5000.9, 5001., 5002.03), \\
m_i^d &= (0.0021141, 0.04176, 2.11584, 4999.43, 5000., 5000.09, 5000.3, 5000.41, 5001.27), \\
m_i^u &= (0.0009744, 0.479892, 136.433, 5000., 5000.2, 5000.3, 5000.4, 5000.5, 5001.92). \tag{B.15}
\end{aligned}$$

The neutral fermion Majorana masses are given by

$$\begin{aligned}
m_i^n &= (3.38664 \cdot 10^{-13}, 8.68414 \cdot 10^{-12}, 5.01938 \cdot 10^{-11}, \\
&4934.06, 4934.06, 5000.55, 5000.55, 5000.61, 5000.61, 5000.89, 5000.9, \\
&5001.13, 5001.14, 5070.58, 5070.59, 10000., 10000., 10000.). \tag{B.16}
\end{aligned}$$

The W-boson couplings are proportional to

$$(U_L^u)^\dagger P_6 U_L^d = \tag{B.17}$$

0.9745	0.2245	0.0036 · e ^{-1.20i}	0.0000	0.0000 · e ^{-0.49i}	0.0000 · e ^{-0.30i}	0.0000 · e ^{-0.43i}	0.0000 · e ^{2.80i}	0.0000 · e ^{-3.10i}	0.0000 · e ^{-3.10i}
0.2244 · e ^{-3.10i}	0.9736	0.0421	0.0000	0.0000	0.0000	0.0000	0.0000 · e ^{-3.10i}	0.0000 · e ^{-3.10i}	0.0000 · e ^{-3.10i}
0.0090 · e ^{-0.38i}	0.0413 · e ^{-3.10i}	0.9991	0.0000 · e ^{0.02i}	0.0000 · e ^{3.10i}	0.0007 · e ^{-3.10i}	0.0000 · e ^{-3.10i}	0.0002 · e ^{-3.10i}	0.0002 · e ^{-3.10i}	-0.0000
0.0000 · e ^{-0.42i}	0.0000 · e ^{-3.10i}	0.0000	0.0000 · e ^{1.50i}	0.9991	0.0007 · e ^{-3.10i}	0.0298 · e ^{-3.10i}	0.0002 · e ^{-3.10i}	0.0000 · e ^{1.40i}	0.0000 · e ^{1.40i}
0.0000 · e ^{-2.80i}	0.0000 · e ^{0.73i}	0.0000 · e ^{-2.40i}	0.7621 · e ^{0.72i}	0.0000 · e ^{3.00i}	0.0000	0.0000 · e ^{-0.33i}	0.0000 · e ^{-2.30i}	0.6468 · e ^{0.72i}	0.0000 · e ^{0.72i}
0.0000 · e ^{-0.22i}	0.0000 · e ^{-3.10i}	0.0000	0.0002 · e ^{-0.03i}	0.0290	0.0025	0.0009 · e ^{-3.10i}	0.0005	0.0002 · e ^{-0.03i}	0.0000 · e ^{-0.03i}
0.0000 · e ^{-0.41i}	0.0000 · e ^{-3.10i}	0.0000 · e ^{-0.01i}	0.0000 · e ^{1.00i}	0.0002 · e ^{-3.10i}	0.0029	0.0000	0.0006	0.0000 · e ^{1.00i}	0.0000 · e ^{1.00i}
0.0000 · e ^{-1.30i}	0.0000 · e ^{2.10i}	0.0000 · e ^{-1.00i}	0.0227 · e ^{-1.00i}	0.0001 · e ^{-3.10i}	0.0028 · e ^{-1.00i}	0.0000 · e ^{-0.73i}	0.0005 · e ^{-1.00i}	0.0193 · e ^{-1.00i}	0.0000 · e ^{-1.00i}
0.0000 · e ^{-0.36i}	0.0000 · e ^{-3.10i}	0.0007 · e ^{0.03i}	0.0001 · e ^{-3.10i}	0.0008 · e ^{0.01i}	0.9819 · e ^{0.03i}	0.0034 · e ^{0.03i}	0.1894 · e ^{0.03i}	0.0000 · e ^{-0.26i}	0.0000 · e ^{-0.26i}

$$(U_L^n)^\dagger P_6 U_L^e = \tag{B.18}$$

0.7900 · e ^{-0.83i}	0.3877 · e ^{2.40i}	0.4748 · e ^{-0.41i}	0.0001 · e ^{2.40i}	0.0000 · e ^{-0.38i}	0.0000 · e ^{-0.59i}	0.0000 · e ^{2.80i}	0.0000 · e ^{-0.59i}	0.0001 · e ^{-0.77i}	0.0000 · e ^{-0.77i}
0.5949 · e ^{1.30i}	0.5746 · e ^{1.70i}	0.5619 · e ^{-1.70i}	0.0002 · e ^{1.70i}	0.0000 · e ^{-1.70i}	0.0000 · e ^{-1.60i}	0.0000 · e ^{1.40i}	0.0000 · e ^{-1.60i}	0.0002 · e ^{-1.50i}	0.0000 · e ^{-1.50i}
0.1482 · e ^{0.13i}	0.7202 · e ^{-1.60i}	0.6774 · e ^{-1.60i}	0.0002 · e ^{-1.60i}	0.0000 · e ^{-1.60i}	0.0000 · e ^{1.60i}	0.0000 · e ^{1.60i}	0.0000 · e ^{1.60i}	0.0002 · e ^{1.60i}	0.0000 · e ^{1.60i}
0.0000 · e ^{-3.10i}	0.0135	0.0000 · e ^{-0.12i}	0.3774	0.0045 · e ^{-2.80i}	0.0206 · e ^{-0.02i}	0.0001 · e ^{-2.80i}	0.0020 · e ^{3.10i}	0.3280	0.0000 · e ^{3.10i}
0.0000 · e ^{-1.60i}	0.0135 · e ^{1.60i}	0.0000 · e ^{1.40i}	0.3774 · e ^{1.60i}	0.0045 · e ^{-1.20i}	0.0206 · e ^{1.60i}	0.0001 · e ^{-1.20i}	0.0020 · e ^{-1.60i}	0.3280 · e ^{1.60i}	0.0000 · e ^{1.60i}
0.0000 · e ^{-3.10i}	0.0000 · e ^{-0.02i}	0.0000 · e ^{-3.10i}	0.0185 · e ^{-0.03i}	0.3424	0.5213 · e ^{-3.10i}	0.1111	0.0509	0.0161 · e ^{-0.03i}	0.0000 · e ^{-0.03i}
0.0000 · e ^{-1.50i}	0.0000 · e ^{1.60i}	0.0000 · e ^{-1.60i}	0.0185 · e ^{1.50i}	0.3473 · e ^{1.60i}	0.5200 · e ^{-1.60i}	0.1113 · e ^{1.60i}	0.0508 · e ^{1.60i}	0.0161 · e ^{1.50i}	0.0000 · e ^{1.50i}
0.0000 · e ^{-3.10i}	0.0000 · e ^{0.16i}	-0.0000	0.0065 · e ^{0.27i}	-0.6148	-0.3247	-0.0200	0.0317	0.0057 · e ^{0.27i}	0.0000 · e ^{0.27i}
0.0000 · e ^{-1.50i}	0.0000 · e ^{1.70i}	0.0000 · e ^{-1.60i}	0.0067 · e ^{1.80i}	0.6120 · e ^{-1.60i}	0.3294 · e ^{-1.60i}	0.0199 · e ^{-1.60i}	0.0322 · e ^{1.60i}	0.0058 · e ^{1.80i}	0.0000 · e ^{1.80i}
0.0000 · e ^{0.06i}	0.0000 · e ^{-3.10i}	0.0000	0.0006 · e ^{0.10i}	0.0192 · e ^{-3.10i}	0.0203 · e ^{-3.10i}	0.0006 · e ^{-3.10i}	0.0020	0.0005 · e ^{0.10i}	0.0000 · e ^{0.10i}
0.0000 · e ^{1.70i}	0.0000 · e ^{-1.50i}	0.0000 · e ^{1.60i}	0.0002 · e ^{1.90i}	0.0205 · e ^{-1.60i}	0.0091 · e ^{-1.60i}	0.0007 · e ^{-1.60i}	0.0009 · e ^{1.60i}	0.0002 · e ^{1.90i}	0.0000 · e ^{1.90i}
0.0000 · e ^{0.04i}	0.0000 · e ^{-3.10i}	0.0000	0.0112	0.0624	0.3418 · e ^{-3.10i}	0.0020	0.0334	0.0097	0.0000 · e ^{-3.10i}
0.0000 · e ^{1.60i}	0.0000 · e ^{-1.60i}	0.0000 · e ^{1.60i}	0.0111 · e ^{1.60i}	0.0619 · e ^{1.60i}	0.3397 · e ^{-1.60i}	0.0020 · e ^{1.60i}	0.0332 · e ^{1.60i}	0.0096 · e ^{1.60i}	0.0000 · e ^{1.60i}
0.0000 · e ^{-3.10i}	0.0135	0.0000 · e ^{-0.12i}	-0.3767	0.0045 · e ^{0.38i}	0.0205 · e ^{3.10i}	0.0001 · e ^{0.38i}	0.0020 · e ^{-0.02i}	-0.3274	0.0000 · e ^{-0.02i}
0.0000 · e ^{-1.60i}	0.0135 · e ^{1.60i}	0.0000 · e ^{1.40i}	0.3767 · e ^{-1.60i}	0.0045 · e ^{2.00i}	0.0205 · e ^{-1.60i}	0.0001 · e ^{1.90i}	0.0020 · e ^{1.60i}	0.3274 · e ^{-1.60i}	0.0000 · e ^{-1.60i}
0.0000 · e ^{1.10i}	0.0000 · e ^{-0.22i}	0.0000 · e ^{-0.56i}	0.0000 · e ^{-0.32i}	0.0000 · e ^{1.90i}	0.0000 · e ^{-0.76i}	0.0000 · e ^{2.00i}	0.0000 · e ^{2.40i}	0.0000 · e ^{-0.32i}	0.0000 · e ^{-0.32i}
0.0000 · e ^{2.70i}	0.0000 · e ^{-0.40i}	0.0000 · e ^{-0.17i}	0.0000 · e ^{-0.27i}	0.0000 · e ^{-3.00i}	0.0000 · e ^{-0.04i}	0.0000 · e ^{-3.00i}	0.0000 · e ^{3.10i}	0.0000 · e ^{-0.27i}	0.0000 · e ^{-0.27i}
0.0000 · e ^{0.23i}	-0.0000	0.0000 · e ^{0.05i}	0.0000	0.0000 · e ^{-2.70i}	0.0000 · e ^{-0.02i}	0.0000 · e ^{-2.70i}	0.0000 · e ^{3.10i}	0.0000	0.0000 · e ^{3.10i}

$$(U_R^u)^\dagger P_6 U_R^d = \tag{B.19}$$

0.0000 · e ^{-0.11i}	0.0000 · e ^{-0.23i}	0.0000 · e ^{-0.26i}	0.0000 · e ^{-3.10i}	0.0000 · e ^{2.80i}	0.0000 · e ^{2.90i}	0.0000 · e ^{3.00i}	0.0000 · e ^{2.90i}	0.0000 · e ^{-3.10i}	0.0000 · e ^{-3.10i}
0.0000	0.0000	0.0000	0.0000 · e ^{-3.10i}	0.0000 · e ^{3.10i}	0.0000 · e ^{-3.10i}				
0.0000	0.0000	0.0000	0.0000 · e ^{0.05i}	0.0000 · e ^{3.10i}	0.0265 · e ^{-3.10i}	0.0001 · e ^{-3.10i}	0.0051 · e ^{-3.10i}	0.0000 · e ^{1.50i}	0.0000 · e ^{1.50i}
-0.0000	-0.0000	0.0000 · e ^{0.90i}	0.0000 · e ^{1.50i}	0.9991	0.0007 · e ^{-3.10i}	0.0298 · e ^{-3.10i}	0.0002 · e ^{-3.10i}	0.0000 · e ^{1.40i}	0.0000 · e ^{1.40i}
0.0000 · e ^{-2.40i}	0.0000 · e ^{-2.40i}	0.0000 · e ^{-2.40i}	0.7622 · e ^{0.72i}	0.0000 · e ^{3.00i}	0.0000	0.0000 · e ^{-0.33i}	0.0000 · e ^{-2.30i}	0.6467 · e ^{0.72i}	0.0000 · e ^{0.72i}
0.0000 · e ^{3.10i}	-0.0000	-0.0000	0.0002 · e ^{-0.03i}	0.0290	0.0025	0.0009 · e ^{-3.10i}	0.0005	0.0002 · e ^{-0.03i}	0.0000 · e ^{-0.03i}
0.0000 · e ^{-3.00i}	0.0000 · e ^{-3.10i}	0.0000 · e ^{3.10i}	0.0000 · e ^{1.00i}	0.0002 · e ^{-3.10i}	0.0029	0.0000	0.0006	0.0000 · e ^{1.00i}	0.0000 · e ^{1.00i}
0.0000 · e ^{2.10i}	0.0000 · e ^{2.10i}	0.0000 · e ^{2.10i}	0.0227 · e ^{-1.00i}	0.0001 · e ^{-3.10i}	0.0028 · e ^{-1.00i}	0.0000 · e ^{-0.73i}	0.0005 · e ^{-1.00i}	0.0193 · e ^{-1.00i}	0.0000 · e ^{-1.00i}
0.0000 · e ^{-3.10i}	0.0000 · e ^{-3.10i}	0.0004 · e ^{-3.10i}	0.0001 · e ^{-3.10i}	0.0008 · e ^{0.01i}	0.9815 · e ^{0.03i}	0.0034 · e ^{0.03i}	0.1893 · e ^{0.03i}	0.0000 · e ^{-0.26i}	0.0000 · e ^{-0.26i}

$$(U_R^n)^\dagger P_6 U_R^e = \tag{B.21}$$

$$\begin{pmatrix}
0.0000 \cdot e^{-0.64i} & 0.0000 \cdot e^{2.50i} & 0.0000 \cdot e^{-0.70i} & 0.0000 \cdot e^{-0.64i} & 0.0000 \cdot e^{1.80i} & 0.0000 \cdot e^{2.80i} & 0.0000 \cdot e^{1.80i} & 0.0000 \cdot e^{-0.29i} & 0.0000 \cdot e^{-0.64i} \\
0.0000 \cdot e^{-1.50i} & 0.0000 \cdot e^{1.60i} & 0.0000 \cdot e^{-1.50i} & 0.0000 \cdot e^{-1.50i} & 0.0000 \cdot e^{-1.70i} & 0.0000 \cdot e^{-2.10i} & 0.0000 \cdot e^{-1.70i} & 0.0000 \cdot e^{1.10i} & 0.0000 \cdot e^{-1.50i} \\
0.0000 \cdot e^{1.70i} & 0.0000 \cdot e^{-1.50i} & 0.0000 \cdot e^{1.60i} & 0.0000 \cdot e^{1.70i} & 0.0000 \cdot e^{-1.40i} & 0.0000 \cdot e^{1.80i} & 0.0000 \cdot e^{-1.40i} & 0.0000 \cdot e^{-1.30i} & 0.0000 \cdot e^{1.70i} \\
0.0000 & -0.0000 & 0.0000 & 0.3825 & 0.0046 \cdot e^{2.80i} & 0.0209 \cdot e^{0.02i} & 0.0002 \cdot e^{2.80i} & 0.0021 \cdot e^{-3.10i} & 0.3324 \\
0.0000 \cdot e^{-1.60i} & 0.0000 \cdot e^{1.60i} & 0.0000 \cdot e^{-1.60i} & 0.3825 \cdot e^{-1.60i} & 0.0046 \cdot e^{1.20i} & 0.0209 \cdot e^{-1.60i} & 0.0002 \cdot e^{1.20i} & 0.0021 \cdot e^{1.60i} & 0.3324 \cdot e^{-1.60i} \\
0.0000 \cdot e^{0.02i} & 0.0000 \cdot e^{-3.10i} & 0.0000 & 0.0185 \cdot e^{0.03i} & 0.3424 & -0.5214 & 0.0111 & 0.0509 & 0.0161 \cdot e^{0.03i} \\
0.0000 \cdot e^{-1.60i} & 0.0000 \cdot e^{1.60i} & 0.0000 \cdot e^{-1.60i} & 0.0185 \cdot e^{-1.50i} & 0.3473 \cdot e^{-1.60i} & 0.5201 \cdot e^{1.60i} & 0.0113 \cdot e^{-1.60i} & 0.0508 \cdot e^{-1.60i} & 0.0161 \cdot e^{-1.50i} \\
0.0000 \cdot e^{-0.13i} & 0.0000 \cdot e^{3.00i} & 0.0000 & 0.0066 \cdot e^{-0.27i} & 0.6148 \cdot e^{-3.10i} & 0.3247 \cdot e^{-3.10i} & 0.0200 \cdot e^{-3.10i} & 0.0317 & 0.0057 \cdot e^{-0.27i} \\
0.0000 \cdot e^{-1.70i} & 0.0000 \cdot e^{1.50i} & 0.0000 \cdot e^{-1.60i} & 0.0067 \cdot e^{-1.80i} & 0.6120 \cdot e^{1.60i} & 0.3294 \cdot e^{1.60i} & 0.0199 \cdot e^{1.60i} & 0.0322 \cdot e^{-1.60i} & 0.0058 \cdot e^{-1.80i} \\
0.0000 \cdot e^{-0.06i} & 0.0000 \cdot e^{3.10i} & 0.0000 & 0.0006 \cdot e^{-0.10i} & -0.0192 & -0.0203 & -0.0006 & 0.0020 & 0.0005 \cdot e^{-0.10i} \\
0.0000 \cdot e^{-1.70i} & 0.0000 \cdot e^{1.40i} & 0.0000 \cdot e^{-1.60i} & 0.0002 \cdot e^{-1.90i} & 0.0205 \cdot e^{1.60i} & 0.0091 \cdot e^{1.60i} & 0.0007 \cdot e^{1.60i} & 0.0009 \cdot e^{-1.60i} & 0.0002 \cdot e^{-1.90i} \\
0.0000 & -0.0000 & 0.0000 & 0.0112 & 0.0624 & -0.3418 & 0.0020 & 0.0334 & 0.0097 \\
0.0000 \cdot e^{-1.60i} & 0.0000 \cdot e^{-1.60i} & 0.0000 \cdot e^{-1.60i} & 0.0111 \cdot e^{-1.60i} & 0.0619 \cdot e^{-1.60i} & 0.3397 \cdot e^{1.60i} & 0.0020 \cdot e^{-1.60i} & 0.0332 \cdot e^{-1.60i} & 0.0096 \cdot e^{-1.60i} \\
-0.0000 & 0.0000 & -0.0000 & 0.3716 \cdot e^{-3.10i} & 0.0044 \cdot e^{-0.38i} & 0.0202 \cdot e^{-3.10i} & 0.0001 \cdot e^{-0.38i} & 0.0020 \cdot e^{0.02i} & 0.3228 \cdot e^{-3.10i} \\
0.0000 \cdot e^{1.60i} & 0.0000 \cdot e^{-1.60i} & 0.0000 \cdot e^{1.60i} & 0.3716 \cdot e^{1.60i} & 0.0044 \cdot e^{-2.00i} & 0.0202 \cdot e^{1.60i} & 0.0001 \cdot e^{-1.90i} & 0.0020 \cdot e^{-1.60i} & 0.3228 \cdot e^{1.60i} \\
0.0000 \cdot e^{-0.34i} & 0.0000 \cdot e^{2.80i} & 0.0000 \cdot e^{-0.34i} & 0.0000 \cdot e^{-0.34i} & 0.0000 \cdot e^{1.50i} & 0.0000 \cdot e^{-0.69i} & 0.0000 \cdot e^{1.50i} & 0.0000 \cdot e^{2.50i} & 0.0000 \cdot e^{-0.34i} \\
0.0000 \cdot e^{-0.22i} & 0.0000 \cdot e^{2.90i} & 0.0000 \cdot e^{-0.22i} & 0.0000 \cdot e^{-0.22i} & 0.0000 \cdot e^{3.00i} & 0.0000 \cdot e^{-0.15i} & 0.0000 \cdot e^{3.00i} & 0.0000 \cdot e^{3.00i} & 0.0000 \cdot e^{-0.22i} \\
0.0000 & -0.0000 & 0.0000 & 0.0000 & 0.0000 \cdot e^{2.70i} & 0.0000 \cdot e^{0.02i} & 0.0000 \cdot e^{2.70i} & 0.0000 \cdot e^{-3.10i} & 0.0000
\end{pmatrix}$$

The upper-left 3×3 block of $U_{uL}^\dagger P_6 U_{dL}$ and $U_{nL}^\dagger P_6 U_{eL}$ correspond to the CKM matrix and hermitian conjugate of the PMNS matrix, respectively. We also note that the W-boson coupling to the SM fermions in the right-handed current are negligible. The leptoquark couplings with $g_4 = 1$ are given by

$$\hat{g}_{dL}^X = \begin{pmatrix}
0.0000 & 0.0000 & 0.0000 & 0.0000 & 0.7067 & 0.0000 & 0.0230 & 0.0000 \cdot e^{-3.10i} & 0.0000 \\
0.0000 & 0.0283 & 0.0001 & 0.0211 & 0.0000 \cdot e^{-3.10i} & 0.7026 & 0.0000 & 0.0686 \cdot e^{-3.10i} & 0.0184 \\
0.0000 \cdot e^{-3.10i} & 0.7065 & 0.0012 & 0.0055 \cdot e^{-3.10i} & 0.0000 \cdot e^{-3.10i} & 0.0279 \cdot e^{-3.10i} & 0.0000 \cdot e^{-3.10i} & 0.0027 & 0.0052 \cdot e^{-3.10i} \\
0.0000 & 0.0007 & -0.5391 & 0.3009 & 0.0000 & -0.0000 & -0.0000 & -0.0001 & -0.3447 \\
-0.7068 & -0.0000 & 0.0000 & 0.0001 & -0.0006 & 0.0000 & 0.0211 & 0.0000 & 0.0001 \\
-0.0002 & -0.0064 & -0.0012 & -0.5235 & 0.0001 & 0.0146 & -0.0027 & -0.1360 & -0.4551 \\
0.0211 & -0.0000 & -0.0000 & -0.0018 & -0.0230 & -0.0001 & 0.7064 & -0.0015 & -0.0016 \\
0.0000 & -0.0012 & -0.0002 & -0.1009 & -0.0000 & 0.0728 & 0.0010 & 0.6905 & -0.0879 \\
-0.0000 & 0.0010 & -0.4576 & -0.3531 & 0.0000 & 0.0000 & 0.0000 & 0.0001 & 0.4074
\end{pmatrix}, \quad (B.22)$$

$$\hat{g}_{dR}^X = \begin{pmatrix}
0.0000 \cdot e^{-3.10i} & 0.0000 \cdot e^{-3.10i} & 0.0000 \cdot e^{-3.10i} & 0.0000 & 0.0230 \cdot e^{-3.10i} & 0.0000 \cdot e^{-3.10i} & 0.7067 & 0.0001 \cdot e^{-3.10i} & 0.0000 \cdot e^{-3.10i} \\
0.0000 \cdot e^{-3.10i} & 0.0000 \cdot e^{-3.10i} & 0.0000 \cdot e^{-3.10i} & 0.0000 & 0.0000 & 0.0687 \cdot e^{-3.10i} & 0.0001 \cdot e^{-3.10i} & 0.7038 \cdot e^{-3.10i} & 0.0001 \cdot e^{-3.10i} \\
0.0000 \cdot e^{-3.10i} & 0.0000 \cdot e^{-3.10i} & 0.0000 \cdot e^{-3.10i} & 0.4638 & 0.0000 & 0.0003 & 0.0001 \cdot e^{-3.10i} & 0.0000 & 0.5338 \cdot e^{-3.10i} \\
0.0000 & -0.0001 & 0.4575 & 0.4070 & -0.0000 & 0.0006 & 0.0000 & -0.0001 & 0.3536 \\
0.0211 & 0.0003 & 0.0000 & 0.0000 & -0.7064 & 0.0002 & -0.0230 & -0.0000 & -0.0000 \\
-0.0046 & 0.1339 & 0.0001 & 0.0007 & -0.0003 & -0.6910 & -0.0000 & 0.0675 & 0.0002 \\
0.7067 & 0.0116 & 0.0000 & 0.0000 & 0.0211 & -0.0024 & 0.0007 & 0.0002 & -0.0000 \\
0.0109 & -0.6942 & -0.0001 & 0.0001 & 0.0000 & -0.1333 & -0.0000 & 0.0131 & 0.0001 \\
-0.0000 & 0.0001 & -0.5392 & 0.3453 & 0.0000 & 0.0004 & -0.0000 & -0.0000 & 0.3001
\end{pmatrix}, \quad (B.23)$$

$$(\hat{g}_{uL}^X)^\dagger = \begin{pmatrix}
0.0029 \cdot e^{-2.00i} & 0.0221 \cdot e^{-2.40i} & 0.2727 \cdot e^{-2.40i} & 0.5584 \cdot e^{-2.30i} & 0.3358 \cdot e^{2.80i} & 0.0163 \cdot e^{-2.30i} & 0.0001 \cdot e^{1.10i} & 0.0171 \cdot e^{-1.60i} & 0.0013 \cdot e^{0.84i} \\
0.0044 \cdot e^{-1.40i} & 0.0329 \cdot e^{-1.70i} & 0.4043 \cdot e^{-1.70i} & 0.4204 \cdot e^{1.80i} & 0.3975 \cdot e^{-2.20i} & 0.0121 \cdot e^{1.80i} & 0.0001 \cdot e^{-1.60i} & 0.0227 \cdot e^{-0.56i} & 0.0032 \cdot e^{1.40i} \\
0.0055 \cdot e^{1.90i} & 0.0414 \cdot e^{1.50i} & 0.5083 \cdot e^{1.50i} & 0.1048 \cdot e^{3.00i} & 0.4784 \cdot e^{-2.30i} & 0.0030 \cdot e^{3.10i} & 0.0000 \cdot e^{-1.90i} & 0.0006 \cdot e^{-0.25i} & 0.0051 \cdot e^{-1.60i} \\
0.0039 \cdot e^{0.32i} & 0.0291 & 0.0042 & 0.0004 \cdot e^{-0.12i} & 0.0111 \cdot e^{-0.72i} & 0.0010 \cdot e^{-3.10i} & 0.0011 \cdot e^{-3.10i} & 0.3539 \cdot e^{-2.10i} & 0.3518 \cdot e^{3.10i} \\
0.0039 \cdot e^{-1.30i} & 0.0291 \cdot e^{-1.60i} & 0.0042 \cdot e^{-1.60i} & 0.0004 \cdot e^{-1.70i} & 0.0111 \cdot e^{-2.30i} & 0.0010 \cdot e^{1.60i} & 0.0011 \cdot e^{1.60i} & 0.3539 \cdot e^{2.60i} & 0.3518 \cdot e^{1.50i} \\
0.1532 & -0.4131 & 0.0318 \cdot e^{0.01i} & 0.0000 & 0.0000 \cdot e^{-0.99i} & 0.0010 & 0.2319 & 0.0002 \cdot e^{-2.10i} & 0.0328 \cdot e^{3.10i} \\
0.1567 \cdot e^{-1.60i} & 0.4130 \cdot e^{1.60i} & 0.0317 \cdot e^{-1.60i} & 0.0001 \cdot e^{1.60i} & 0.0000 \cdot e^{-2.60i} & 0.0046 \cdot e^{-1.60i} & 0.2297 \cdot e^{-1.60i} & 0.0002 \cdot e^{2.60i} & 0.0327 \cdot e^{1.60i} \\
-0.4755 & -0.1260 & 0.0151 \cdot e^{-0.11i} & 0.0005 & 0.0000 \cdot e^{3.00i} & 0.0166 \cdot e^{-3.10i} & 0.0855 & 0.0001 \cdot e^{-2.30i} & 0.0154 \cdot e^{3.00i} \\
0.4743 \cdot e^{1.60i} & 0.1297 \cdot e^{1.60i} & 0.0154 \cdot e^{-1.70i} & 0.0004 \cdot e^{-1.60i} & 0.0000 \cdot e^{1.50i} & 0.0147 \cdot e^{1.60i} & 0.0865 \cdot e^{-1.60i} & 0.0001 \cdot e^{2.40i} & 0.0157 \cdot e^{1.40i} \\
-0.0165 & -0.0109 & 0.0010 \cdot e^{-0.06i} & 0.0145 \cdot e^{-3.10i} & 0.0001 \cdot e^{2.40i} & 0.4993 & 0.0113 \cdot e^{-3.10i} & 0.0001 \cdot e^{-2.20i} & 0.0024 \cdot e^{3.10i} \\
0.0156 \cdot e^{1.60i} & 0.0030 \cdot e^{1.60i} & 0.0004 \cdot e^{-1.70i} & 0.0145 \cdot e^{1.60i} & 0.0001 \cdot e^{0.82i} & 0.4995 \cdot e^{-1.60i} & 0.0051 \cdot e^{1.60i} & 0.0001 \cdot e^{2.50i} & 0.0017 \cdot e^{1.50i} \\
0.0113 \cdot e^{3.10i} & -0.2451 & 0.0199 & 0.0004 & 0.0000 \cdot e^{-0.17i} & 0.0157 \cdot e^{-3.10i} & 0.4345 \cdot e^{-3.10i} & 0.0000 \cdot e^{0.97i} & 0.0188 \cdot e^{3.10i} \\
0.0114 \cdot e^{1.60i} & 0.2436 \cdot e^{1.60i} & 0.0198 \cdot e^{-1.60i} & 0.0001 \cdot e^{-1.60i} & 0.0000 \cdot e^{-1.70i} & 0.0064 \cdot e^{1.60i} & 0.4356 \cdot e^{1.60i} & 0.0000 \cdot e^{-0.60i} & 0.0187 \cdot e^{1.50i} \\
0.0037 \cdot e^{-2.80i} & -0.0275 & 0.0148 & 0.0004 \cdot e^{-3.10i} & 0.0100 \cdot e^{-0.72i} & 0.0009 & 0.0009 & 0.3526 \cdot e^{-2.10i} & 0.3530 \cdot e^{-0.03i} \\
0.0037 \cdot e^{1.90i} & 0.0275 \cdot e^{1.60i} & 0.0148 \cdot e^{-1.60i} & 0.0004 \cdot e^{1.70i} & 0.0100 \cdot e^{-2.30i} & 0.0009 \cdot e^{-1.60i} & 0.0009 \cdot e^{-1.60i} & 0.3526 \cdot e^{2.60i} & 0.3529 \cdot e^{-1.60i} \\
0.0000 \cdot e^{0.36i} & 0.0000 \cdot e^{0.34i} & 0.0000 \cdot e^{0.21i} & 0.0000 \cdot e^{2.00i} & 0.0000 \cdot e^{3.00i} & 0.0000 \cdot e^{3.00i} & 0.0000 \cdot e^{0.39i} & 0.0000 \cdot e^{-1.40i} & 0.0000 \cdot e^{-2.90i} \\
0.0000 \cdot e^{0.53i} & 0.0000 \cdot e^{0.24i} & 0.0000 \cdot e^{0.40i} & 0.0000 \cdot e^{0.48i} & 0.0000 \cdot e^{2.60i} & 0.0000 \cdot e^{3.10i} & 0.0000 \cdot e^{0.21i} & 0.0000 \cdot e^{-2.00i} & 0.0000 \cdot e^{-2.90i} \\
0.0000 \cdot e^{0.32i} & 0.0000 & -0.0000 & -0.0000 & 0.0000 \cdot e^{2.40i} & 0.0006 & 0.0006 \cdot e^{-3.10i} & 0.0006 \cdot e^{1.00i} & 0.0000 \cdot e^{3.10i}
\end{pmatrix}, \quad (B.24)$$

$$(\hat{g}_{uL}^X)^\dagger = \begin{pmatrix}
0.0029 \cdot e^{-2.00i} & 0.0221 \cdot e^{-2.40i} & 0.2727 \cdot e^{-2.40i} & 0.5584 \cdot e^{-2.30i} & 0.3358 \cdot e^{2.80i} & 0.0163 \cdot e^{-2.30i} & 0.0001 \cdot e^{1.10i} & 0.0171 \cdot e^{-1.60i} & 0.0013 \cdot e^{0.84i} \\
0.0044 \cdot e^{-1.40i} & 0.0329 \cdot e^{-1.70i} & 0.4043 \cdot e^{-1.70i} & 0.4204 \cdot e^{1.80i} & 0.3975 \cdot e^{-2.20i} & 0.0121 \cdot e^{1.80i} & 0.0001 \cdot e^{-1.60i} & 0.0227 \cdot e^{-0.56i} & 0.0032 \cdot e^{1.40i} \\
0.0055 \cdot e^{1.90i} & 0.0414 \cdot e^{1.50i} & 0.5083 \cdot e^{1.50i} & 0.1048 \cdot e^{3.00i} & 0.4784 \cdot e^{-2.30i} & 0.0030 \cdot e^{3.10i} & 0.0000 \cdot e^{-1.90i} & 0.0006 \cdot e^{-0.25i} & 0.0051 \cdot e^{-1.60i} \\
0.0039 \cdot e^{0.32i} & 0.0291 & 0.0042 & 0.0004 \cdot e^{-0.12i} & 0.0111 \cdot e^{-0.72i} & 0.0010 \cdot e^{-3.10i} & 0.0011 \cdot e^{-3.10i} & 0.3539 \cdot e^{-2.10i} & 0.3518 \cdot e^{3.10i} \\
0.0039 \cdot e^{-1.30i} & 0.0291 \cdot e^{-1.60i} & 0.0042 \cdot e^{-1.60i} & 0.0004 \cdot e^{-1.70i} & 0.0111 \cdot e^{-2.30i} & 0.0010 \cdot e^{1.60i} & 0.0011 \cdot e^{1.60i} & 0.3539 \cdot e^{2.60i} & 0.3518 \cdot e^{1.50i} \\
0.1532 & -0.4131 & 0.0318 \cdot e^{0.01i} & 0.0000 & 0.0000 \cdot e^{-0.99i} & 0.0010 & 0.2319 & 0.0002 \cdot e^{-2.10i} & 0.0328 \cdot e^{3.10i} \\
0.1567 \cdot e^{-1.60i} & 0.4130 \cdot e^{1.60i} & 0.0317 \cdot e^{-1.60i} & 0.0001 \cdot e^{1.60i} & 0.0000 \cdot e^{-2.60i} & 0.0046 \cdot e^{-1.60i} & 0.2297 \cdot e^{-1.60i} & 0.0002 \cdot e^{2.60i} & 0.0327 \cdot e^{1.60i} \\
-0.4755 & -0.1260 & 0.0151 \cdot e^{-0.11i} & 0.0005 & 0.0000 \cdot e^{3.00i} & 0.0166 \cdot e^{-3.10i} & 0.0855 & 0.0001 \cdot e^{-2.30i} & 0.0154 \cdot e^{3.00i} \\
0.4743 \cdot e^{1.60i} & 0.1297 \cdot e^{1.60i} & 0.0154 \cdot e^{-1.70i} & 0.0004 \cdot e^{-1.60i} & 0.0000 \cdot e^{1.50i} & 0.0147 \cdot e^{1.60i} & 0.0865 \cdot e^{-1.60i} & 0.0001 \cdot e^{2.40i} & 0.0157 \cdot e^{1.40i} \\
-0.0165 & -0.0109 & 0.0010 \cdot e^{-0.06i} & 0.0145 \cdot e^{-3.10i} & 0.0001 \cdot e^{2.40i} & 0.4993 & 0.0113 \cdot e^{-3.10i} & 0.0001 \cdot e^{-2.20i} & 0.0024 \cdot e^{3.10i} \\
0.0156 \cdot e^{1.60i} & 0.0030 \cdot e^{1.60i} & 0.0004 \cdot e^{-1.70i} & 0.0145 \cdot e^{1.60i} & 0.0001 \cdot e^{0.82i} & 0.4995 \cdot e^{-1.60i} & 0.0051 \cdot e^{1.60i} & 0.0001 \cdot e^{2.50i} & 0.0017 \cdot e^{1.50i} \\
0.0113 \cdot e^{3.10i} & -0.2451 & 0.0199 & 0.0004 & 0.0000 \cdot e^{-0.17i} & 0.0157 \cdot e^{-3.10i} & 0.4345 \cdot e^{-3.10i} & 0.0000 \cdot e^{0.97i} & 0.0188 \cdot e^{3.10i} \\
0.0114 \cdot e^{1.60i} & 0.2436 \cdot e^{1.60i} & 0.0198 \cdot e^{-1.60i} & 0.0001 \cdot e^{-1.60i} & 0.0000 \cdot e^{-1.70i} & 0.0064 \cdot e^{1.60i} & 0.4356 \cdot e^{1.60i} & 0.0000 \cdot e^{-0.60i} & 0.0187 \cdot e^{1.50i} \\
0.0037 \cdot e^{-2.80i} & -0.0275 & 0.0148 & 0.0004 \cdot e^{-3.10i} & 0.0100 \cdot e^{-0.72i} & 0.0009 & 0.0009 & 0.3526 \cdot e^{-2.10i} & 0.3530 \cdot e^{-0.03i} \\
0.0037 \cdot e^{1.90i} & 0.0275 \cdot e^{1.60i} & 0.0148 \cdot e^{-1.60i} & 0.0004 \cdot e^{1.70i} & 0.0100 \cdot e^{-2.30i} & 0.0009 \cdot e^{-1.60i} & 0.0009 \cdot e^{-1.60i} & 0.3526 \cdot e^{2.60i} & 0.3529 \cdot e^{-1.60i} \\
0.0000 \cdot e^{0.36i} & 0.0000 \cdot e^{0.34i} & 0.0000 \cdot e^{0.21i} & 0.0000 \cdot e^{2.00i} & 0.0000 \cdot e^{3.00i} & 0.0000 \cdot e^{3.00i} & 0.0000 \cdot e^{0.39i} & 0.0000 \cdot e^{-1.40i} & 0.0000 \cdot e^{-2.90i} \\
0.0000 \cdot e^{0.53i} & 0.0000 \cdot e^{0.24i} & 0.0000 \cdot e^{0.40i} & 0.0000 \cdot e^{0.48i} & 0.0000 \cdot e^{2.60i} & 0.0000 \cdot e^{3.10i} & 0.0000 \cdot e^{0.21i} & 0.0000 \cdot e^{-2.00i} & 0.0000 \cdot e^{-2.90i} \\
0.0000 \cdot e^{0.32i} & 0.0000 & -0.0000 & -0.0000 & 0.0000 \cdot e^{2.40i} & 0.0006 & 0.0006 \cdot e^{-3.10i} & 0.0006 \cdot e^{1.00i} & 0.0000 \cdot e^{3.10i}
\end{pmatrix}, \quad (B.25)$$

$$\begin{pmatrix}
0.0000 \cdot e^{2.50i} & 0.0000 \cdot e^{2.50i} & 0.0000 \cdot e^{2.50i} & 0.0000 \cdot e^{-0.92i} & 0.0000 \cdot e^{1.30i} & 0.0000 \cdot e^{2.20i} & 0.0000 \cdot e^{1.50i} & 0.0000 \cdot e^{-0.07i} & 0.0000 \cdot e^{-1.10i} \\
0.0000 \cdot e^{1.60i} & 0.0000 \cdot e^{1.60i} & 0.0000 \cdot e^{1.60i} & 0.0000 \cdot e^{-1.40i} & 0.0000 \cdot e^{0.83i} & 0.0000 \cdot e^{1.70i} & 0.0000 \cdot e^{-1.60i} & 0.0000 \cdot e^{-0.59i} & 0.0000 \cdot e^{1.50i} \\
0.0000 \cdot e^{-1.60i} & 0.0000 \cdot e^{-1.60i} & 0.0000 \cdot e^{-1.60i} & 0.0000 \cdot e^{1.60i} & 0.0000 \cdot e^{0.85i} & 0.0000 \cdot e^{-1.60i} & 0.0000 \cdot e^{1.60i} & 0.0000 \cdot e^{-0.57i} & 0.0000 \cdot e^{1.50i} \\
0.0000 \cdot e^{-0.01i} & 0.0000 & 0.3486 & 0.0033 \cdot e^{-0.38i} & 0.3582 \cdot e^{-0.72i} & 0.0003 \cdot e^{-3.00i} & 0.0005 \cdot e^{-0.04i} & 0.0101 \cdot e^{1.00i} & 0.0051 \cdot e^{-3.10i} \\
0.0000 \cdot e^{-1.60i} & 0.0000 \cdot e^{-1.60i} & 0.3486 \cdot e^{-1.60i} & 0.0032 \cdot e^{-2.00i} & 0.3582 \cdot e^{-2.30i} & 0.0000 \cdot e^{2.90i} & 0.0002 \cdot e^{-1.70i} & 0.0105 \cdot e^{-0.57i} & 0.0051 \cdot e^{1.60i} \\
0.0011 \cdot e^{-3.10i} & 0.2320 & -0.0100 & 0.2425 \cdot e^{-3.10i} & 0.0170 \cdot e^{-0.69i} & 0.0064 \cdot e^{-3.10i} & 0.0015 & 0.0012 \cdot e^{0.99i} & 0.3700 \cdot e^{-0.03i} \\
0.0047 \cdot e^{1.60i} & 0.2298 \cdot e^{-1.60i} & 0.0099 \cdot e^{1.60i} & 0.2460 \cdot e^{1.60i} & 0.0170 \cdot e^{-2.30i} & 0.0063 \cdot e^{1.60i} & 0.0013 \cdot e^{-1.60i} & 0.0014 \cdot e^{-0.58i} & 0.3691 \cdot e^{-1.60i} \\
0.0166 & 0.0855 & -0.0062 & 0.4345 & 0.0059 \cdot e^{-1.00i} & 0.0130 & 0.0008 & 0.0006 \cdot e^{1.00i} & 0.2310 \cdot e^{-0.03i} \\
0.0147 \cdot e^{-1.60i} & 0.0865 \cdot e^{-1.60i} & 0.0063 \cdot e^{1.60i} & 0.4326 \cdot e^{-1.60i} & 0.0061 \cdot e^{-2.60i} & 0.0131 \cdot e^{-1.60i} & 0.0007 \cdot e^{-1.60i} & 0.0007 \cdot e^{-0.57i} & 0.2344 \cdot e^{-1.60i} \\
-0.4995 & -0.0112 & -0.0004 & 0.0136 & 0.0005 \cdot e^{-0.83i} & 0.0012 & 0.0007 \cdot e^{-3.10i} & 0.0008 \cdot e^{1.00i} & 0.0144 \cdot e^{-0.03i} \\
0.4997 \cdot e^{1.60i} & 0.0051 \cdot e^{1.60i} & 0.0002 \cdot e^{1.60i} & 0.0145 \cdot e^{-1.60i} & 0.0002 \cdot e^{-2.60i} & 0.0007 \cdot e^{-1.60i} & 0.0003 \cdot e^{1.60i} & 0.0003 \cdot e^{-0.57i} & 0.0065 \cdot e^{-1.60i} \\
0.0156 & -0.4344 & -0.0065 & 0.0444 \cdot e^{-3.10i} & 0.0102 \cdot e^{-0.72i} & 0.0000 \cdot e^{-3.10i} & 0.0001 & 0.0016 \cdot e^{1.00i} & 0.2427 \cdot e^{-0.03i} \\
0.0063 \cdot e^{-1.60i} & 0.4355 \cdot e^{1.60i} & 0.0065 \cdot e^{1.60i} & 0.0440 \cdot e^{1.60i} & 0.0101 \cdot e^{-2.30i} & 0.0004 \cdot e^{1.60i} & 0.0005 \cdot e^{-1.60i} & 0.0012 \cdot e^{-0.57i} & 0.2412 \cdot e^{-1.60i} \\
-0.0000 & -0.0000 & 0.3581 & 0.0031 \cdot e^{2.80i} & 0.3479 \cdot e^{2.40i} & 0.0007 \cdot e^{3.10i} & 0.0006 \cdot e^{0.03i} & 0.0109 \cdot e^{-2.10i} & 0.0237 \cdot e^{-0.02i} \\
0.0000 \cdot e^{1.60i} & 0.0000 \cdot e^{1.60i} & 0.3582 \cdot e^{-1.60i} & 0.0031 \cdot e^{1.20i} & 0.3479 \cdot e^{0.85i} & 0.0003 \cdot e^{1.50i} & 0.0003 \cdot e^{-1.50i} & 0.0105 \cdot e^{2.60i} & 0.0237 \cdot e^{-1.60i} \\
0.0000 \cdot e^{-0.27i} & 0.0000 \cdot e^{-0.45i} & 0.0000 \cdot e^{-2.70i} & -0.0160 & 0.0090 \cdot e^{-1.20i} & 0.5537 & 0.3132 \cdot e^{0.47i} & 0.3081 \cdot e^{-2.60i} & 0.0017 \cdot e^{-2.70i} \\
0.0000 \cdot e^{-0.32i} & 0.0000 \cdot e^{-0.19i} & 0.0000 \cdot e^{0.17i} & 0.0047 \cdot e^{1.60i} & 0.0145 \cdot e^{-0.88i} & 0.1627 \cdot e^{-1.50i} & 0.4850 \cdot e^{-3.00i} & 0.4879 \cdot e^{-2.30i} & 0.0028 \cdot e^{0.12i} \\
-0.0012 & -0.0012 & -0.0012 & 0.0119 & 0.0123 \cdot e^{-0.72i} & 0.4080 \cdot e^{-3.10i} & 0.4083 & 0.4081 \cdot e^{-2.10i} & 0.0010 \cdot e^{-0.03i}
\end{pmatrix},$$

The Yukawa couplings $h_{qq'}$ defined in Eq. (3.38) are given by

$$h_{dd} = 0.00000183 \cdot e^{-0.01i}, \quad h_{uu} = 0.00000182 \cdot e^{-0.01i}, \quad h_{du} = 0.00000183 \cdot e^{-0.01i}, \quad (\text{B.26})$$

where the Yukawa coupling in the gauge basis, h is set to be identity matrix.

Finally we summarize the prediction of observables at this benchmark point, lower and upper limits in Table 4. We take $\tan \beta = 50$ and $m_H = 3.0$ TeV to calculate the neutral meson mixing. The benchmark point explains the $b \rightarrow s\mu\mu$ anomaly. On the other hand it is hard to explain the $b \rightarrow c\tau\nu$ anomaly. The all experimental constraints listed in the table are satisfied and the tuning level defined in Eq. (2.41) is about 0.1%.

Table 4: The values of predictions at this benchmark point, lower and upper limit are shown. The value of the fine-tuning parameter is $\Delta_{\text{FT}}^{-1} = 1.39 \times 10^3$.

observable	prediction	lower limit	upper limit	Ref.
$\text{Re}\Delta C_9$ ($b \rightarrow s\mu\mu$ anomaly)	-0.505	-0.59	-0.41	[84]
ΔC_V ($b \rightarrow c\tau\nu$ anomaly)	2.75×10^{-8}	5.2×10^{-2}	0.124	[85]
$\text{BR}(B \rightarrow e\nu)$	8.74×10^{-12}	0	9.8×10^{-7}	[90]
$\text{BR}(B \rightarrow \mu\nu)$	3.88×10^{-7}	2.90×10^{-7}	1.07×10^{-6}	[90]
$\text{BR}(B \rightarrow \tau\nu)$	8.82×10^{-5}	8.5×10^{-5}	1.33×10^{-4}	[90]
$\text{BR}(B_c \rightarrow e\nu)$	2.20×10^{-9}	0	0.6	[111]
$\text{BR}(B_c \rightarrow \mu\nu)$	9.79×10^{-5}	0	0.6	[111]
$\text{BR}(B_c \rightarrow \tau\nu)$	2.39×10^{-2}	0	0.6	[111]
$\text{BR}(K_L \rightarrow e\mu)$	3.04×10^{-13}	0	4.7×10^{-12}	[90]
$\text{BR}(B_d \rightarrow e\tau)$	1.27×10^{-18}	0	2.8×10^{-5}	[90]
$\text{BR}(B_d \rightarrow \mu\tau)$	4.70×10^{-13}	0	2.2×10^{-5}	[90]
$\text{BR}(B_d \rightarrow \mu e)$	5.46×10^{-13}	0	2.8×10^{-9}	[90]
$\text{BR}(B_d \rightarrow ee)$	2.47×10^{-15}	0	8.3×10^{-8}	[90]
$\text{BR}(B_d \rightarrow \mu\mu)$	1.00×10^{-10}	0	3.9×10^{-10}	[90]
$\text{BR}(B_d \rightarrow \tau\tau)$	2.34×10^{-8}	0	2.1×10^{-3}	[90]
$\text{BR}(B_s \rightarrow e\tau)$	2.83×10^{-18}	-	-	[90]
$\text{BR}(B_s \rightarrow \mu\tau)$	7.51×10^{-13}	0	4.2×10^{-5}	[90]
$\text{BR}(B_s \rightarrow \mu e)$	7.99×10^{-13}	0	5.4×10^{-9}	[90]
$\text{BR}(B_s \rightarrow ee)$	7.48×10^{-14}	0	2.8×10^{-7}	[90]
$\text{BR}(B_s \rightarrow \mu\mu)$	3.81×10^{-9}	2.2×10^{-9}	3.8×10^{-9}	[90]
$\text{BR}(B_s \rightarrow \tau\tau)$	7.16×10^{-7}	0	6.8×10^{-3}	[90]
$\text{BR}(\mu \rightarrow e)^{\text{Al}}$	7.67×10^{-16}	0	6×10^{-17}	[91]
$\text{BR}(\mu \rightarrow e)^{\text{Au}}$	9.37×10^{-16}	0	3×10^{-13}	[93](prospect)
$ C_{B_d} $	0.94	0.83	1.27	[100, 101]
$\text{Arg}C_{B_d}$	-0.75	-5.6	1.6	[100, 101]
$ C_{B_s} $	1.03	0.93	1.29	[100, 101]
$\text{Arg}C_{B_s}$	-1.71×10^{-2}	-1.36	2.2	[100, 101]
$\text{Im}C_K$	0.92	0.88	1.36	[100, 101]
$\text{BR}(\mu \rightarrow e\gamma)$	3.69×10^{-14}	0	4.2×10^{-13}	[96]
$\text{BR}(\tau \rightarrow e\gamma)$	4.38×10^{-15}	0	3.3×10^{-8}	[90]
$\text{BR}(\tau \rightarrow \mu\gamma)$	5.09×10^{-9}	0	4.4×10^{-8}	[90]

References

- [1] W. Buchmuller, R. Ruckl, and D. Wyler, *Leptoquarks in Lepton - Quark Collisions*, *Phys. Lett. B* **191** (1987) 442–448. [Erratum: *Phys.Lett.B* 448, 320–320 (1999)].
- [2] Y. Sakaki, M. Tanaka, A. Tayduganov, and R. Watanabe, *Testing leptoquark models in $\bar{B} \rightarrow D^{(*)}\tau\bar{\nu}$* , *Phys. Rev. D* **88** (2013), no. 9 094012, [[arXiv:1309.0301](#)].
- [3] M. Bauer and M. Neubert, *Minimal Leptoquark Explanation for the $R_{D^{(*)}}$, R_K , and $(g-2)_g$ Anomalies*, *Phys. Rev. Lett.* **116** (2016), no. 14 141802, [[arXiv:1511.01900](#)].
- [4] S. Fajfer and N. Košnik, *Vector leptoquark resolution of R_K and $R_{D^{(*)}}$ puzzles*, *Phys. Lett. B* **755** (2016) 270–274, [[arXiv:1511.06024](#)].
- [5] D. Bečirević, S. Fajfer, N. Košnik, and O. Sumensari, *Leptoquark model to explain the B -physics anomalies, R_K and R_D* , *Phys. Rev. D* **94** (2016), no. 11 115021, [[arXiv:1608.08501](#)].
- [6] B. Bhattacharya, A. Datta, J.-P. Guévin, D. London, and R. Watanabe, *Simultaneous Explanation of the R_K and $R_{D^{(*)}}$ Puzzles: a Model Analysis*, *JHEP* **01** (2017) 015, [[arXiv:1609.09078](#)].
- [7] X.-Q. Li, Y.-D. Yang, and X. Zhang, *Revisiting the one leptoquark solution to the $R(D^{(*)})$ anomalies and its phenomenological implications*, *JHEP* **08** (2016) 054, [[arXiv:1605.09308](#)].
- [8] R. Barbieri, C. W. Murphy, and F. Senia, *B -decay Anomalies in a Composite Leptoquark Model*, *Eur. Phys. J. C* **77** (2017), no. 1 8, [[arXiv:1611.04930](#)].
- [9] S. Sahoo, R. Mohanta, and A. K. Giri, *Explaining the R_K and $R_{D^{(*)}}$ anomalies with vector leptoquarks*, *Phys. Rev. D* **95** (2017), no. 3 035027, [[arXiv:1609.04367](#)].
- [10] N. Assad, B. Fornal, and B. Grinstein, *Baryon Number and Lepton Universality Violation in Leptoquark and Diquark Models*, *Phys. Lett. B* **777** (2018) 324–331, [[arXiv:1708.06350](#)].
- [11] D. Buttazzo, A. Greljo, G. Isidori, and D. Marzocca, *B -physics anomalies: a guide to combined explanations*, *JHEP* **11** (2017) 044, [[arXiv:1706.07808](#)].
- [12] L. Di Luzio, A. Greljo, and M. Nardecchia, *Gauge leptoquark as the origin of B -physics anomalies*, *Phys. Rev. D* **96** (2017), no. 11 115011, [[arXiv:1708.08450](#)].
- [13] D. Bečirević and O. Sumensari, *A leptoquark model to accommodate $R_K^{\text{exp}} < R_K^{\text{SM}}$ and $R_{K^*}^{\text{exp}} < R_{K^*}^{\text{SM}}$* , *JHEP* **08** (2017) 104, [[arXiv:1704.05835](#)].
- [14] A. Angelescu, D. Bečirević, D. Faroughy, and O. Sumensari, *Closing the window on single leptoquark solutions to the B -physics anomalies*, *JHEP* **10** (2018) 183, [[arXiv:1808.08179](#)].
- [15] S. Iguro, T. Kitahara, Y. Omura, R. Watanabe, and K. Yamamoto, *D^* polarization vs. $R_{D^{(*)}}$ anomalies in the leptoquark models*, *JHEP* **02** (2019) 194, [[arXiv:1811.08899](#)].
- [16] C. Cornella, J. Fuentes-Martin, and G. Isidori, *Revisiting the vector leptoquark explanation of the B -physics anomalies*, *JHEP* **07** (2019) 168, [[arXiv:1903.11517](#)].

- [17] J. C. Pati and A. Salam, *Lepton Number as the Fourth Color*, *Phys. Rev. D* **10** (1974) 275–289. [Erratum: *Phys.Rev.D* 11, 703–703 (1975)].
- [18] Z. Poh, S. Raby, and Z.-z. Wang, *Pati-Salam SUSY GUT with Yukawa unification*, *Phys. Rev. D* **95** (2017), no. 11 115025, [arXiv:1703.09309].
- [19] L. Calibbi, A. Crivellin, and T. Li, *Model of vector leptoquarks in view of the B-physics anomalies*, *Phys. Rev. D* **98** (2018), no. 11 115002, [arXiv:1709.00692].
- [20] M. J. Dolan, T. P. Dutka, and R. R. Volkas, *Lowering the scale of Pati-Salam breaking through seesaw mixing*, arXiv:2012.05976.
- [21] **LHCb** Collaboration, R. Aaij et al., *Measurement of Form-Factor-Independent Observables in the Decay $B^0 \rightarrow K^{*0}\mu^+\mu^-$* , *Phys. Rev. Lett.* **111** (2013) 191801, [arXiv:1308.1707].
- [22] **LHCb** Collaboration, R. Aaij et al., *Angular analysis of the $B^0 \rightarrow K^{*0}\mu^+\mu^-$ decay using 3 fb^{-1} of integrated luminosity*, *JHEP* **02** (2016) 104, [arXiv:1512.04442].
- [23] **LHCb** Collaboration, R. Aaij et al., *Test of lepton universality with $B^0 \rightarrow K^{*0}\ell^+\ell^-$ decays*, *JHEP* **08** (2017) 055, [arXiv:1705.05802].
- [24] **LHCb** Collaboration, R. Aaij et al., *Test of lepton universality using $B^+ \rightarrow K^+\ell^+\ell^-$ decays*, *Phys. Rev. Lett.* **113** (2014) 151601, [arXiv:1406.6482].
- [25] **LHCb** Collaboration, R. Aaij et al., *Search for lepton-universality violation in $B^+ \rightarrow K^+\ell^+\ell^-$ decays*, *Phys. Rev. Lett.* **122** (2019), no. 19 191801, [arXiv:1903.09252].
- [26] **Belle** Collaboration, A. Abdesselam et al., *Test of lepton flavor universality in $B \rightarrow K^*\ell^+\ell^-$ decays at Belle*, arXiv:1904.02440.
- [27] **Belle** Collaboration, A. Abdesselam et al., *Measurement of $\mathcal{R}(D)$ and $\mathcal{R}(D^*)$ with a semileptonic tagging method*, arXiv:1904.08794.
- [28] **LHCb** Collaboration, R. Aaij et al., *Measurement of CP-Averaged Observables in the $B^0 \rightarrow K^{*0}\mu^+\mu^-$ Decay*, *Phys. Rev. Lett.* **125** (2020), no. 1 011802, [arXiv:2003.04831].
- [29] **BaBar** Collaboration, J. Lees et al., *Evidence for an excess of $\bar{B} \rightarrow D^{(*)}\tau^-\bar{\nu}_\tau$ decays*, *Phys. Rev. Lett.* **109** (2012) 101802, [arXiv:1205.5442].
- [30] **BaBar** Collaboration, J. Lees et al., *Measurement of an Excess of $\bar{B} \rightarrow D^{(*)}\tau^-\bar{\nu}_\tau$ Decays and Implications for Charged Higgs Bosons*, *Phys. Rev. D* **88** (2013), no. 7 072012, [arXiv:1303.0571].
- [31] **LHCb** Collaboration, R. Aaij et al., *Measurement of the ratio of branching fractions $\mathcal{B}(\bar{B}^0 \rightarrow D^{*+}\tau^-\bar{\nu}_\tau)/\mathcal{B}(\bar{B}^0 \rightarrow D^{*+}\mu^-\bar{\nu}_\mu)$* , *Phys. Rev. Lett.* **115** (2015), no. 11 111803, [arXiv:1506.08614]. [Erratum: *Phys.Rev.Lett.* 115, 159901 (2015)].
- [32] **Belle** Collaboration, M. Huschle et al., *Measurement of the branching ratio of $\bar{B} \rightarrow D^{(*)}\tau^-\bar{\nu}_\tau$ relative to $\bar{B} \rightarrow D^{(*)}\ell^-\bar{\nu}_\ell$ decays with hadronic tagging at Belle*, *Phys. Rev. D* **92** (2015), no. 7 072014, [arXiv:1507.03233].

- [33] **Belle** Collaboration, Y. Sato et al., *Measurement of the branching ratio of $\bar{B}^0 \rightarrow D^{*+} \tau^- \bar{\nu}_\tau$ relative to $\bar{B}^0 \rightarrow D^{*+} \ell^- \bar{\nu}_\ell$ decays with a semileptonic tagging method*, *Phys. Rev. D* **94** (2016), no. 7 072007, [[arXiv:1607.07923](#)].
- [34] **Belle** Collaboration, S. Hirose et al., *Measurement of the τ lepton polarization and $R(D^*)$ in the decay $\bar{B} \rightarrow D^* \tau^- \bar{\nu}_\tau$* , *Phys. Rev. Lett.* **118** (2017), no. 21 211801, [[arXiv:1612.00529](#)].
- [35] **LHCb** Collaboration, R. Aaij et al., *Test of Lepton Flavor Universality by the measurement of the $B^0 \rightarrow D^{*-} \tau^+ \nu_\tau$ branching fraction using three-prong τ decays*, *Phys. Rev. D* **97** (2018), no. 7 072013, [[arXiv:1711.02505](#)].
- [36] **LHCb** Collaboration, R. Aaij et al., *Angular analysis of the $B^+ \rightarrow K^{*+} \mu^+ \mu^-$ decay*, [arXiv:2012.13241](#).
- [37] F. U. Bernlochner, Z. Ligeti, M. Papucci, and D. J. Robinson, *Combined analysis of semileptonic B decays to D and D^* : $R(D^{(*)})$, $|V_{cb}|$, and new physics*, *Phys. Rev. D* **95** (2017), no. 11 115008, [[arXiv:1703.05330](#)]. [Erratum: *Phys.Rev.D* 97, 059902 (2018)].
- [38] D. Bigi, P. Gambino, and S. Schacht, *$R(D^*)$, $|V_{cb}|$, and the Heavy Quark Symmetry relations between form factors*, *JHEP* **11** (2017) 061, [[arXiv:1707.09509](#)].
- [39] M. Bordone, M. Jung, and D. van Dyk, *Theory determination of $\bar{B} \rightarrow D^{(*)} \ell^- \bar{\nu}$ form factors at $\mathcal{O}(1/m_c^2)$* , *Eur. Phys. J. C* **80** (2020), no. 2 74, [[arXiv:1908.09398](#)].
- [40] **HFLAV** Collaboration, Y. S. Amhis et al., *Averages of b -hadron, c -hadron, and τ -lepton properties as of 2018*, [arXiv:1909.12524](#).
- [41] S. Iguro and R. Watanabe, *Bayesian fit analysis to full distribution data of $\bar{B} \rightarrow D^{(*)} \ell \bar{\nu}$: $|V_{cb}|$ determination and new physics constraints*, *JHEP* **08** (2020), no. 08 006, [[arXiv:2004.10208](#)].
- [42] B. Bhattacharya, A. Datta, D. London, and S. Shivashankara, *Simultaneous Explanation of the R_K and $R(D^{(*)})$ Puzzles*, *Phys. Lett. B* **742** (2015) 370–374, [[arXiv:1412.7164](#)].
- [43] R. Barbieri, G. Isidori, A. Pattori, and F. Senia, *Anomalies in B -decays and $U(2)$ flavour symmetry*, *Eur. Phys. J. C* **76** (2016), no. 2 67, [[arXiv:1512.01560](#)].
- [44] D. Das, C. Hati, G. Kumar, and N. Mahajan, *Towards a unified explanation of $R_{D^{(*)}}$, R_K and $(g-2)_\mu$ anomalies in a left-right model with leptoquarks*, *Phys. Rev. D* **94** (2016) 055034, [[arXiv:1605.06313](#)].
- [45] A. Greljo and B. A. Stefanek, *Third family quark–lepton unification at the TeV scale*, *Phys. Lett. B* **782** (2018) 131–138, [[arXiv:1802.04274](#)].
- [46] L. Di Luzio, J. Fuentes-Martin, A. Greljo, M. Nardecchia, and S. Renner, *Maximal Flavour Violation: a Cabibbo mechanism for leptoquarks*, *JHEP* **11** (2018) 081, [[arXiv:1808.00942](#)].
- [47] M. Bordone, C. Cornella, J. Fuentes-Martin, and G. Isidori, *A three-site gauge model for flavor hierarchies and flavor anomalies*, *Phys. Lett. B* **779** (2018) 317–323, [[arXiv:1712.01368](#)].
- [48] M. Bordone, C. Cornella, J. Fuentes-Martin, and G. Isidori, *Low-energy signatures of the PS^3 model: from B -physics anomalies to LFV*, *JHEP* **10** (2018) 148, [[arXiv:1805.09328](#)].

- [49] J. Fuentes-Martín and P. Stangl, *Third-family quark-lepton unification with a fundamental composite Higgs*, *Phys. Lett. B* **811** (2020) 135953, [arXiv:2004.11376].
- [50] J. Fuentes-Martín, G. Isidori, M. König, and N. Selimović, *Vector Leptoquarks Beyond Tree Level III: Vector-like Fermions and Flavor-Changing Transitions*, *Phys. Rev. D* **102** (2020) 115015, [arXiv:2009.11296].
- [51] D. Guadagnoli, M. Reboud, and P. Stangl, *The Dark Side of 4321*, *JHEP* **10** (2020) 084, [arXiv:2005.10117].
- [52] W. Altmannshofer, S. Gori, M. Pospelov, and I. Yavin, *Quark flavor transitions in $L_\mu - L_\tau$ models*, *Phys. Rev.* **D89** (2014) 095033, [arXiv:1403.1269].
- [53] A. Crivellin, G. D’Ambrosio, and J. Heeck, *Explaining $h \rightarrow \mu^\pm \tau^\mp$, $B \rightarrow K^* \mu^+ \mu^-$ and $B \rightarrow K \mu^+ \mu^- / B \rightarrow K e^+ e^-$ in a two-Higgs-doublet model with gauged $L_\mu - L_\tau$* , *Phys. Rev. Lett.* **114** (2015) 151801, [arXiv:1501.00993].
- [54] S. Raby and A. Trautner, *Vectorlike chiral fourth family to explain muon anomalies*, *Phys. Rev.* **D97** (2018), no. 9 095006, [arXiv:1712.09360].
- [55] S. F. King, *Flavourful Z' models for $R_{K^{(*)}}$* , *JHEP* **08** (2017) 019, [arXiv:1706.06100].
- [56] A. Falkowski, S. F. King, E. Perdomo, and M. Pierre, *Flavourful Z' portal for vector-like neutrino Dark Matter and $R_{K^{(*)}}$* , *JHEP* **08** (2018) 061, [arXiv:1803.04430].
- [57] J. Kawamura, S. Raby, and A. Trautner, *Complete vectorlike fourth family and new $U(1)'$ for muon anomalies*, *Phys. Rev. D* **100** (2019), no. 5 055030, [arXiv:1906.11297].
- [58] J. Kawamura, S. Raby, and A. Trautner, *Complete vectorlike fourth family with $U(1)'$: A global analysis*, *Phys. Rev. D* **101** (2020), no. 3 035026, [arXiv:1911.11075].
- [59] B. Gripaios, M. Nardecchia, and S. A. Renner, *Linear flavour violation and anomalies in B physics*, *JHEP* **06** (2016) 083, [arXiv:1509.05020].
- [60] P. Arnan, L. Hofer, F. Mescia, and A. Crivellin, *Loop effects of heavy new scalars and fermions in $b \rightarrow s \mu^+ \mu^-$* , *JHEP* **04** (2017) 043, [arXiv:1608.07832].
- [61] B. Grinstein, S. Pokorski, and G. G. Ross, *Lepton non-universality in B decays and fermion mass structure*, *JHEP* **12** (2018) 079, [arXiv:1809.01766].
- [62] P. Arnan, A. Crivellin, M. Fedele, and F. Mescia, *Generic Loop Effects of New Scalars and Fermions in $b \rightarrow s \ell^+ \ell^-$ and a Vector-like 4th Generation*, arXiv:1904.05890.
- [63] C.-W. Chiang and H. Okada, *A simple model for explaining muon-related anomalies and dark matter*, arXiv:1711.07365.
- [64] J. M. Cline and J. M. Cornell, *$R(K^{(*)})$ from dark matter exchange*, *Phys. Lett.* **B782** (2018) 232–237, [arXiv:1711.10770].
- [65] J. Kawamura, S. Okawa, and Y. Omura, *Interplay between the $b \rightarrow s \ell \ell$ anomalies and dark matter physics*, *Phys. Rev.* **D96** (2017), no. 7 075041, [arXiv:1706.04344].

- [66] B. Barman, D. Borah, L. Mukherjee, and S. Nandi, *Correlating the anomalous results in $b \rightarrow s$ decays with inert Higgs doublet dark matter and muon $(g - 2)$* , [arXiv:1808.06639](#).
- [67] D. G. Cerdeño, A. Cheek, P. Martín-Ramiro, and J. M. Moreno, *B anomalies and dark matter: a complex connection*, *Eur. Phys. J. C* **79** (2019), no. 6 517, [[arXiv:1902.01789](#)].
- [68] G. Arcadi, L. Calibbi, M. Fedele, and F. Mescia, *Systematic approach to B-physics anomalies and t-channel dark matter*, [arXiv:2103.09835](#).
- [69] A. Crivellin, C. Greub, and A. Kokulu, *Explaining $B \rightarrow D\tau\nu$, $B \rightarrow D^*\tau\nu$ and $B \rightarrow \tau\nu$ in a 2HDM of type III*, *Phys. Rev. D* **86** (2012) 054014, [[arXiv:1206.2634](#)].
- [70] M. Tanaka and R. Watanabe, *New physics in the weak interaction of $\bar{B} \rightarrow D^{(*)}\tau\bar{\nu}$* , *Phys. Rev. D* **87** (2013), no. 3 034028, [[arXiv:1212.1878](#)].
- [71] A. Celis, M. Jung, X.-Q. Li, and A. Pich, *Sensitivity to charged scalars in $B \rightarrow D^{(*)}\tau\nu_\tau$ and $B \rightarrow \tau\nu_\tau$ decays*, *JHEP* **01** (2013) 054, [[arXiv:1210.8443](#)].
- [72] A. Crivellin, A. Kokulu, and C. Greub, *Flavor-phenomenology of two-Higgs-doublet models with generic Yukawa structure*, *Phys. Rev. D* **87** (2013), no. 9 094031, [[arXiv:1303.5877](#)].
- [73] A. Crivellin, J. Heeck, and P. Stoffer, *A perturbed lepton-specific two-Higgs-doublet model facing experimental hints for physics beyond the Standard Model*, *Phys. Rev. Lett.* **116** (2016), no. 8 081801, [[arXiv:1507.07567](#)].
- [74] C.-H. Chen and T. Nomura, *Charged-Higgs on $R_{D^{(*)}}$, τ polarization, and FBA*, *Eur. Phys. J. C* **77** (2017), no. 9 631, [[arXiv:1703.03646](#)].
- [75] S. Iguro and K. Tobe, *$R(D^{(*)})$ in a general two Higgs doublet model*, *Nucl. Phys. B* **925** (2017) 560–606, [[arXiv:1708.06176](#)].
- [76] S. Iguro and Y. Omura, *Status of the semileptonic B decays and muon $g-2$ in general 2HDMs with right-handed neutrinos*, *JHEP* **05** (2018) 173, [[arXiv:1802.01732](#)].
- [77] S. Iguro, Y. Omura, and M. Takeuchi, *Test of the $R(D^{(*)})$ anomaly at the LHC*, *Phys. Rev. D* **99** (2019), no. 7 075013, [[arXiv:1810.05843](#)].
- [78] R. Alonso, B. Grinstein, and J. Martin Camalich, *Lifetime of B_c^- Constrains Explanations for Anomalies in $B \rightarrow D^{(*)}\tau\nu$* , *Phys. Rev. Lett.* **118** (2017), no. 8 081802, [[arXiv:1611.06676](#)].
- [79] A. Akeroyd and C.-H. Chen, *Constraint on the branching ratio of $B_c \rightarrow \tau\bar{\nu}$ from LEP1 and consequences for $R(D^{(*)})$ anomaly*, *Phys. Rev. D* **96** (2017), no. 7 075011, [[arXiv:1708.04072](#)].
- [80] P. Hung, A. Buras, and J. Bjorken, *Petite Unification of Quarks and Leptons*, *Phys. Rev. D* **25** (1982) 805.
- [81] G. Valencia and S. Willenbrock, *Quark - lepton unification and rare meson decays*, *Phys. Rev. D* **50** (1994) 6843–6848, [[hep-ph/9409201](#)].
- [82] M. Borsato, V. V. Gligorov, D. Guadagnoli, D. Martinez Santos, and O. Sumensari, *Effective-field-theory arguments for pursuing lepton-flavor-violating K decays at LHCb*, *Phys. Rev. D* **99** (2019), no. 5 055017, [[arXiv:1808.02006](#)].

- [83] M. J. Baker, J. Fuentes-Martín, G. Isidori, and M. König, *High- p_T signatures in vector-leptoquark models*, *Eur. Phys. J. C* **79** (2019), no. 4 334, [arXiv:1901.10480].
- [84] M. Algueró, B. Capdevila, A. Crivellin, S. Descotes-Genon, P. Masjuan, J. Matias, M. Novoa Brunet, and J. Virto, *Emerging patterns of New Physics with and without Lepton Flavour Universal contributions*, *Eur. Phys. J. C* **79** (2019), no. 8 714, [arXiv:1903.09578]. [Addendum: *Eur.Phys.J.C* 80, 511 (2020)].
- [85] S. Iguro, M. Takeuchi, and R. Watanabe, *Testing Leptoquark/EFT in $\bar{B} \rightarrow D^{(*)}l\bar{\nu}$ at the LHC*, arXiv:2011.02486.
- [86] S. Antusch and V. Maurer, *Running quark and lepton parameters at various scales*, *JHEP* **11** (2013) 115, [arXiv:1306.6879].
- [87] **ATLAS** Collaboration, G. Aad et al., *Search for high-mass dilepton resonances using 139 fb⁻¹ of pp collision data collected at $\sqrt{s} = 13$ TeV with the ATLAS detector*, *Phys. Lett. B* **796** (2019) 68–87, [arXiv:1903.06248].
- [88] **ATLAS** Collaboration, M. Aaboud et al., *Combination of the searches for pair-produced vector-like partners of the third-generation quarks at $\sqrt{s} = 13$ TeV with the ATLAS detector*, *Phys. Rev. Lett.* **121** (2018), no. 21 211801, [arXiv:1808.02343].
- [89] J. Heeck and D. Teresi, *Pati-Salam explanations of the B-meson anomalies*, *JHEP* **12** (2018) 103, [arXiv:1808.07492].
- [90] **Particle Data Group** Collaboration, P. Zyla et al., *Review of Particle Physics*, *PTEP* **2020** (2020), no. 8 083C01.
- [91] **SINDRUM II** Collaboration, W. H. Bertl et al., *A Search for muon to electron conversion in muonic gold*, *Eur. Phys. J. C* **47** (2006) 337–346.
- [92] **DeeMe** Collaboration, H. Natori, *DeeMe experiment - An experimental search for a mu-e conversion reaction at J-PARC MLF*, *Nucl. Phys. B Proc. Suppl.* **248-250** (2014) 52–57.
- [93] **COMET** Collaboration, Y. Kuno, *A search for muon-to-electron conversion at J-PARC: The COMET experiment*, *PTEP* **2013** (2013) 022C01.
- [94] **Mu2e** Collaboration, R. J. Abrams et al., *Mu2e Conceptual Design Report*, arXiv:1211.7019.
- [95] L. Lavoura, *General formulae for $f(1) \rightarrow f(2)\gamma$* , *Eur. Phys. J.* **C29** (2003) 191–195, [hep-ph/0302221].
- [96] **MEG** Collaboration, A. Baldini et al., *Search for the lepton flavour violating decay $\mu^+ \rightarrow e^+\gamma$ with the full dataset of the MEG experiment*, *Eur. Phys. J. C* **76** (2016), no. 8 434, [arXiv:1605.05081].
- [97] **MEG II** Collaboration, A. M. Baldini et al., *The design of the MEG II experiment*, *Eur. Phys. J.* **C78** (2018), no. 5 380, [arXiv:1801.04688].
- [98] A. J. Buras, S. Jager, and J. Urban, *Master formulae for Delta F=2 NLO QCD factors in the standard model and beyond*, *Nucl. Phys.* **B605** (2001) 600–624, [hep-ph/0102316].

- [99] A. J. Buras, *Weak Hamiltonian, CP violation and rare decays*, in *Probing the standard model of particle interactions. Proceedings, Summer School in Theoretical Physics, NATO Advanced Study Institute, 68th session, Les Houches, France, July 28-September 5, 1997. Pt. 1, 2*, pp. 281–539, 1998. [hep-ph/9806471](#).
- [100] **UTfit** Collaboration, M. Bona et al., *The 2004 UTfit collaboration report on the status of the unitarity triangle in the standard model*, *JHEP* **07** (2005) 028, [[hep-ph/0501199](#)].
- [101] **UTfit** Collaboration, M. Bona et al., *Model-independent constraints on $\Delta F = 2$ operators and the scale of new physics*, *JHEP* **03** (2008) 049, [[arXiv:0707.0636](#)].
- [102] L. Di Luzio, M. Kirk, A. Lenz, and T. Rauh, *ΔM_s theory precision confronts flavour anomalies*, *JHEP* **12** (2019) 009, [[arXiv:1909.11087](#)].
- [103] R. N. Mohapatra and R. E. Marshak, *Local B-L Symmetry of Electroweak Interactions, Majorana Neutrinos and Neutron Oscillations*, *Phys. Rev. Lett.* **44** (1980) 1316–1319. [Erratum: *Phys.Rev.Lett.* 44, 1643 (1980)].
- [104] D. G. Phillips, II et al., *Neutron-Antineutron Oscillations: Theoretical Status and Experimental Prospects*, *Phys. Rept.* **612** (2016) 1–45, [[arXiv:1410.1100](#)].
- [105] **Super-Kamiokande** Collaboration, K. Abe et al., *The Search for $n - \bar{n}$ oscillation in Super-Kamiokande I*, *Phys. Rev. D* **91** (2015) 072006, [[arXiv:1109.4227](#)].
- [106] **Flavour Lattice Averaging Group** Collaboration, S. Aoki et al., *FLAG Review 2019*, [arXiv:1902.08191](#).
- [107] V. Cirigliano, R. Kitano, Y. Okada, and P. Tuzon, *On the model discriminating power of $\mu \rightarrow e$ conversion in nuclei*, *Phys. Rev. D* **80** (2009) 013002, [[arXiv:0904.0957](#)].
- [108] P. Junnarkar and A. Walker-Loud, *Scalar strange content of the nucleon from lattice QCD*, *Phys. Rev. D* **87** (2013) 114510, [[arXiv:1301.1114](#)].
- [109] R. Kitano, M. Koike, and Y. Okada, *Detailed calculation of lepton flavor violating muon electron conversion rate for various nuclei*, *Phys. Rev. D* **66** (2002) 096002, [[hep-ph/0203110](#)]. [Erratum: *Phys.Rev.D* 76, 059902 (2007)].
- [110] T. Suzuki, D. F. Measday, and J. Roalsvig, *Total Nuclear Capture Rates for Negative Muons*, *Phys. Rev. C* **35** (1987) 2212.
- [111] M. Blanke, A. Crivellin, S. de Boer, T. Kitahara, M. Moscati, U. Nierste, and I. Nišandžić, *Impact of polarization observables and $B_c \rightarrow \tau \nu$ on new physics explanations of the $b \rightarrow c \tau \nu$ anomaly*, *Phys. Rev. D* **99** (2019), no. 7 075006, [[arXiv:1811.09603](#)].